The Effect of the Interphase/Interface Region on Creep and Creep Rupture of Thermoplastic Composites

By

Yeou Shin Chang

Dissertation submitted to the Faculty of the
Virginia Polytechnic Institute and State University
in partial fulfillment of the requirements for the degree of
Doctor of Philosophy
in
Materials Engineering Science Program

APPROVED:

David A. Dillard
D. A. Dillard, Chairman

D. G. Baird

Alfred C. Loos
A. C. Loos

Wayne W. Stinchcomb
W. W. Stinchcomb

T. C. Ward
T. C. Ward

May, 1992

Blacksburg, Virginia

The Effect of the Interphase/Interface Region on Creep and Creep Rupture of Thermoplastic Composites

By

Yeou Shin Chang

David A. Dillard, Chairman

Materials Engineering Science Program

(ABSTRACT)

The effect of the interphase/interface region on the static mechanical properties, creep and creep rupture behavior of thermoplastic (J2) composites was investigated. The mechanical properties of the J2 composites were altered by systematic changes in fiber surface chemistry. Four fiber systems were used including the AU4, AS4(1) & (2), and AS4CGP fibers. (AS4(1) and AS4(2) represent different batch numbers.) Surface energies and chemistry of carbon fibers were examined using the Dynamic Contact Angle (DCA) method and X-ray Photoelectron Spectroscopoy (XPS), respectively. The mesoindentation technique was used to measure the interfacial shear strengths (ISS) of the composites.

For the same batch of the composites, the ISS ratios for AS4(2)/J2 to AU4/J2 and AS4CGP/J2 to AU4/J2 were 1.22 and 1.24, respectively. The mechanical properties of these composites in the fiber direction were insensitive to the ISS. The transverse and shear moduli of the J2 composites

were also not affected by the ISS. The static strengths, in general, ordered themselves from strong to weak as follows: AS4(2)/J2> AS4CGP/J2> AU4/J2. However, the creep rupture strength revealed a different ordering: AS4CGP/J2> AS4(2)/J2> AU4/J2. This suggests that static mechanical properties may not be a good indicator for long term mechanical performance. Experimental results showed that the interphase/interface region did not affect the degradation rates of the creep rupture strength of the J2 composites.

DMA creep tests were performed at elevated temperatures for J2 composites. A master curve of each composite was generated. The shift factors obeyed the Arrhenius type equation. The activation energies of composites were approximately the same. The creep response of the AU4/J2, AS4(2)/J2, and AS4CGP/J2 composites were not dependent upon the ISS.

Severe delaminations were observed in the AS4(1)/J2 composite laminates. The $([\pm 45/90_2]_s)$ laminate tensile strength of AS4(1)/J2 composite was less than that of AS4(2)/J2 and AS4CGP/J2 composite. The creep rupture strength of the AS4(1)/J2 composite laminates degraded about two times faster than that of the other three composite systems.

ACKNOWLEDGEMENTS

The author wishes to express his sincere appreciation to Professor D. A. Dillard for his advice and guidance during the entire endeavor of the author's graduate studies. The suggestions and criticisms from the committee members and Professor K. L. Reifsnider are also appreciated. Special thanks are due to the Virginia Institute for Material Systems for supporting this research. The author also gratefully acknowledges the help of Dr. S. Khan of E. I. DuPont de Nemours Co. in supplying the J2 prepregs for this study.

Many valuable suggestions from Dr. G. P. Carman, Dr. B. Tang, Mr. K. Jayaraman and Mr. J. J. Lesko are also appreciated. The author also thanks Mr. P. Commercon and Ms. J. Chin for their help in analyzing the surface properties of carbon fibers. Thanks are due to Mr. Danny Reed for his assistance in preparing specimens.

The author is deeply grateful to his father, parents-in-law, wife, and son for their constant and endless love, encouragement and patience during the course of this study.

Table of Contents

1. INTRODUCTION 1

REFERENCES 10

2. LITERATURE REVIEW 13

2.1 Characterization of the Interfacial Region: Surface Properties of Fibers 14
2.1.1 X-ray Photoelectron Spectroscopy (XPS) 15
2.1.2 Scanning Electron Microscopy (SEM) 18
2.1.3 Inverse Gas Chromatography (IGC) 18
2.1.4 Dynamic Contact Angle (DCA) Measurement 21
2.1.5 Summary 22

2.2 Characterization of the Interfacial Region: Mechanical Test Approaches on Composites 23
2.2.1 Micro-Mechanical Tests 24
2.2.2 Macro-Mechanical Tests 26
2.2.3 Dynamic Mechanical Analysis (DMA) 27
2.2.4 Summary 28

2.3 Effect of the Interphase on the Mechanical Properties of Polymeric Composites 29
2.3.1 Static Mechanical Properties 29
2.3.2 Fractogrphy Analysis by SEM 31
2.3.3 Interphase Effect on Creep and Creep Rupture ... 32
2.3.4 Summary 35

REFERENCES 36

3. EXPERIMENTAL 42

3.1 Materials 42
3.1.1 Characteristic of the Prepregs 44
3.1.2 Manufacturing of Composite Panels 45
3.1.3 Quality of Composite Panels 46
3.1.4 Dimensions and Stacking Sequence of Composites . 47
3.1.5 Thermal History of the Specimens 47

3.2 Test Procedures 50
3.2.1 Surface Properties of Fibers 50
3.2.2 DMA Tests 52
3.2.3 Meso-Indentation Tests 52
3.2.4 Mechanical Tests 52
3.2.5 Creep Tests 54
3.2.6 Creep Rupture Tests 55

3.3 Fiber Volume Fraction 56

3.4 SEM Fractography Analysis 56

REFERENCES 57

4. CHARACTERIZATION OF THE INTERPHASE 59

4.1 XPS Results 59

4.2 IGC Results 60

4.3 DCA Results 62

4.4 Characteristics of AS4CGP Fibers 63

4.5 Topology of Fiber Surfaces 67

4.6 Interfacial Shear Strength of J2 Composites 67

4.7 Summary 70

REFERENCES 71

5. MECHANICAL PROPERTIES OF J2 COMPOSITES 73

5.1 Characteristic of the Composites 73

5.2 Mechanical Properties of J2 Composites 74
5.2.1 $[0]_8$ Tensile Tests 74
5.2.2 $[90]_{12}$ Tensile Tests 85
5.2.3 $[\pm 45]_{2s}$ Tensile Tests 93
5.2.4 Iosipescu Tests 98
5.2.5 $[\pm 45/90_2]_s$ Tensile Tests 105

5.3 Summary 109

REFERENCES 109

6. CREEP AND CREEP RUPTURE OF J2 COMPOSITES 111

6.1 Dynamic Mechanical Properties of Composites ... 111

6.2 Creep and Creep Rupture of J2 Composites 117

6.3 Summary 126

REFERENCES 131

7. COMPARISON BETWEEN AS4(1)/J2 AND AS4(2)/J2 COMPOSITES 133

7.1 Surface Properties of AS4(1) and AS4(2) Fibers 133

7.2 DMA Results 134

7.3 Mechanical Properties of AS4(1)/J2 and AS4(2)/J2 Composites 135

7.4 Creep and Creep Rupture of AS4(1)/J2 AS4(2)/J2 Composites 138

7.5 Summary 145

REFERENCES 148

8. CONCLUSIONS AND RECOMMENDATIONS 149

8.1 Conclusions 149

8.2 Recommendations 151

REFERENCES 152

VITA 154

List of Illustrations

Figure 1-1: Creep rupture tests for AS4(1)/J2 composite laminates at 100°C, 120°C, and 140°C 5

Figure 1-2: Dynamic mechanical properties of AS4(1)/J2 $[90]_{12}$ lamina 7

Figure 1-3: Dynamic mechanical properties of T300/934 composite lamina ($[90]_{12}$) 8

Figure 3-1: Chemical structure of J2 resin 43

Figure 3-2: Voids in a AU4/J2 laminate ($[\pm 45/90_2]_s$) ... 48

Figure 4-1: The acid/base characteristic of the AS4CGP fiber 61

Figure 4-2: SEM photomicrograph for the AS4CGP fibers .. 65

Figure 4-3: DSC traces of the epoxy sizing 66

Figure 4-4: SEM photomicrograph for (a) AU4 fiber; (b) AS4(2) fiber; and (c) AS4CGP fiber 68

Figure 5-1: Broken fibers randomly distributed in the AU4/J2 composite panels 75

Figure 5-2: Fiber distribution in the cross section for (a) AU4/J2; (b) AS4(2)/J2; and (c) AS4CGP/J2 specimen 76

Figure 5-3: Stress-strain curves of $[0]_8$ tension tests for (a) AU4/J2; (b) AS4(2)/J2; and (c) AS4CGP/J2 composites 80

Figure 5-4: Photo of failed $[0]_8$ specimens 83

Figure 5-5: Stress-strain curves of $[90]_{12}$ tension tests for (a) AU4/J2; (b) AS4(2)/J2; and (c) AS4CGP/J2 composites 86

Figure 5-6: SEM photomicrographs of failed $[90]_{12}$ specimens for (a) AU4/J2; (b) AS4(2)/J2; and (c) AS4CGP/J2 composites 91

Figure 5-7: Shear stress-shear strain curves of [±45] tension tests for (a) AU4/J2; (b)

AS4(2)/J2; and (c) AS4CGP/J2 composites 94

Figure 5-8: Photo of failed $[\pm 45]_{2s}$ specimens 97

Figure 5-9: SEM photomicrographs of failed $[\pm 45]_{2s}$ specimens for (a) AU4/J2; (b) AS4(2)/J2; and (c) AS4CGP/J2 composites 99

Figure 5-10: Shear stress-shear strain curves of Iosipescu tests for (a) AU4/J2; (b) AS4(2)/J2; and (c) AS4CGP/J2 composites ... 101

Figure 5-11: SEM photomicrographs of failed Iosipescu specimens for (a) AU4/J2; (b) AS4(2)/J2; and (c) AS4CGP/J2 composites..... 106

Figure 5-12: Photos of failed $[\pm 45/90_2]_s$ specimens 108

Figure 6-1: Traces of log(E′) vs. tan(δ) for (a) $[0]_8$; (b) $[\pm 45]_{2s}$; and (c) $[90]_{12}$ specimens 114

Figure 6-2: Typical creep compliance curves at elevated temperatures for the AS4CGP/J2 ($[90]_{12}$) .. 119

Figure 6-3: Master curves of J2 composites ($[90]_{12}$) .. 120

Figure 6-4: Master curves of J2 composites ($[\pm 45]_{2s}$) . 121

Figure 6-5: Arrhenius plot for J2 composites 123

Figure 6-6: Creep rupture tests at 120°C for AU4/J2, AS4(2)/J2, and AS4CGP/J2 laminates 125

Figure 6-7: SEM photomicrographs of failed specimens with intermediate creep rupture life for (a) AU4/J2; (b) AS4(2)/J2; and (c) AS4CGP/J2 127

Figure 6-8: SEM photomicrographs of failed specimens with long creep rupture life for (a) AU4/J2 (b) AS4(2)/J2; and (c) AS4CGP/J2 ... 129

Figure 7-1: Traces of log(E′,E") vs. temperature for unannealed AS4(1)/J2 and annealed AS4(1)/J2 and AS4(2)/J2 specimens 136

Figure 7-2: Photo of failed AS4(1)/J2 specimens ($[\pm 45/90_2]_s$) 139

Figure 7-3: Master curves of AS4(1)/J2 and AS4(2)/J2 specimens ($[90]_{12}$) 140

Figure 7-4: A redrawn figure for creep rupture results of (a) Figure 1-1 and (b) Figure 6-6 142

Figure 7-5: Normalized creep rupture strengths of J2 composites 144

Figure 7-6: SEM photomicrographs of failed specimens with intermediate creep rupture life for (a) AS4(1)/J2 and (b) AS4(2)/J2 146

Figure 7-7: SEM photomicrographs of failed specimens with long creep rupture life for (a) AS4(1)/J2 and (b) AS4(2)/J2 composites 147

List of Tables

Table 2-1: XPS results of carbon fibers (reference) ... 16

Table 2-2: XPS results of carbon fibers (reference) ... 17

Table 2-3: IGC results of carbon fibers (reference) ... 20

Table 2-4: IGC results of carbon fibers (reference) ... 20

Table 2-5: Surface energies of carbon fibers (references) 22

Table 2-6: Interfacial shear strengths of composites (references) 25

Table 2-7: Mechanical properties of composites (references) 30

Table 2-8: Mechanical properties of composites (reference) 31

Table 3-1: Mechanical properties of carbon fibers and J2 polymer (references) 43

Table 3-2: Typical dimensions of the testing specimens. 49

Table 4-1: XPS results of carbon fibers 60

Table 4-2: Surface energies of carbon fibers and interfacial shear strength of composites ... 62

Table 5-1: Mechanical properties of J2 composites 78

Table 6-1: T_g and height of the tan(δ) peak 112

Table 7-1: XPS results of AS4(1) and AS4(2) fibers ... 134

Table 7-2: Mechanical properties of AS4(1)/J2 and AS4(2)/J2 137

Chapter 1

INTRODUCTION

The increasing use of polymeric composites as structural components is due partly to the high ratio of strength to weight, i.e., weight saving. Historically, advanced polymeric composites have been made from thermoset matrices, e.g., epoxies, polyesters, and polyimides. The nature of the crosslink structure in thermosetting polymers results in composites with low fracture toughness, which is of major concern to the aerospace industries [1-2]. On the other hand, chemical reaction that is taking place during the curing process to form the crosslink structure may result in good adhesion between the fiber and matrix. In general, good fiber-matrix adhesion yields good static mechanical properties of composites [3-4].

The adhesion of carbon fibers to thermosetting polymers has been investigated by several researchers recently [3-8]. Madhukar and Drzal [3-4] have reviewed a series of their research papers published in the past few years. They have investigated AU4, AS4, and AS4C carbon fibers in an epoxy to study the interfacial properties of single fiber composites. The AU4 fiber is a PAN based carbon fiber with no further conditioning. The AU4 fiber may be further processed with a

proprietary treatment, an electrolytic oxidation treatment, to yield the AS4 fiber. The AS4C fiber is produced from the AS4 fiber by the addition of a solvent deposited epoxy sizing.

Madhukar and Drzal [3] have found that the ratio of the interfacial shear strength (ISS) from single fiber fragmentation tests (SFFT) for AU4:AS4:AS4C fibers in epoxy was 1.0:1.7:2.2. In the same study, they have also shown that the ratio of in-plane shear strength, measured by ASTM D3518, for the AU4:AS4:AS4C composite lamina was 1.0:2.0:2.7. These results show that composite performance is significantly affected by the properties of the interphase region. Although, the mechanical properties of thermoset composites can be improved by altering the fiber surface properties, the fracture toughness of the thermoset composites is still low [1-2]. Thus, instead of using thermosetting polymers for advanced applications, thermoplastic polymers are being considered as alternate matrices.

Thermoplastic polymers that have high glass transition temperatures, high fracture toughness, and good damage tolerance and impact resistance, are found to be an alternative to replace thermosetting polymers [1-2]. Thermoplastic polymers do not undergo chemical reaction during the consolidation process, however. Due to this

characteristic, thermoplastic polymers do not form as strong a bond to carbon fibers as thermosetting polymers do. For thermoset composites, it has been found that weak fiber-matrix bonding results in poor short-term static mechanical properties [3]. Therefore, it is need to investigate the interfacial adhesion of carbon fibers to thermoplastic polymers and the consequential influence on the mechanical properties of the thermoplastic composites.

Viscoelastic behavior is a characteristic of all polymers and polymer matrix composites. It is generally believed that carbon fibers do not creep substantially under a long term loading; and the source for the viscoelastic behavior of polymeric composites is the polymer matrices. Several researchers [9-13] have investigated the creep and creep rupture behavior of the thermoset composites at elevated temperatures. Dillard [10-11] has observed that the creep rupture strength degraded less than 10% in four decades of time for most T300/934 composite laminates, at temperatures as high as 16°C below transition temperature, T_g. This reduction has also been shown to be reasonably independent of the stacking sequence of the tested laminates [11].

It has been reported that the viscoelastic behavior of thermoplastic composites will be no better or possibly worse than that of thermoset composites [1]. In addition,

previous creep rupture results revealed that the creep rupture strength of the thermoplastic composite laminates ($[\pm 45/90_2]_s$ of AS4(1)/J2) degraded about 19% within four decades of time period, as shown in Figure 1-1 [14]. This rate is substantially (~2x) faster than that observed for T300/934 laminates. Several possibilities were suggested to explain this discrepancy. First, the thermoplastic matrix lacks the crosslink structure present in thermosetting systems. Secondly, the testing temperatures used in the creep rupture studies of the two composite systems are different. Thirdly, the interphase properties of fiber/matrix in the thermoset and thermoplastic composites are different. And, finally, the thermoplastic composite may exhibit a greater degree of nonlinear behavior than does a thermoset composite.

It is generally accepted that the storage moduli, at temperatures well below T_g, are about the same for most polymers [15]. At temperatures beyond the T_g, the moduli of non-crosslinked polymers decrease several orders of magnitude whereas the moduli of crosslinked polymers remain constant [15]. For most applications of interest, the operation temperatures of structural composite components are below the T_g. Even over long periods of time, high performance composites remain in the glassy regime for most applications. Thus, the lack of a crosslink structure

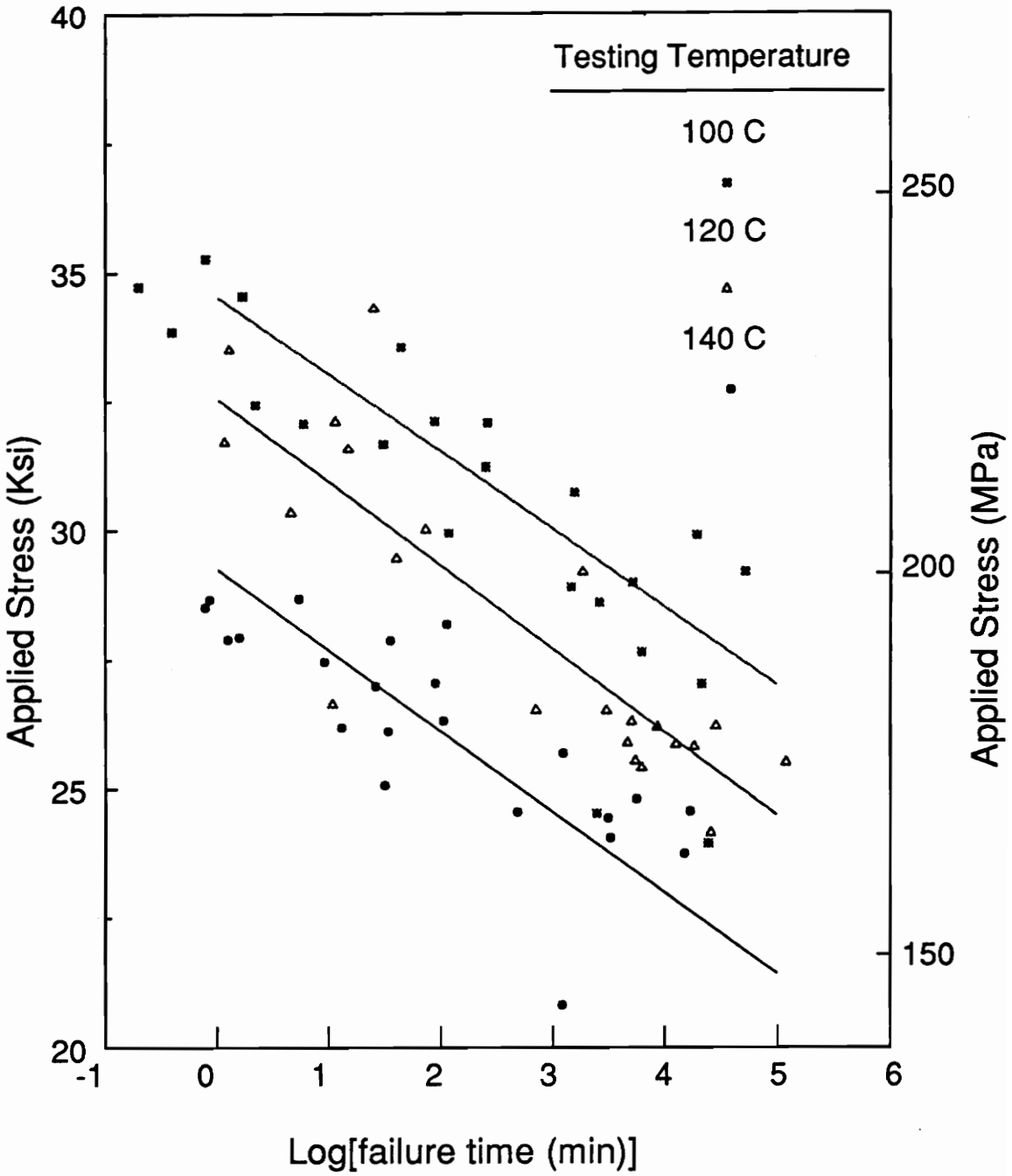

Figure 1-1: Creep rupture tests for AS4(1)/J2 composite laminates ([45/-45/90(2)]s) at 100 C, 120 C, and 140 C.

should not affect the short range molecular motion below T_g.

Creep rupture tests were performed at temperatures as high as 140°C for AS4(1)/J2 composites, as indicated in Figure 1-1 [14]. This temperature was approximately 27°C below the transition temperature of J2 composites, as shown in Figure 1-2. In addition, this temperature was well below the onset temperature of the transition region, as illustrated in Figure 1-2. Whereas T300/934 composites were tested at temperatures close to the onset temperature of the transition region, as shown in Figure 1-3. Thus, one would expect that T300/934 composites might degrade faster than AS4(1)/J2 composites. However, the preliminary creep rupture results of the AS4(1)/J2 composites showed a contradiction to the expectation. Hence, the second factor appears not to be a major concern.

With regards to the third factor, thermoplastic composites, in general, possess "poor" fiber/matrix interfacial strength as compared to thermoset composites. Bascom et al. [5] have employed single fiber fragmentation tests to measure the interfacial adhesion of AS4 fiber in a thermoset (DGEBA/m-PDA) and several thermoplastic (polysulfone, polycarbonate, polyetherimide, and polyphenylene oxide) resins. The results indicate greater adhesion was obtained in thermoset composites than in thermoplastic composites. This difference could affect

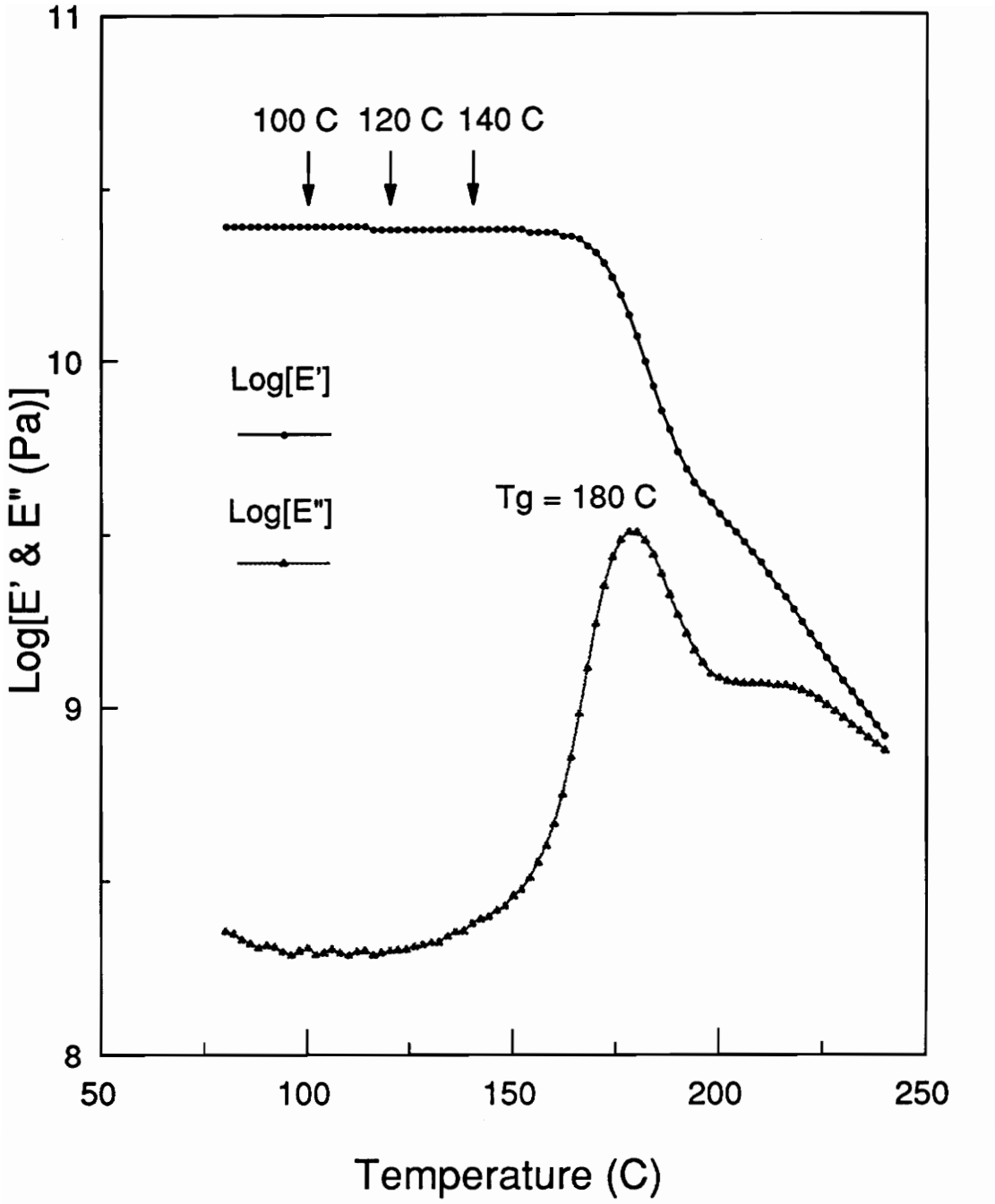

Figure 1-2: Dynamic mechanical properties of AS4(1)/J2 [90](12) lamina. Creep rupture tests for the AS4(1)/J2 composite laminates were conducted at 100 C, 120 C, and 140 C, which were well below the transition region.

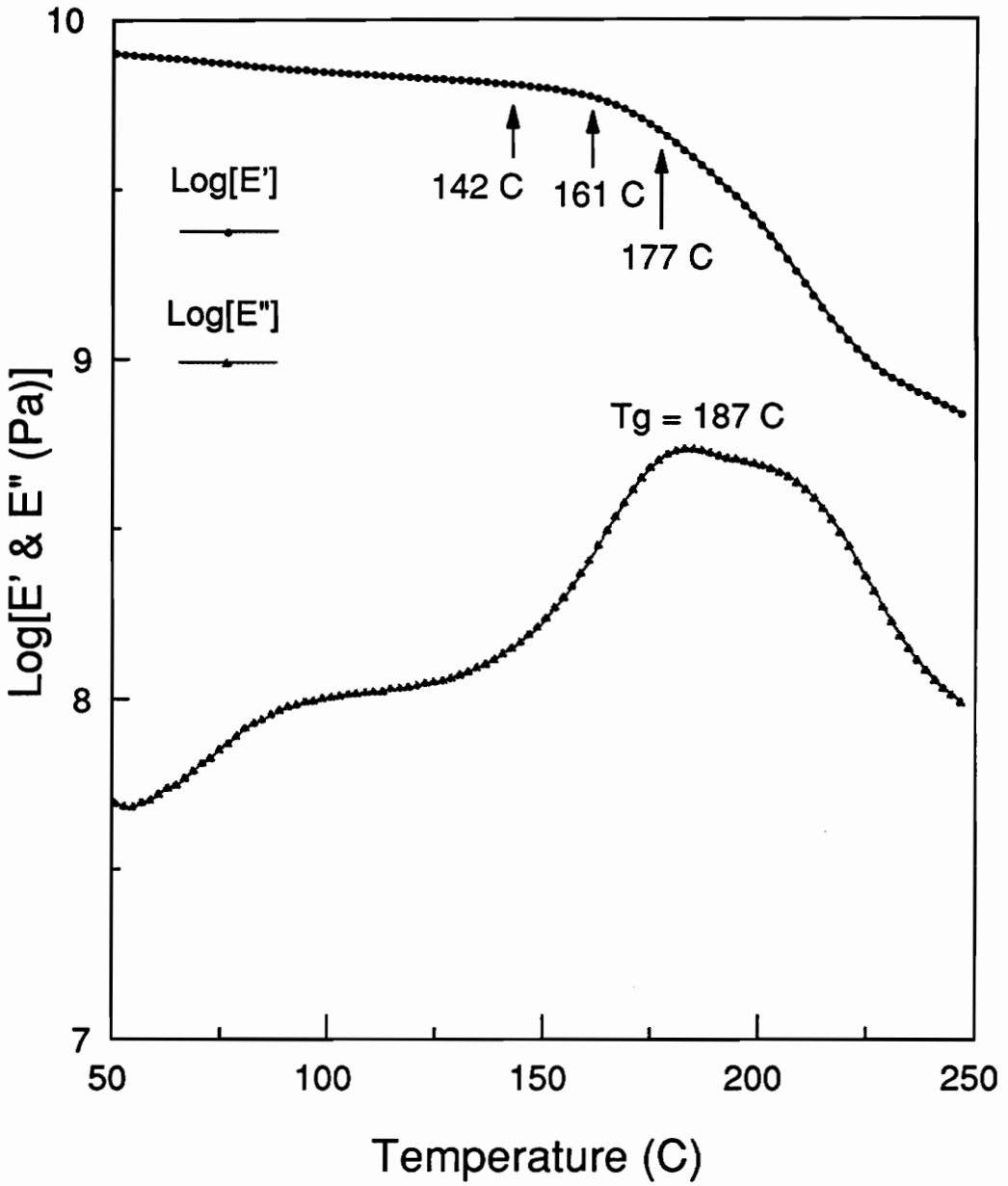

Figure 1-3: Dynamic mechanical properties of T300/934 [90](12) lamina. Creep rupture tests for the T300/934 composite laminates were conducted at 142 C, 161 C, and 177 C, which were close to the transition region.

creep rupture behavior.

As far as the fourth factor is concerned, Schapery [16] has indicated that viscoelastic behavior of polymeric composites is due to viscoelastic flow in the matrix as well as internal flaw formation and growth. At high stress levels, the viscoelastic behavior of the composite becomes severely nonlinear due to unrecoverable damage, (e.g., interfacial debonding, matrix cracking, and delamination). The formation of these damage modes may ultimately be related to the interphase/interface properties.

Thus, the two latter factors could be considered as a single effect, i.e., an interphase response. Consequently, we were led to consider the interphase effect in determining the degradation rate and creep rupture strength for these composites. We thus considered the following question. Would it be possible to enhance the resistance to creep by controlling the fiber-matrix bond quality? Thus, the main objective of the present research is to investigate the effects of the interphase/interface properties on the long term (creep and creep rupture) behavior of the polymeric composites at high temperatures.

In this dissertation, Chapter Two will detail a literature review. Experimental procedures for the present research are described in Chapter Three. The experimental results are discussed in Chapters Four through Seven. In

Chapter Four, the author presents and discusses the results regarding the surface properties of the carbon fibers and its consequential effect on fiber-matrix adhesion. The effect of the interfacial adhesion on the mechanical properties of the J2 composites is discussed in Chapter Five. Next, the effect of the interphase region on creep and creep rupture behavior of the J2 composites is discussed in Chapter Six. A comparison between two batches of J2 composites, AS4(1)/J2 and AS4(2)/J2, is presented in Chapter Seven. Finally, Chapter Eight presents the conclusions of the present research and recommendations for the future study.

REFERENCES

[1] National Materials Advisory Board, "The Place for Thermoplastics in Structural Components", National Research Council, USA, 1987.

[2] Leach, D. C., "Continuous Fiber Reinforced Thermoplastic Matrix Composites," in Advanced Composites, Ed. by Patridge, I. K., Elsevier Applied Science, 1989.

[3] Madhukar, M. S. and Drzal, L. T., "Fiber-Matrix Adhesion and Its Effect on Composite Mechanical Properties: I. Inplane and Interlaminar Shear Behavior of Graphite/Epoxy Composites", Journal of Composite Materials, Vol. 25, 1991, pp. 932-957.

[4] Madhukar, M. S. and Drzal, L. T., "Fiber-Matrix Adhesion and Its Effect on Composite Mechanical Properties: II. Longitudinal (0°) and Transverse (90°) Tensile and Flexure Behavior of Graphite/Epoxy

Composites", Journal of Composite Materials, Vol. 25, 1991, pp. 958-991.

[5] Bascom, W. D., Yon, K. J., Jensen, R. M., Cordner, L., "The Adhesion of Carbon Fibers to Thermoset and Thermoplastic Polymers," Journal of Adhesion, Vol. 34, 1991, pp. 79-98.

[6] Schultz, J., Lavielle, L., and Martin, C., "The Role of the Interface in Carbon Fiber-Epoxy Composites," Journal of Adhesion, Vol. 23, 1987, pp. 45-60.

[7] Norita, T., Matsui, J., and Matsuda, H. S., "Effect of Surface Treatment of Carbon Fiber on Mechanical Properties of CFRP", in Composite Interfaces, Ed. by, Ishida, H. and Koenig, J. L., Elsevier Science Publishing Co., 1986, pp. 123-132.

[8] Bolvari, A. E. and Ward, T. C., "Determination of Fiber-Matrix Adhesion and Acid-Base Interactions," in Inverse Gas Chromatography: Characterization of Polymers and Other Materials, Ed. Lloyd, D. R., Ward, T. C., and Schreiber, H. P., ACS Symposium Series 391, 1989.

[9] Brinson, H. F., Griffith, W. I., and Morris, D. H., "Creep Rupture of Polymer-Matrix Composites", Presented at the 4th SESA International Congress on Experimental Mechanics, Boston, 1980.

[10] Dillard, D. A., Morris, D. H., and Brinson, H. F., "Environmental Effects and Viscoelastic Behavior of Laminated Graphite/Epoxy Composites", Environmental Degradation of Engineering Materials, Virginia Polytechnic Institute and State University, September, 1981, pp. 445-53.

[11] Dillard, D. A., Ph.D. Dissertation., "Creep and Creep Rupture of Laminated Graphite/Epoxy Composites", Virginia Polytechnic Institute and State University, March, 1981.

[12] Tuttle, M. E. and Brinson, H. F., "Prediction of the Long-Term Creep Compliance of General Composite Laminates", Experimental Mechanics, Vol. 26, 1986, pp. 89-102.

[13] Lin, K. Y., and Hwang, I. H., "Analytical and Experimental Studies on Creep Behavior of Polymeric

Matrix Composites", Proceedings 17th Congress of the International Council of Aeronautical Sciences (ICAS), Stockholm, Sweden, September, 9-14, 1990.

[14] Chang, Y. S., Lesko, J. J., Reifsnider, K. L., and Dillard, D. A., "The Effect of the Interphase/Interface Region on Creep and Creep Rupture of Thermoplastic Composites," Presented at ASTM Symposium on High Temperature and Environmental Effect of Polymeric Composites, at San Diego, October 15-16, 1991.

[15] Aklonis, J. J. and MacKnight, W. J., Chapter 3, in Introduction to Polymer Viscoelasticity, 2nd Edition, John Wiley, NY, 1983.

[16] Schapery, R. A., "Stress Analysis of Viscoelastic Composite Materials", in Journal of Composite Materials, Vol. 1, pp.228, 1967.

Chapter 2

LITERATURE REVIEW

It has been found that the mechanical performance of composites is affected by the properties of the interfacial region in composites [1-3]. This interfacial region, i.e., interphase, may have different properties than the bulk matrix. For thermoset composites, the interphase may be formed in several ways;

- the formation of the interfacial region is due to the fiber/matrix interaction which results in immobilizing the molecular motion [4],
- the interfacial region is formed because of the preferential adsorption of one of the resin formulation components [5,6],
- the composition of the interfacial region varies from bulk matrix to fiber surface because the fiber surface coating may not dissolve in the bulk matrix completely [7,8].

For thermoplastic composites, Pangelinan et al. [9] have proposed that molecular chains of low molecular weight form an interphase next to the fiber surface because of an entropic driving force. A segregation between low and high molecular weight molecular chains is formed at the

interphase [9]. It is reasonable to assume that the entropic driving force is a mutual attraction between the fiber surface and low molecular weight chains. Therefore, fiber surface properties may affect the interfacial properties of thermoplastic composites.

These researchers [4-9] have proposed several possible mechanisms to form a interfacial region between the fiber and matrix. Thus, the properties of the interfacial region can be changed by altering fiber surface treatments and/or adding an additional sizing. Consequently, composites made from fibers with different surface treatments (and/or sizings) but in the same matrix will possess different interfacial properties and final mechanical performance.

2.1 Characterization of the Interfacial Region: Surface Properties of Fibers

Several techniques have been developed over the years to study surfaces and interfaces [10]. These surface analysis techniques reveal chemical properties and topology of material surfaces. The results of the surface analysis can then be used to understand the possible bonding mechanisms of the adherend with a primer and/or adhesive; and to analyze the possible failure modes, including cohesive, adhesive, and mixed modes. The adhesion of fibers to matrix may also be studied by using surface analysis

techniques for the same reason.

The X-ray Photoelectron Spectroscopy (XPS) technique is perhaps the most useful tool in analyzing surface chemistry and compositions of the adherend (or fiber). The Scanning Electron Microscopy (SEM) technique has been used to examine the topology of the adherend (or fiber) before the bonding process and after the failure of the joint. The Inverse Gas Chromatography (IGC) technique, based on the adsorptive theory, has been employed to determine the surface energies of the fiber and matrix. The Dynamic Contact Angle (DCA) method measures the dispersive and polar energies of materials, and thus can be employed to predict the degree of fiber-matrix interaction. The applications of these techniques will be discussed in the following sections.

2.1.1 X-ray Photoelectron Spectroscopy (XPS)

In adhesive bonding, the interaction of the adherend with the primer and/or adhesive is controlled by the chemical properties of the adherend surface [10]. The concept is also applied to fiber-matrix adhesion. The XPS technique that is used to analyze the chemical compositions of adherend surfaces has been employed to examine the fiber surface properties [11-14]. For carbon fibers without special chemical treatments, the XPS results reveal the compositions of nitrogen, oxygen, and carbon on the fiber

surfaces.

Bolvari and Ward [11] have used the XPS technique to investigate the properties of carbon fiber surfaces, including AU4 and AS4. Table 2-1 [11] lists the XPS results of the atomic percentages of the carbon fibers. For the purposes of the comparison, fiber critical lengths (measured by single fiber fragmentation test, SFFT) in thermoplastic polymers are also listed in Table 2-1. Kelly and Davis [15] have proposed that the fiber-matrix adhesion can be correlated to the fiber critical length of the fragmentation test. The shorter the fiber critical length, the better the interfacial adhesion. Bolvari and Ward's results have suggested that a higher percentage of oxygen and nitrogen compositions will yield better adhesion between the fiber and matrix. Thus, the XPS results provide a basic understanding of the interfacial adhesion of the fiber and matrix.

Table 2-1 XPS Results of Carbon Fibers (Ref. [11])

Fibers	Carbon (%)	Oxygen (%)	Nitrogen (%)	Fiber Critical* Length mm
AU4	89.5	8.5	2	0.59
AS4	79.7	14.5	5.8	0.44

* : fibers are in polysulfone; measured by SFFT.

Hodge et al. [12] have studied the surface chemistry of

carbon fibers (non-optimized, surface controlled, and additional surface treatment) and their influences on the interfacial adhesion in PEEK polymer. Their XPS results are summarized in Table 2-2 and show a similar trend to Bolvari and Ward's observations. Bascom et al. [13] have studied the interfacial adhesion for the AS1 and AS4 fibers to thermoplastic polymers including polyphenylene oxide, polycarbonate, polyetherimide, and polysulfone and have found the same trend as those of Refs. [11-12]. Yip and Lin [14] have investigated the interfacial adhesion of various carbon fiber systems to EPON-828/V-40. They have observed that the oxygen concentration increases from the untreated carbon fiber to the carbon fibers treated with various chemical reagents. The transverse tensile strengths of chemical treated carbon fiber composites are greater than those of the untreated carbon fiber composites.

Table 2-2 XPS Results of Carbon Fibers (Ref. [12])

Fibers	Carbon (%)	Oxygen (%)	Nitrogen (%)	W_a (mJ/m^2)*
Non-Optimized	95.5	2.2	2.1	71.9
Surface Controlled	88.5	7.3	4	86.6
Additional Surface Treatment	83.0	11.9	4.8	84.0

* : work of adhesion measured by contact angle measurement.

2.1.2 Scanning Electron Microscopy (SEM)

For mechanical interlocking, one of the four adhesion mechanisms [10], the morphology of the adherend governs the level of the bonding between the primer (and/or adhesive) and adherend. From a microscopic view point, a rough adherend yields stronger bond than a smooth adherend [10]. Thus the SEM technique used to examine the morphology of the adherend can be employed to study the topology of the fiber surfaces [13,14].

Yip and Lin [14] have employed the SEM technique to study the effect of surface roughness on fiber-matrix adhesion for various carbon fiber-EPON-828/V-40 systems. They have attributed the increase in adhesion to the increase in fiber surface roughness caused by treatment with chemical reagents. However, Bascom et al. [13] have observed that rough AS1 fibers yield a weaker adhesion than smooth AS4 fibers in several thermoplastic polymers. The reasons were given as follows: the surface treatment (1) cleaned the AS1 fiber surface and (2) stabilized the chemical compositions on the AS4 fiber surface.

2.1.3 Inverse Gas Chromatography (IGC)

It has been shown that the chemical compositions of the fiber surface affect the adhesion between the fiber and matrix. However, the XPS technique does not reveal the

bonding mechanisms between the fiber and matrix. According to Bolvari and Ward [11], the adhesion of the fiber to matrix can be best described by the adsorptive theory. The adsorptive theory predicts that the maximum adhesion is obtained when the adhesive comes into intimate contact with the substrate. Fowkes [16] has proposed that the work of adhesion is dominated by the non-dispersive (acid-base) and dispersive energies. Since the IGC technique is based on the adsorptive theory, it is appropriate to employ the IGC technique to further understand the bonding mechanisms between the fiber and matrix. Several researchers [11,13,17] have employed the IGC technique to characterize the dispersive and non-dispersive interactions for the fiber and matrix.

Schultz et al. [17] have applied the IGC technique to investigate the dispersive (γ^D_s) and non-dispersive interactions between carbon fibers (untreated, oxidized, and coated fibers) and epoxy (DGEBA-DDS). They have also conducted SFFT to measure the interfacial shear strength (ISS) of the corresponding composites. Table 2-3 [17] shows that γ^D_s of the untreated fiber is the highest; whereas the coated fiber has the lowest γ^D_s. On the other hand, the interfacial adhesion of the treated fibers is stronger than that of the untreated fibers, as shown in Table 2-3. Bolvari and Ward [11] have also observed that the γ^D_s of the

AU4 (untreated) fiber is greater than that of the AS4 (treated) fiber, as shown in Table 2-4. As suggested by Fowkes [16], Bolvari and Ward results [11] have suggested the non-dispersive interactions are key factors in determining the interfacial adhesion for the fiber to matrix.

Table 2-3 IGC Results of Carbon Fibers (Ref. [17])

Fibers	γ^D_s [mJ/m^2]	ISS (MPa)*
Untreated	50±4	101
Oxidized	49±2	113
Coated**	36±3	135

* : Fibers are in epoxy (DGEBA-DDS); measured by SFFT.
**: the oxidized fibers with a sizing.

Table 2-4 IGC Results of Carbon Fibers (Ref. [11])

Fibers	γ^D_s [mJ/m^2]	Fiber Critical* Length, mm
AU4	65.1	.59
AS4	47.5	.44

* : Fibers are in polysulfone; measured by SFFT.

Schultz et al. [17] have concluded that (a) the untreated fiber has an average acid character; (b) the oxidized fiber has a strong acid character; (c) the coated fiber has both strong acid and base character; (d) the epoxy

has both acid and base character. According to Refs. [18,19], the non-dispersive interactions are acid-base interactions. Thus, only an acid and a base can develop strong interactions. Furthermore, there will be no interaction between two materials that are both acids or both bases even though both materials may have high surface polarities. As a result, it is expected that the coated fiber yields the highest ISS; whereas the lowest ISS is for the untreated fiber.

2.1.4 Contact Angle Measurement

An alternative approach to determine the dispersive and polar energies of the fiber surface is the contact angle measurement [12,17]. Schultz et al. [17] have used the contact angle method to determine the dispersive (γ^D_s) and polar (γ^P_s) energies of untreated, oxidized, and coated fibers, as shown in Table 2-5. The results show that γ^P_s of the oxidized fiber increases twice as much as that of the untreated fiber. However, γ^D_s of the oxidized fiber is approximately the same with that of the untreated fiber. The additional sizing of the coated fiber reduces γ^D_s to the lowest; whereas the sizing does not improve the polar energy after the fiber has been oxidized (surface treated.) The contact angle measurements show good agreement with the ISS of the corresponding epoxy composites (DGEBA-DDS) [17].

Hodge et al. [12] have also measured γ^D_s and γ^P_s by contact angle measurements for non-optimized, surface treated, and additional sizing treated fibers, as shown in Table 2-5. A good correlation between the transverse tensile flexural strength of the PEEK composites and the γ^D_s and γ^P_s has been observed. Thus, Hodge's results are consistent with the Schultz's results [17].

Table 2-5 γ^D_s and γ^P_s of Carbon Fibers (Ref. [12,17])

Fibers	γ^D_s	γ^P_s	$\gamma^D_s + \gamma^P_s$	[MPa]
Untreated	50±8	7±3	57	101*
Oxidized	48±10	15±4	63	113*
Coated	34±6	13±3	47	135*
Non-Optimized	27.15	8.51	35.7	53.6**
Surface Controlled	26.1	22.3	48.4	152.5**
Additional Sizing	24	21.5	45.5	157.6**

* : Measured by SFFT in Ref [17].
**: Measured by transverse flexural tests in Ref [12].

2.1.5 Summary

These researchers [10-19] have suggested that the surface treatments promote the adhesion for the fiber to matrix. The purpose of the surface treatment is to remove the weak surface layer from carbon fibers and thus promote fiber-matrix adhesion [20]. The additional sizing shows little effect on the enhancement of the adhesion for the

surface treated fibers [12,14,17]. The increase of the surface roughness may enhance the mechanical interlocking between the fiber and matrix and thus yield a better adhesion. However, the inconsistent observations between Bascom et al. [13] and Yip and Lin [14] may be due to the following reasons. In Bascom's study [13], the AS4 fiber were obtained by a proprietary electrochemical surface treatment on the AS1 fiber. The treatment removed the weak surface layer from the AS1 fibers only and thus resulted in the smooth surface on the AS4 fibers. On the other hand, Yip and Lin [14] used chemical reagents including HNO_3, H_2O_2, and O_2 to treat carbon fibers. These chemical reagents not only removed the weak surface layer from carbon fiber but also etched the carbon fiber surfaces. Consequently, rough carbon surfaces were resulted. Hence, the roughness of the carbon surface may have improved the fiber-matrix adhesion in the Yip's study.

2.2 Characterization of the Interfacial Region: Mechanical Test Approaches on Composites

In the previous sections, it has been shown that the adhesion level of the fiber/matrix can be characterized through chemical analysis methods, i.e., XPS, IGC, and DCA techniques. However, these techniques do not reveal the strength of the interfacial region in composites. Thus it

is necessary to perform a mechanical test to measure the strength of the interfacial region. Several methods have been developed to measure the ISS of composites. For single fiber tests (micro-mechanical tests), there are the fiber pull out test [21-24], critical fiber length test [1,2,11,13,23], and micro-indentation test [25]. The short beam shear test [26,27,28], transverse tension test [27,28], transverse flexure test [27,28], and meso-indentation test [29] are employed for composite laminate samples (macro-mechanical tests). In addition to the micro-mechanical tests, the dynamic mechanical analysis (DMA) technique has been used to examine the interfacial effect on the viscoelastic behavior of composites [30-32]. However, the DMA technique does not measure the strength of composites.

2.2.1 Micro-Mechanical Tests

Jacques and Favre [23] have investigated the interfacial adhesion of untreated and surface treated high strength (HT) and T-300 carbon fibers in epoxy (DGEBA) composites. Both SFFT and pull-out tests have been performed to determine the ISS of the composites. They have observed that the ISS's of the surface treated HT composites are greater than those of untreated HT composites for both testing methods. Their results have confirmed the other published results [24] in that surface treated carbon fiber

composites have higher ISS than untreated carbon fiber composites, as shown in Table 2-6 [23,24,25]. However, the ISS's measured by SFFT is higher than those measured by pull-out tests. Mandell and Grande [25] have used both SFFT and micro-indentation tests to measure the ISS's of E-glass fibers in epoxy and polyester. Again, the ISS of the composite measured by the SFFT is different from that measured by micro-indentation test.

Table 2-6 Interfacial shear strength of composites

Fibers	SFFT ISS, MPa	Pull-out ISS, MPa	Micro-indentaion ISS, MPa
*Treated HT in DGEBA	44	65.5	
*Untreated HT in DGEBA	12.2	28	
*Treated T300 in DGEBA	46.3	58	
*Untreated T300 in DGEBA	30.5	55	
**Treated HT in epoxy		10	
**Untreated HT in epoxy		55	
***E-Glass in epoxy	79		56
***E-Glass in polyester	28		23

*: from Ref. [23]; **: from Ref. [24]; ***: from Ref. [25].

2.2.2 Macro-Mechanical Tests

Adams et al. [26] have conducted transverse flexural tests to measure the interfacial strength of three composite systems including AU4, AS4, AS4C (epoxy sized AS4) fibers in EPON-828/mPDA. For the purpose of comparison, Adams et al. have also carried out short-beam shear tests for the above composite systems. Their results have revealed that the transverse flexural strength ratio of AS4C/AU4 was ~2.8, and ~1.3 for AS4/AU4, which were in a good agreement with Drzal [27,28]. Adams et al. [26] have concluded that the transverse flexural tests are sensitive to the fiber surface treatments and sizing. Hodge et al. [12] have also performed the transverse flexural tests on non-optimized, surface controlled, and sized carbon fibers in PEEK. Hodge's results are also consistent with Adams et al. [26].

The meso-indentation technique, used to measure the ISS of the "composites", was developed here at Virginia Tech by the Materials Response Group [29]. By using the meso-indentation technique, Lesko et al. [29] have reported that the ISS of AU4, AS4, and AS4C fibers in Epon-828/mPDA were 71.4, ~103, and ~109 MPa, respectively, which are higher than those reported by Madhukar and Drzal [1,2]. (It is to be noted that the specimens, Lesko et al. [29] used for meso-indentation tests, were supplied by Drzal.) These high ISS values may be due to the large fiber volume fraction in

the tested regions [29].

2.2.3 Dynamic Mechanical Analysis (DMA)

Since polymer matrices are viscoelastic materials, it is reasonable to assume that the interfacial region of composites have time and temperature dependent properties. Thus, instead of using static tests, the interphase may be characterized by measuring the dynamic mechanical properties of composites in a desired temperature range.

Reed [30] has used a DuPont DMA-980 to study the dynamic mechanical properties of glass/epoxy composites. Reed [30] has shown that the composites with fiber direction between 0 and 30 degrees had an additional transition above T_g. Reed has proposed that the additional transition might be due to an interphase being formed between glass fibers and epoxy. Thomason [31] has employed a DuPont DMA-982 to investigate the interphase/interface of glass fiber/epoxy composites. He has shown similar results to Reed [30] in that an additional transition occurring above the T_g on the composites having fiber orientation between 0 and 30 degrees. Thomason [31] has claimed that the additional transition was an artifact which resulted from a complex interaction between design of the instrument, heating rate, thermal conductivity of sample, etc. On the other hand, he observed a minor transition occurring below the T_g and

assigned the minor transition to the interphase of the treated glass fiber/epoxy composite. For this particular composite specimen, Thomason [7] has also used Scanning Secondary Ion Mass Spectrometry (SSIMS) to identify the existence of the interphase. Ko et al. [32] have used a torsional dynamic mechanical analyzer to characterize the graphite fiber/epoxy composites. Their results have shown that treated graphite fiber/epoxy composites have a higher T_g. There is no additional transition shown in this study, however.

2.2.4 Summary

The results obtained from the micro- and macro-mechanical tests are sensitive to the surface treatments and/or sizing of carbon fibers, as discussed in the previous sections. However, the ISS of the SFFT, micro-indentation, and pull-out tests are inconsistent with each other. The advantages and disadvantages of using these methods has been discussed in detail in Refs. [33-37].

To date, the published results [31-32] show the influence of the interface region on the dynamic mechanical properties of composites. It is noticed that these researchers used thermoset composites for their study. For thermoplastic composites, it is generally known that the interfacial adhesion between the fiber and matrix is poor

[13]. Thus, a question is raised. How significant is the effect of fiber-matrix adhesion on the dynamic mechanical properties of thermoplastic composites?.

2.3 Effect of the Interphase on the Mechanical Properties of Polymeric Composites

It has been shown that the interphase properties affect the ISS of composites. Thus one would expect that the mechanical properties of composite lamina, for example, longitudinal tensile strength (modulus), transverse tensile strength (modulus), and shear strength (modulus), are influenced by altering the interphase properties [1,2]. In general, poor interfacial adhesion results in weak mechanical properties of the composite lamina [1,2], which has been verified through the interpretation of SEM photomicrographs of the fracture surfaces of the failed specimens. Clean fiber surfaces are observed in failed composite specimens that have poor adhesion between fibers and matrix, whereas matrix is observed adhering to fiber surfaces in composites having good interfacial adhesion between fibers and matrix [1,2].

2.3.1 Static Mechanical Properties

The effect of the interphase on the static mechanical properties of the composites has been investigated by

several researchers [1,2,38]. Refs. [1,2] provide a comprehensive review in the field of the influence of fiber-matrix adhesion on the mechanical properties of composites. Table 2-7 shows that the mechanical properties of the composites are enhanced with the improvement of the ISS in the composites. In the matrix dominated direction, the mechanical properties of both AS4 and AS4C composite systems are significantly affected by the ISS.

Table 2-7 Mechanical Properties of Composites (Ref [1,2])

Tests	AU4*	AS4*	AS4C*
0° Tension Strength, MPa Young's Modulus, GPa	 1403±107 130±8.7	 1890±143 138±4.7	 2044±256 150±8.6
90° Tension Strength, MPa Young's Modulus, GPa	 18±3.9 8.9±0.6	 34.2±6.2 9.8±0.6	 41.2±4.74 10.3±0.6
±45° In-plane** Shear Strength, MPa Shear Modulus, GPa	 37.2±1.8 9.1±1.5	 72.2±12.4 6.2±0.5	 97.5±7.4 6.0±0.2
ISS***, MPa	37.2	68.3	81.4

* : Carbon fibers in EPON-828/mPDA.
** : Measured by ASTM D3518.
***: Measured by SFFT.

Norita et al. [38] have investigated the interfacial adhesion of four different surface treated carbon fibers (untreated, 1/2, 1, and 2 times of the current production treatment level) in epoxy (Toray #3620). (Note that no sizing was applied to the surface treated carbon fibers in

their study.) The consequent effect on the mechanical properties of the corresponding composites have also been studied, as shown in Table 2-8. In addition, they have also investigated the mechanical properties of composite laminates. Their results have shown that the surface treatments promote interfacial adhesion and improved mechanical properties of composites from the untreated to treated carbon fibers. However, the interfacial adhesion and mechanical properties of composites are not enhanced further as the surface treatment time increases beyond 1/2.

Table 2-8 Mechanical Properties of Composites (Ref. [38])

	0*	1/2*	1*	2*
0° Tension Strength MPa Young's Modulus GPa	 1950 143	 1900 143	 1820 142	 1740 142
90° Tension Strength MPa Young's Modulus GPa	 28 9.5	 42 9.1	 50 9.1	 50 9.4
$[\pm 45]_s$ In-plane** Shear Strength MPa Shear Modulus GPa	 63 4.5	 136 4.5	 130 4.6	 126 4.5
$[0/\pm 45/90]_s$ Tension Strength MPa	 576	 574	 565	 544

* : level of surface treatment (times).
**: Measured by ASTM D3518.

2.3.2 Fractography Analysis By SEM

Madhukar and Drzal [1,2] have also shown SEM

photomicrographs of the fracture surfaces of failed specimens. Clean fiber surfaces have been observed for AU4/EPON-828/mPDA composites, which suggests poor adhesion in this composite system. On the other hand, matrix debris are present on the AS4 and AS4C fiber surfaces indicating good adhesion in these composite systems. The SEM results are consistent with the trend of the mechanical properties of the composites. The application of the SEM technique for the fractography and failure analysis of composites has been reviewed in detail by Bascom and Gweon [39].

2.3.3 Interphase Effect on Creep and Creep Rupture

To date, most efforts have been made to investigate the interfacial effect on the static mechanical properties of composite lamina. There are few published papers discussing the effect of the interphase/interface region on creep and creep rupture properties of polymeric composites. Thus, the following review was based on the recent published results in the field of the creep and creep rupture behavior of polymeric composites.

Yeow [40] has studied the creep response of the T300/934 composites at various temperatures. He has found that the fiber direction compliance (S_{11}) and fiber/transverse coupling compliance (S_{12}) were time independent. Dillard [41] has used the non-linear Findley

power law to represent the transverse (S_{22}) and shear (S_{66}) compliance of the T300/934 composites at 160°C. The numerical representations of the S_{22} and S_{66} were then incorporated into a computer program (VISLAP), based on lamination theory, to predict the creep compliance and rupture time of general laminates at 160°C. The prediction of the program agrees with the experimental results in matrix dominated laminates. However, for the fiber dominated laminates, the predictions and experimental data are inconsistent because lamination theory assumes no interlaminar deformations [41]. Gramoll [42] has examined the thermoviscoelastic behavior of Kevlar 49 in 7714A epoxy composites. Gramoll [42] has observed that both matrix and fiber exhibited viscoelastic behavior. A PC version of the VISLAP program, utilizing Prony series, has been developed to predict the viscoelastic response of composite laminates. The predictions of the program are in good agreement with four-week creep tests for unidirectional, multi-directional laminates. Lin and Hwang [43] have developed a finite element program to predict the creep strain of IM7/8551-7 laminates ($[90_2/\pm45/90/\pm45/90]_s$) at 121°C. The predictions have been verified with experimental results including strain gage measurements and Moire interferometry.

Chung et al. [44] have used a micro-mechanical model to predict the steady state creep of PEKK-based thermoplastic

composites at 121°C. The PEKK-based composites include continuous fiber and long discontinuous fiber systems. The creep model utilizes the matrix creep properties and assumes that creep strain in the fiber direction is negligible and that the fiber does not creep. Chung et al. [44] have found that the long discontinuous fiber system is more resistant to creep. Papanicolaou and Baxevanakis [45] have investigated the creep behavior of continuous carbon fiber reinforced polyamide composites. They have developed a computer program to described the creep response of the composites. To best describe the creep behavior of the investigated composites, this computer program utilized a repetitive procedure to find an appropriate combination of spring-dashpots elements. They have claimed that the experimental results and the theoretical prediction are in a good agreement.

Brinson et al. [46] have conducted creep rupture tests on T300/934 unidirectional lamina at various temperatures. They have found that the agreement between experimental results and creep rupture models were poor. They have also observed different viscoelastic behavior in various batches of composites. Dillard et al. [47] have also carried out the creep rupture tests at three different temperatures for T300/934 composite laminates. Dillard et al. [47] have employed a modified rate equation [48] to model the creep

rupture results with a good agreement.

2.3.4 Summary

The properties of the interphase do affect the final mechanical properties of composites, as discussed in the previous section. The interfacial adhesion level is not enhanced significantly when only the surface treatment is applied, regardless of using the various chemical reagents and surface treatment time [12,38]. However, the fiber-matrix adhesion can be further promoted by coating an additional sizing on the surface treated carbon fibers. This results in a moderate enhancement of mechanical properties of thermoset composites, as demonstrated in Refs. [1,2]. On the other hand, Hodge et al. [12] have shown minor improvement in the mechanical properties of sized carbon fibers reinforced PEEK composites.

A number of papers regarding the viscoelastic behavior of polymeric composites have been published during the last decade. (See Ref. [49] for a detailed review.) However, the influence of the interfacial adhesion on the creep behavior of composites has not been studied yet. Efforts are also needed to investigate how fiber-matrix adhesion affects the creep life of composites.

REFERENCES

[1] Madhukar, M. S. and Drzal, L. T., "Fiber-Matrix Adhesion and Its Effect on Composite Mechanical Properties: I. Inplane and Interlaminar Shear Behavior of Graphite/Epoxy Composites", Journal of Composite Materials, Vol. 25, 1991, pp. 932-957.

[2] Madhukar, M. S. and Drzal, L. T., "Fiber-Matrix Adhesion and Its Effect on Composite Mechanical Properties: II. Longitudinal (0°) and Transverse (90°) Tensile and Flexure Behavior of Graphite/Epoxy Composites", Journal of Composite Materials, Vol. 25, 1991, pp. 958-991.

[3] Fife, B, Peacock, J. A., and Barlow, C. Y., "The Role of Fiber-Matrix Adhesion in Continuous Carbon Fiber Reinforced Thermoplastic Composites: A Microstructural Study," in 6th International Conference for Composite Materials (ICCM-VI), Vol. 5, 1987, pp. 439-447.

[4] Ishida, H. and Koenig, J. L., "The Reinforcement Mechanism of Fiber-Glass-Reinforced Plastics Under Wet Conditions: A Review", Polymer Engineering and Science, V. 18, 1978, pp. 128-145.

[5] Lipatov, Y. S., Fabulyak, F. G., and Shifrin, V. V., "The Effect of Chemical Modification on the Surface of a Filler on the Behavior of a Polymer in Boundary Layers of Different Thickness", Polymer Science of U.S.S.R., V. 18, 1976, pp. 866-870.

[6] DiBenedetto, A. T. and Lex, P. J., "Evaluation of Surface Treatments for Glass Fibers in Composite Materials," Polymer Engineering and Science, Vol. 29, No. 8, 1989, pp. 543-555.

[7] Thomason, J. L., "Investigation of the Interphase in Glass-Fiber-Reinforced Epoxy Composites", Interfaces in Polymer, Ceramic, and Metal Matrix Composites, Ed. H. Ishida, Elsevier Science, New York, 1988, pp. 503-512.

[8] Hoh, K., Ishida, H., and Koenig, J. L., "The diffusion of Epoxy Resin into a Silane Coupling Agent Interphase," in Composite Interfaces, Ed. by Ishida, H. and Koenig, J. L., Elsevier Science, New York, 1986, pp. 251-263.

[9] Pangelinan, A. B., McCullough, R. L., and Kelly, M. J.,

"Polymer Molecular Weight Distributions Near Surfaces and Their Effects on Thermoplastic Composite Properties", Presented at the AIChE Annual Symposium, San Francisco, November 7, 1989.

[10] Davis, G. D., "Characterization of Surfaces," in Adhesive Bonding, Chapter 6, Ed. by Lee, L.-H., Plenum Press, 1991.

[11] Bolvari, A. E. and Ward, T. C., "Determination of Fiber-Matrix Adhesion and Acid-Base Interactions," in Inverse Gas Chromatography: Characterization of Polymers and Other Materials, Ed. Lloyd, D. R., Ward, T. C., and Schreiber, H. P., ACS Symposium Series 391, 1989.

[12] Hodge, D. J., Middlemiss, B. A., and Peacock, J. A., "Correlation Between Fiber Surface Energetics and Fiber-Matrix Adhesion in Carbon Fiber Reinforced PEEK Composites," in Materials Research Society Symposium Proceedings, Vol. 170, Ed. by Pantano, C. G. and Chen, E. J. H., pp. 327-338.

[13] Bascom, W. D., Yon, K. J., Jensen, R. M., Cordner, L., "The Adhesion of Carbon Fibers to Thermoset and Thermoplastic Polymers," Journal of Adhesion, Vol. 34, 1991, pp. 79-98.

[14] Yip, P. W. and Lin, S. S., "Effect on Surface Oxygen on Adhesion of Carbon Fiber Reinforced Composites," in Materials Research Society Symposium Proceedings, Vol. 170, Ed. by Pantano, C. G. and Chen, E. J. H., pp. 339-344.

[15] Kelly, A. and Davis, G. J., "The Principles of the Fiber Reinforcement of Metal," Metallurgical Review, Vol. 10(37), 1965, pp. 1.

[16] Fowkes, F. M., "Determination of Interfacial Tensions, Contact Angles, and Dispersion Forces in Surfaces by Assuming Additivity of Intermolecular Interactions in Surfaces," Journal of Physical Chemistry, Vol. 66, 1962, p. 382.

[17] Schultz, J., Lavielle, L., and Martin, C., "The Role of the Interface in Carbon Fiber-Epoxy Composites," Journal of Adhesion, Vol. 23, 1987, pp. 45-60.

[18] Schultz, J., Cazeneuve, C., Shanahan, M. E. R., Donnet,

J. B., "Fiber Surface Energy Characterization," Journal of Adhesion, Vol. 12, 1981, pp. 221-231.

[19] Gutmann, V., The Donor Acceptor Approach to Molecular Interactions, Plenum Press, 1978.

[20] Drzal, L. T., "Composite Interphase Characterization," in SAMPE Journal, Vol. 19(5), 1983, pp.7-13.

[21] Piggot, M. R., "Tailored Interphases in Fiber Reinforced Polymers," in Materials Research Society Symposium Proceedings, Vol. 170, Ed. by Pantano, C. G. and Chen, E. J. H., pp. 265-274.

[22] Penn, L. S., and Lee, S. M., "Interpretation of Experimental Results in the Single Pull-Out Filament Test", Journal of Composites Technology and Research, V. 11(1), Spring, 1989, pp. 23-30.

[23] Jacques, D. and Favre, J. P., "Determination of the Interfacial Shear Strength by Fiber Fragmentation in Resin Systems with a Small Rupture Strain," in 6th International Congress on Composite Materials, Vol. 5, London, 1987.

[24] Favre, J. R., "Characterization of Fiber/Resin Bonding in Composites Using Pull-Out Test," International Journal of Adhesion and Adhesives, October, 1981, pp. 311.

[25] Mandell, J. F., Grande, D. H., Tsiang, T. H., and McGarry, F. J., "A Modified Microdebonding Test for Direct in-situ Fiber/Matrix Bond Strength Determination in Fiber Composites", Composite Materials: Testing and Design, Seventh Conference, Philadelphia, April, 1984.

[26] Adams, D. F., King, T. R., and Blackketter, D. M., "Evaluation of the Transverse Flexure Test Method for Composite Materials", Composite Science and Technology, V. 39, 1990, pp. 341-353.

[27] Drzal, L. T., Rich, M. J., and Subramoney S., "The Interdependence Between Fiber-Matrix Adhesion and Composite Properties", Proceedings of the American Society for Composites, 3rd Technical Conference, 25-29, September, 1988, Seattle, Washington.

[28] Drzal, L. T., "Fiber-Matrix Interphase Structure and its Effect on Adhesion and Composite Mechanical

Properties", Controlled Interphases in Composite Materials, Ed. H. Ishida, Elsevier Science, New York, 1990.

[29] Lesko, J.J., Carman, G. P., Dillard, D. A., and Reifsnider, K. L., "Indentation Testing of Composite Materials as a Tool for Measuring Interfacial Quality," submitted for publication ASTM STP, March, 1991.

[30] Reed, K. E., "Dynamic Mechanical Analysis of Fiber Reinforced Composites", Polymer Composites, V. 1(1), 1980, pp. 44-49.

[31] Thomason, J. L., "Investigation of Composite Interphase Using Dynamic Mechanical Analysis: Artifacts and Reality", Polymer Composites, V. 11(2), 1990, pp. 105-113.

[32] Ko, Y. S., Forsman, W. C., and Dziemianowicz, T. S., "Carbon Fiber-Reinforced Composites:Effect of Fiber Surface on Polymer Properties", Polymer Engineering and Science, Vol. 22(13), 1982, pp. 805-814.

[33] Piggot, M. R., "The Interface - an Overview," in 36th International SAMPE Symposium, at San Diego, CA, April 15-18, 1991, pp. 1773-1786.

[34] Narkis, M., Chen, E. J. H., and Pipes, R. B., "Review of Methods for Characterization of Interfacial Fiber-Matrix Interactions," in Polymer Composites, Vol. 9(4), 1988, pp. 245-251.

[35] Verpoest, I., Desaeger, M., and Keunings, R., "Critical Review of Direct Micromechanical Test Methods for Interfacial Strength Measurements in Composites," in Controlled Interphases in Composite Materials, Ed. by Ishida, H., Elsevier Science, 1990, pp. 653-666.

[36] Jayaraman, K., Reifsnider, K. L., and Swain, R. E., "The Interphase in Unidirectional Fiber-Reinforced Composites I: A Review of Characterization Methods," Submitted to Journal of Composites Technology and Research (in review), 1991.

[37] Herrera-Franco, P. J. and Drzal, L. T., "Comparison of Methods for the Measurement of Fiber/Matrix Adhesion in Composites," Composites, Vol. 23, No. 1, 1992, pp. 2-27.

[38] Norita, T., Matsui, J., and Matsuda, H. S., "Effect of Surface Treatment of Carbon Fiber on Mechanical Properties of CFRP", in Composite Interfaces, Ed. by, Ishida, H. and Koenig, J. L., Elsevier Science Publishing Co., 1986, pp. 123-132.

[39] Bascom, W. D. and Gweon, S. Y., "Fractography and Failure Mechanisms of Carbon Fiber-Reinforced Composite Materials," Chapter 9, in Fractography and Failure Mechanisms of Polymers and Composites, Ed. by Roulin-Moloney, A. C., 1989, Elsvier Science.

[40] Yeow, Y. T., Ph.D. Dissertation, "The Time-Temperature Behavior of Graphite/Epoxy Laminates," Virginia Polytechnic Institute and State University, 1978.

[41] Dillard, D. A., Ph.D. Dissertation, "Creep and Creep Rupture of Laminated Graphite/Epoxy Composites," Virginia Polytechnic Institute and State University, March, 1981.

[42] Gramoll, K. C., Ph.D. Dissertation, "Thermo-viscoelastic Characterization of Viscoelastic Composite Materials," Virginia Polytechnic Institute and State University, March, 1988.

[43] Lin, K. Y., and Hwang, I. H., "Analytical and Experimental Studies on Creep Behavior of Polymeric Matrix Composites", Proceedings 17th Congress of the International Council of Aeronautical Sciences (ICAS), Stockholm, Sweden, September, 9-14, 1990, pp. 1938-1944.

[44] Chung, I, Sun, C. T., and Chang, I. Y., "Modeling of Steady State Creep in PEKK-Based Thermoplastic Composites," in Proceedings of the American Society for Composites: 6th Technical Conference, on October 7-9, 1991, at Albany, New York, pp. 234-255.

[45] Papanicolaou G. C. and Baxevanakis C, "Viscoelastic Modelling of Continuous Carbon Fiber Reinforced Thermoplastics'" Proceedings 17th Congress of the International Council of Aeronautical Sciences (ICAS), Stockholm, Sweden, September, 9-14, 1990, pp.1945-1950.

[46] Brinson, H. F., Griffith, W. I., and Morris, D. H., "Creep Rupture of Polymer-Matrix Composites", Presented at the 4th SESA International Congress on Experimental Mechanics, Boston, 1980.

[47] Dillard, D. A., Morris, D. H., and Brinson, H. F., "Environmental Effects and Viscoelastic Behavior of Laminated Graphite/Epoxy Composites", Environmental Degradation of Engineering Materials, Virginia Polytechnic Institute and State University, September, 1981, pp. 445-53.

[48] Slonimskii, G. L., Askadskii, A. A., and Kazantseva, V. V., "Mechanism of Rupture of Solid Polymers", Polymer Mechanics, V. 5, 1977, pp. 647-651.

[49] Hastie, R. L, Ph.D. Dissertation, "The Effect of Physical Aging on the Creep Response of a Thermoplastic Composite," Virginia Polytechnic Institute and State University, May, 1991.

Chapter 3

EXPERIMENTAL

3.1 Materials

Four composite systems have been used in this study: AS4(1), AU4, AS4(2), and AS4CGP fibers embedded in J2 resin. The number in the parentheses denotes the batch number; regardless of the batch number, the AU4 fiber is a PAN based carbon fiber with no further finishing, which causes fibers to be loose in a tow. The AS4 fiber is based on the AU4 fiber and has a proprietary surface treatment - electrolytic oxidation. The AS4CGP fiber is obtained by coating the AS4 fiber with a water based epoxy sizing (~0.4% w.t.). The surface appearance of both AS4(2) and AS4CGP fibers are shiny; and both fibers are not loose when compared to the AU4 fiber. J2 resin, manufactured by DuPont Co., is an amorphous polyamide copolymer with a chemical structure shown in Figure 3-1.

Table 3-1 is the list of the mechanical properties of carbon fibers (obtained from supplier's data sheet [1]) and J2 resin (from Ref. [2]). The mechanical properties of AS4(1) fiber are not listed in Table 3-1 because the fiber was not purchased by the author. DuPont Co. purchased AS4(1) fibers and made AS4(1)/J2 prepreg (Lot# TT1164-3368)

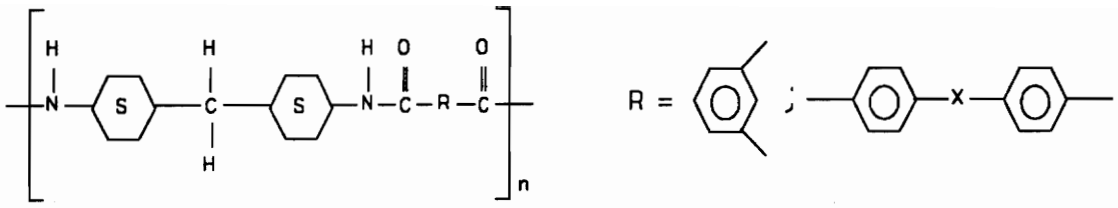

Figure 3-1: Chemical structure of J2 resin.

which was received in October, 1989. AU4, AS4(2), and AS4CGP fibers were purchased by VPI in December, 1990 and sent to DuPont for prepregging. AU4/J2 (Lot# TT1206-4070), AS4(2)/J2 (Lot# TT1205-4069), and AS4CGP/J2 (Lot# TT1207-4071) prepregs were also made by DuPont and received in April 1991. The prepregs were stored in sealed plastic bags to reduce moisture uptake.

Table 3-1 Mechanical Properties of Carbon Fibers and J2

Materials	Young's Modulus (GPa)	Tensile Strength (GPa)	Strain to Failure (%)	Density (Kg/m^3)
AU4	234.4	3.61	1.56	1770
AS4(2)	241.3	3.76	1.57	1780
AS4CGP	262.0	4.10	1.62	1770
J2	3.2	0.10	25.0	1150

3.1.1 Characteristic of the Prepregs

The prepregs were in film stacking form. The fibers, except those next to the films, had little contact with the J2 resins for all prepregs. For the AS4(1)/J2 prepreg, bare fibers were seen in several small regions on both sides. The author had tried to avoid using the prepreg containing these bare-fiber regions. Unfortunately, these regions were spread out on both sides, and hence the author had to use the prepregs containing minimum amount of bare-fiber regions to make composite panels. It was noticed that the resin was not uniform in the AU4/J2 prepreg. However, the cause of this non-uniformity was not clear. Also, there were many broken fibers in the films of the AU4/J2 prepreg. One possible reason was given here. Since the AU4 fiber was hard to handle, it was possible that AU4 fibers were damaged in the process of making the AU4/J2 prepregs. In the AS4CGP/J2 prepreg, there were gaps between fibers in some regions. The AS4(2)/J2 prepregs had an overall good quality.

Unlike fiber impregnated prepregs, the stacking film prepregs caused the fibers to be loose when cut; and the fibers were easily pulled away from the film. This was especially the cases in AS4(1)/J2 and AU4/J2 prepregs. In summary, due to the nature of the high viscosity of thermoplastic polymers, it is initially difficult to wet the

entire fiber bundle. However, full infusion of J2 resin will take place during consolidation [3].

3.1.2 Manufacturing of Composite Panels

Composite panels were manufactured in the Fabrication Laboratory of the Center for Composite Materials and Structures (CCMS) at VPI from the supplied prepregs. The consolidation procedures of the J2 prepregs were provided by the DuPont Co. Sections were cut from the prepregs and stacked in a mold with the desired orientations. The mold was placed in a vacuum oven at 100°C for 16 hours to ensure the prepregs were dry prior to the consolidation procedure. A Tetrahedron hot press (capacity: 1000 Kg) was used to consolidate the panel(s). The hot press was preheated to 295°C before placing the mold with the prepregs in the hot press. A contact pressure, less than 35 KPa, was introduced until the mold reached a temperature of 285°C. The pressure was increased gradually to 170 KPa within 10 min. In the meantime, the hot press temperature was raised to 295°C at a rate of 1 °C/min. The pressure was then increased to 2 MPa and maintained for 20 minutes at 295°C. The hot press was then cooled to room temperature with the assistance of forced air within 2 hours.

A 203 mm by 203 mm mold was initially made to manufacture composite panels. However, cavities were

detected in the central part of the panels. Efforts had been made to avoid yielding the cavities when performing the first consolidation procedures. For instance, the author had extended the dwell time from 20 min. to 30 min. at 295°C. However, this approach did not produce a good quality panel. Thus, these panels were then taken through an additional consolidation process to improve their quality. The causes for the cavities in these panels were not clear. Because of this time consuming process in making good panels, the author decided to use a 152 mm by 152 mm mold to make most composite panels. Only two panels (203 mm by 203 mm) of each composite system with good quality were made for tensile longitudinal tests ($[0]_8$). Later, the author was successful in making two panels per press by placing a 152 mm by 152 mm steel plate between the panels. This method saved time and cost in fabricating composite panels. By using this method, most panels, except some AU4/J2 panels, were made with good quality.

3.1.3 Quality of Composite Panels

The composite panels were inspected by using the ultrasonic C-scan technique. Few composite panels were found to have defects with the predominant number being AU4/J2 and AS(1)/J2 composites. These composite panels were re-consolidated to remove these defects. However, some

defects were not detected by the the C-scan. For example, Figure 3-2 reveals voids in a failed AU4/J2 laminate $[\pm 45/90_2]_s$.

3.1.4 Dimensions and Stacking Sequence of Composites

In this study, ASTM testing methods were used to characterize mechanical properties of composites. Thus specimens were cut with desired dimensions to meet ASTM requirements. The dimensions of specimens are listed in Table 3-2. The dimensions of specimens used for Dynamic Mechanical Analysis (DuPont DMA-983) are also listed in Table 3-2. It should be noted that there was no specific size for the DMA specimens.

3.1.5 Thermal History of the Specimens

Specimens cut from composite panels were polished and dried in a vacuum oven at 100°C for 16 hours. After the drying process, the AS4(1)/J2 specimens were stored in a desiccator prior to conducting tests. For static mechanical tests, the AS4(1)/J2 specimens were tested as-fabricated. For the short term creep and DMA tests, both thermal treated and as-made AS4(1)/J2 specimens were tested. It should be noted that the author did not consider different thermal history of the AS4(1)/J2 specimens might be a significant factor when the preliminary investigation was performed.

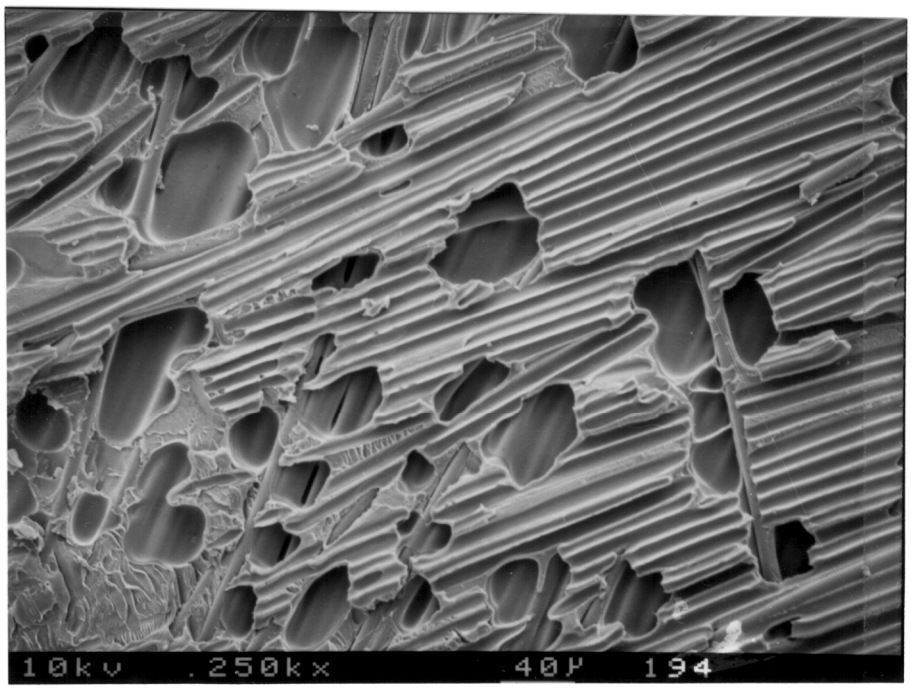

Figure 3-2: Micro-voids in the AU4/J2 composite laminate ($[\pm 45/90_2]_s$).

Table 3-2 Typical dimensions of the testing specimens.

ASTM Test Method	Length (mm)	Width (mm)	Thickness (mm)
ASTM D3039 Longitudinal Tensile Tests $[0]_8$	202	12.5	1
ASTM D3039 Transverse Tensile Tests $[90]_{12}$	152	25.4	1.5
ASTM D3518 Inplane Shear Tensile Test [±45]	152	25.4	1
Iosipescu Tests* $[90]_{20}$	50	19	2.5
Creep Rupture Tests $[\pm 45/90_2]_s$	152	25.4	1
Dynamic Mechanical Analysis Tests	40	10	1 - 1.5

* : A modified test procedure is described in detail in Ref. [4].

The three other composite specimens, AU4/J2, AS4(2)/J2, and AS4CGP/J2, were annealed at 175°C for 48 hours and then cooled to room temperature at a cooling rate of 0.1 °C/min. This thermal treatment was to ensure the specimens had the same thermal history. The annealed specimens were stored in the desiccator prior to performing tests. For the creep, creep rupture, and static tests, only annealed specimens were used. For the short term creep (DMA creep mode) and DMA tests, both annealed and unannealed specimens were used.

3.2 Test Procedures

3.2.1 Surface Properties of Fibers

The chemical compositions of carbon fiber surfaces were determined by using a Perkin-Elmer X-ray Photoelectron Spectroscope (XPS). For AU4, AS4(2), and AS4CGP systems, fibers were obtained from both spools and prepregs. However, AS4(1) fibers were obtained from the AS4(1)/J2 prepreg only because the author did not have a spool of the AS4(1) fiber. The fibers were packed in a sample holder and stored in a desiccator at room temperature prior to performing XPS tests.

A Hewlett-Packard Gas Chromatography (Model 5890) equipped with a flame ionization detector was used to characterize the non-dispersive and dispersive components of surface energy for the carbon fibers. A prior study [5,6] had obtained IGC results for AU4 and AS4 fibers. Thus, for the IGC tests, only the AS4CGP fiber was characterized in this study. The AS4CGP fibers, twenty-two 1 m long tows, were packed in a 1 m stainless steel column (internal diameter 4.4 mm). Helium was used as the carrier gas and methane as the non-interacting marker. The flow rate was 13.5 ml/min and the injector temperature was 40°C. The column was conditioned at 100°C overnight. Wilkinson [7] described the step-by-step operation procedures in his

dissertation, which was used as a guide for the present study.

The surface energies of the carbon fibers were also determined by the Dynamic Contact Angle (DCA) method. By attaching the fiber to an electrobalance, the force, F, was measured and recorded during immersion and emersion cycles in a liquid. The force changed due to the menisci of the liquid raised or lowered at the interfaces. The force was then used to calculate the surface energies of the carbon fibers. The detailed theory and experimental procedures were reported in Refs. [8,9].

Surface topology of each fiber system was also examined by using a scanning electron microscopy (SEM). Fibers used for the SEM topology study were obtained from both prepregs and spools. Several short sections of AS4CGP fibers were placed in a oven at 100°C for 16 hours; the temperature was then raised up to 295°C and maintained for 20 min. This procedure was intended to simulate the heating process of consolidation cycles. The surface of the thermal treated AS4CGP fibers were then examined by SEM.

The DuPont DSC-910 was used to characterize the T_g of the epoxy sizing of the AS4CGP fiber. The AS4CGP fibers were chopped and packed in an unpressured sample pan. The unsealed pan was placed in a vacuum oven and treated with the same thermal cycle described in the previous paragraph.

The unsealed pan was removed from the oven and quickly sealed.

3.2.2 DMA Tests

The temperature dependent properties of J2 composites, including $[0]_8$, $[10]_8$, $[\pm45]_{2s}$, $[90]_{12}$, and $[\pm45/90_2]_s$, were measured by DMA-983. Temperature was scanned from 80°C to 200°C at a heating rate of 2 °C/min, as suggested by Thomason [10]. The frequencies used for the DMA tests were 0.32, 1, and 3.2 Hz.

3.2.3 Meso-Indentaton Tests

The interfacial shear strengths of J2 composites were determined using the meso-indentation tests. Short sections were cut from lamina ($[0]_{12}$) with right angle edges so that the indentor was pushed parallel to the fiber direction. The sections were placed in a specimen holder and then polished using the Buehler polishing machine. A very fine surface was necessary for the indentation tests. The experimental set-up and data interpretation for this test method were described elsewhere [11,12].

3.2.4 Mechanical Tests

ASTM D3039 and D3518 were followed to determine the mechanical properties of composites including longitudinal

tensile strength (modulus), transverse tensile strength (modulus), and inplane shear strength (modulus). Strain in the specimens was measured by resistance strain gages, which were purchased from Measurement Group Co. Two elements (90° 'tee' rosette) strain gages (CEA-06-125UT-350) were used to measure both longitudinal and transverse strains for both longitudinal and inplane tensile tests. Uniaxial strain gages (CEA-06-250UN-350) were used for the transverse tensile tests.

Strain gages were bonded on both sides of the specimens. An M-bond 610 adhesive was used to bond the strain gages on the specimens. The curing cycle of the M-bond 610 adhesive is described in detail in Ref [13]. The specimens bonded with strain gages were placed in a programmable oven (Fisher Scientific Isotemp-838F) to cure the adhesive. A heating rate of 2 °C/min was used to raise oven temperature to 150°C. This temperature was maintained for 4 hours and then cooled to room temperature. Post cure, at 160°C for 2 hours, was also performed for the adhesive as recommended in Ref [13].

A Vishay-2110, a signal conditioner and amplifier system, was used to generate conditioned output voltages from strain gages. The signals from the Vishay-2110 were collected by an IBM-XT equipped with a data acquisition board (Data Translation). Static tests were conducted using

an MTS 445 servohydraulic testing machine (capacity: 20 Kip). The cross-head speed was set at 1 mm/min for all the static tests.

The Iosipescu tests were performed using a modified Wyoming testing fixture. The Iosipescu tests also measured the shear modulus and interlaminar shear strength of composite laminae. Strain gages (EA-13-062TV-350) were used on the Iosipescu specimens. A Universal screw driven machine was employed for the tests. The cross-head speed was 1 mm/min. The testing and data reduction procedures are described in detail in Ref [4].

3.2.5 Creep Tests

A duPont DMA-983 is also capable of performing creep and recovery tests at a variety of temperature ranges. The advantages of using a DMA-983 for creep and recovery tests were: a) a very small strain was generated, which ensured the creep tests were in the linear range; b) because of DMA-983 being fully programmable, it saved time when performing creep and recovery tests at elevated temperatures.

Thus, a DMA-983 was also used to conduct short term creep and recovery tests at elevated temperatures, from 110°C to 160°C, for annealed and unannealed J2 composite lamina ($[90]_{12}$ and $[\pm 45]_{2s}$). The initial temperature interval was 15°C when temperature was below 140°C. Later,

the interval was then changed to 5°C when temperature was 140°C. A cycle, 10-minute creep and 40-minute recovery tests, was performed at each temperature. Several creep compliance curves were then generated after the creep and recovery tests. The time-temperature superposition principle (TTSP), described in detailed in Ref. [14], was used to shift creep compliance curves with respect to a reference curve. Shift factors were then obtained and plotted as a function of inverse temperature. The activation energies of J2 composites were determined based on an Arrhenius equation.

3.2.6 Creep Rupture Tests

Creep rupture tests were conducted for AS4(1)/J2 composite laminates ($[\pm 45/90_2]_s$) at 100°C, 120°C, and 140°C. (Note that the specimens were not annealed.) However, creep rupture tests at 120°C were conducted for annealed AU4/J2, AS4(2)/J2, and AS4CGP/J2 composite laminates ($[\pm 45/90_2]_s$). All creep rupture tests were performed in lever arm machines equipped with ovens. Specimens were placed in the ovens for an hour to ensure the equilibrium temperatures were reached prior to applying loads to the specimens. A timer was placed below the lever arm so that the timer was switched off when the specimen failed in order to record the failure time.

3.3 Fiber Volume Fraction

Fiber volume fractions of the composites were determined according to ASTM D3171. A short section, approximately 30 mm x 8 mm, was cut from each representative lamina (laminates). The volume (V_c) and weight (W_c) of each section were measured before dissolving the section in a flask filled with 1-Methyl-2-Pyrrolidinone (200 ml). The flask was heated until polymer dissolved in the solvent. The solution became brown and fibers floated to the solution. The solution was filtered and the fibers were washed with acetone. This process was continued until clean acetone was observed. The fibers with filter paper were then placed in a vacuum oven at 100°C for 10 hours and weighed the fibers (W_f). With the known fiber density (d_f) (Table 3-1), the fiber volume fraction was determined by the following equation:

$$V_f = \left(\frac{W_f}{d_f}\right) / \left(\frac{W_c}{d_c}\right) \qquad (3.1)$$

3.4 SEM Fractography Analysis

A scanning electron microscopy (SEM) was employed to examine the fracture surfaces of failed specimens including creep rupture and static tests. A small composite section

was carefully cut to avoid any contamination of the fracture surfaces. The section was then coated with gold by a sputtering process and was ready to be investigated. A Perkin-Elmer SEM was used for this investigation.

REFERENCES

[1] Hercules Co., Material Data Sheet.

[2] DuPont Co., Preliminary Data Sheet for "J2 Polymer Thermoplastic Resin Impregnated Tapes and Fabrics", E-89563-1.

[3] Leach, D. C., "Continuous Fiber Reinforced Thermoplastic Matrix Composites," in Advanced Composites, Ed. by Patridge, I. K., Elsevier Applied Science, 1989.

[4] Budiman, H. T, Masters Thesis, "An Assessment of Subscale Notched Specimens for Composites Shear Property Measurement," Virginia Polytechnic Institute and State University, December, 1991.

[5] Wilkinson, S. P., Ph.D. Dissertation, "Toughened Bismaleimides: Their Carbon Fiber Composites and Interphase Evaluation," Virginia Polytechnic Institute and State University, December, 1991.

[6] Schultz, J., Lavielle, L., and Martin, C., "The Role of the Interface in Carbon Fiber-Epoxy Composites," Journal of Adhesion, Vol. 23, 1987, pp. 45-60.

[7] Bolvari, A. E. and Ward, T. C., "Determination of Fiber-Matrix Adhesion and Acid-Base Interactions," in Inverse Gas Chromatography: Characterization of Polymers and Other Materials, Ed. Lloyd, D. R., Ward, T. C., and Schreiber, H. P., ACS Symposium Series 391, 1989.

[8] Schultz, J., Cazeneuve, C., Shanahan, M. E. R., and Donnet, J. B., "Fiber Surface Energy Characterization," Journal of Adhesion, Vol. 12, 1981, pp. 221-231.

[9] Commercon, P. and Wightman, J. P., "Surface Characterization of Plasma Treated Carbon Fibers and Adhesion to a Thermoplastic Polymer," Submitted to Journal of Adhesion, April, 1992.

[10] Thomason, J. L. and Morsink, J. B. W., "Investigation of the Interphase in Glass-Fiber-Reinforced Epoxy Composites", in Interfaces in Polymer, Ceramic, and Metal Matrix Composites, Ed. by Ishida, H., Elsevier Science Publishing Co., 1988, pp. 503-512.

[11] Lesko, J.J., Carman, G. P., Dillard, D. A., and Reifsnider, K. L., "Indentation Testing of Composite Materials as a Tool for Measuring Interfacial Quality," submitted for publication ASTM STP, March, 1991.

[12] Carman, G. P., Lesko, J. J., Reifsnider, K. L., and Dillard, D. A., "Micromechanical Model of Composite Materials Subjected to Ball Indentation," Submitted to Journal of Composite Materials, October, 1991.

[13] Micro-measurement Division, Measurement Group, Inc., Strain Gage Installation Bulletin B-130-11.

[14] Aklonis, John J. and MacKnight, William J., Chapter 3, in Introduction to Polymer Viscoelasticity, Second Edition, John Wiley, New York, 1983.

Chapter 4

CHARACTERIZATION OF THE INTERPHASE

This chapter discusses the results of the XPS, IGC, DCA, and meso-indentation tests and the relationships between each other. The XPS results reveal atomic percentages on the surface of the AU4, AS4(2), and AS4CGP fibers. Both IGC and DCA results suggest good adhesion is expected for the AS4(2) and AS4CGP fibers. The interfacial shear strengths (determined by meso-indentation tests) are consistent with the IGC and DCA results.

4.1 XPS Results

The XPS results are shown in Table 4-1. The atomic percentages of the AU4 and AS4(2) fibers are consistent with reported values [1]. The compositions of oxygen and nitrogen for both AS4(2) and AS4CGP fibers are greater than those of the AU4 fiber. The increase of the oxygen composition of the AS4 and AS4CGP fibers is due to the surface treatment imparting active groups (e.g., -C=O) on carbon fiber surfaces [2]. It has been shown that higher concentrations of nitrogen and oxygen on carbon fiber surfaces correlate with better adhesion between the fiber and matrix [3]. Thus, one would expect better adhesion in

the AS4(2)/J2 and AS4CGP/J2 composites than in the AU4/J2 composites, as will be demonstrated later.

Table 4-1 XPS Results of Carbon Fibers

Fiber	Carbon	Oxygen	Nitrogen
AU4	95.6%	2.7%	1.7%
AS4(2)	85.9%	11.6%	2.5%
AS4CGP	83.3%	16.1%	0.6%

4.2 IGC Results

The IGC results of AS4CGP fiber are shown in Figure 4-1. The dispersive component of the surface energy (γ_s^D) of AS4CGP fibers was obtained according to Ref. [1,4], and found to have a value of 26.1 mJ/m^2. Bolvari and Ward [1] have found that the values of γ_s^D for the AU4* and AS4* fiber were 65.1 and 47.5 mJ/m^2, respectively. (Note "*" represents these carbon fibers were used by Bolvari and Ward.) They have attributed the low γ_s^D of the AS4* fiber to the surface treatment resulting in increasing the polarity of the AS4* fiber. They have also observed that the AS4* fiber has better adhesion to thermoplastic polymers than the AU4* fiber does. Therefore, an even lower γ_s^D of the AS4CGP fiber is expected to result in good adhesion to thermoplastic polymers.

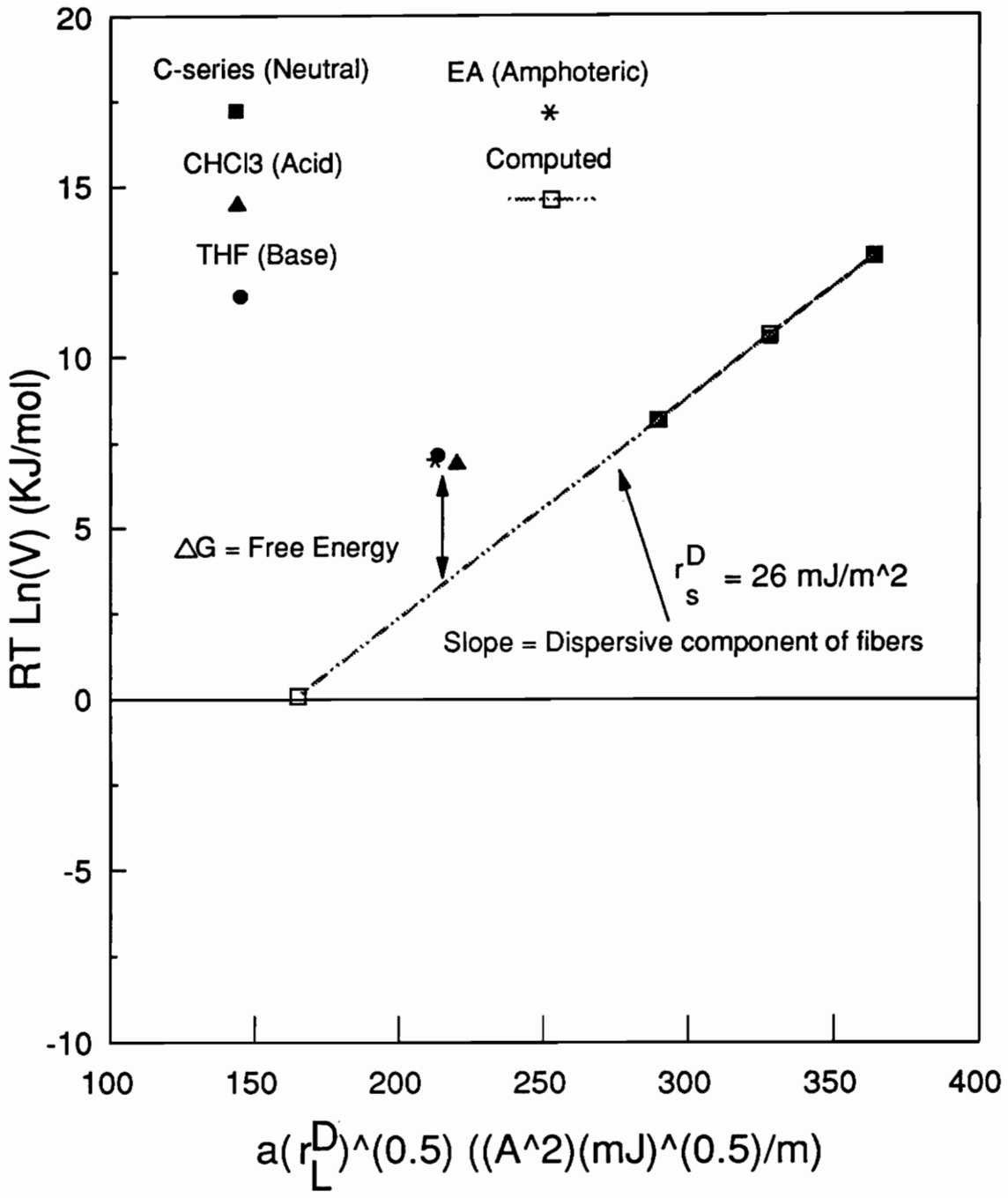

Figure 4-1: Illustrations of the acid/base characteristic of the AS4CGP fiber at 40 C.

4.3 DCA Results

The surface energies of the AU4, AS4(2), and AS4CGP fibers obtained by the DCA method are summarized in Table 4-2. The dispersive component (γ^D_s) of the surface energy for AU4 and AS4(2) fibers is consistent with the findings of Bolvari and Ward [1]. It is noticed that the dispersive component of the AS4CGP fiber obtained by the DCA method is same as that obtained by the IGC method.

Table 4-2 Surface Energy of Carbon Fibers and ISS of Composites

Fibers	γ^D_s (mJ/m^2)	γ^P_s (mJ/m^2)	I^P_{sf} (mJ/m^2)	ISS (MPa)
AU4	73	4	18*	77.2 (54.0%)**
AS4(2)	47	15	35*	~96.5 (54.7%)**
AS4CGP	26	17	37*	~96.5 (53.7%)**

* : Fibers in formamid (γ^P_l = 18.7 mJ/m^2).
** : Number in the parentheses denotes fiber volume fraction.

The non-dispersive component of surface energy (γ^P_s) of the carbon fibers is approximately four times that of the AU4 fiber. This suggests that the proprietary treatment increases the polarity of the AS4(2) and AS4CGP fibers, according to Bolvari and Ward [1]. In addition, the non-dispersive interaction (I^P_{sf}) of the AS4(2) and AS4CGP fibers is approximately two times that of the AU4 fiber. As

discussed in the literature [6-7], the non-dispersive interactions (I^P_{sf}) are acid-base interactions and only an acid and a base may result in acid-base interactions. It has been shown [1,8] that the non-dispersive interaction is a key factor in determining the interfacial adhesion between the fiber and matrix. Schultz et al. [8] have reported that the AU4 fiber has a weak acid character; the AS4 fiber has a strong acid character; AS4C (an epoxy sizing on the AS4 fiber) has both strong acid and base characters. Because J2 polymer has two polar groups (-N-), which is a base, good interfacial adhesion is expected for the AS4(2) and AS4CGP fibers to the thermoplastic polymers, as suggested by Schultz et al. [8].

4.4 Characteristics of AS4CGP Fibers

It is noticed that the epoxy sizing (0.4% by weight) of the AS4CGP fiber, normally used in epoxy matrices, is not optimized for the J2. An epoxy may not undergo full cure if a curing agent is not present. However, the epoxy may undergo polymerization at high temperatures, e.g., at 295°C [9]. Therefore, the epoxy sizing of the AS4CGP fiber may be in a partially cured state at consolidation temperatures. The author has placed the AS4CGP fiber at 100°C for 16 hours to investigate the state of the epoxy sizing. A portion of the AS4CGP fiber has been further treated at 295°C for 30

min, which simulates the thermal cycle of the consolidation procedures of making J2 composites. Both thermal treated AS4CGP fibers have been examined by the SEM. Figure 4-2 is the SEM photomicrograph of the AS4CGP fiber that have been treated at 295°C for 30 min. It is noticed that the epoxy sizing coalesced between the AS4CGP fibers. This suggests that the epoxy sizing may be partially cured after thermal treatments. The T_g of the epoxy sizing is also characterized by DSC and is found to be -10°C, as shown in Figure 4-3. The T_g of the epoxy sizing is very close to the T_g of EPON-828 [10]. Since EPON-828 is a commonly used matrix, it is possible that the epoxy sizing has a similar formula to the EPON-828. However, the real chemical structure of the epoxy sizing is not clear at the present time.

Because of the low viscosity of the epoxy sizing at the consolidation temperature, the epoxy sizing may mix with the J2 polymer. Thomason [11] has employed the SIMS technique to show the diffusion of a sizing in a polymer matrix, which may support the present observation. Thus, the properties of the interphase in AS4CGP/J2 composites will be different from those in AS4(2)/J2 composites. It is possible that a more compliant interphase results in the AS4CGP/J2 composites because of the presence of the partially cured epoxy sizing.

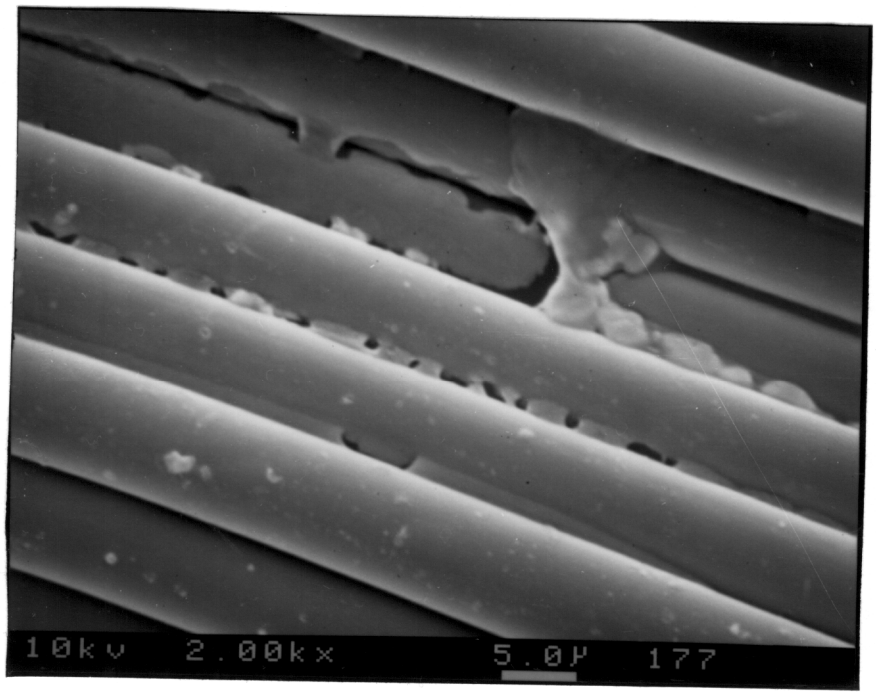

Figure 4-2: SEM photomicrograph for the AS4CGP fibers (at 295°C for 30 min.)

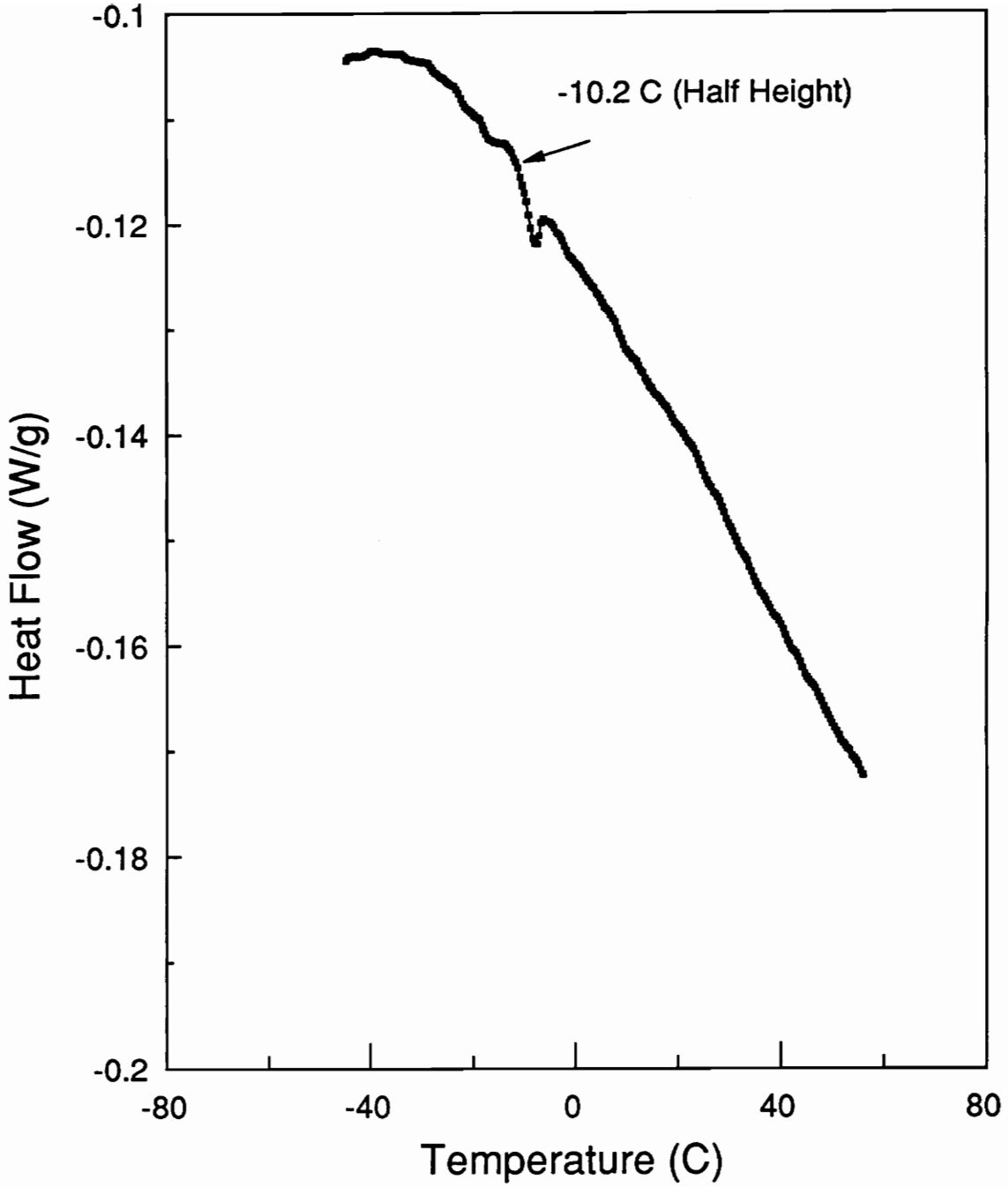

Figure 4-3: DSC traces for the epoxy sizing of the AS4CGP fibers.

4.5 Topology of Fiber Surfaces

Figure 4-4 contains the SEM photomicrographs for the surface topology of AU4, AS4(2), and AS4CGP fibers. It is seen that the AU4 fiber has a rougher surface than both AS4(2) and AS4CGP fibers. However, the rough AU4 fiber does not possess "good" adhesion, as will be demonstrated later. Bascom et al. [3]. have also observed that the AS1 fiber (equivalent to AU4 fibers) has a rougher surface but weaker interfacial adhesion. The present observations are consistent with Bascom et al. [3]. This abnormal phenomenon is explained as follows. Drzal [12] has suggested that the surface treatment is (a) to remove weak layers at fiber surfaces and (b) then to impart chemically active groups on fiber surfaces resulting in increasing the surface polarity. Thus, the characteristic of the rough surface on the AU4 fiber seems not to contribute to increasing fiber-matrix adhesion.

4.6 Interfacial Shear Strength (ISS) of J2 Composites

The ISS of the J2 composites are also given in Table 4-2. The data obtained from the meso-indentation test was collected in the form of a stress-strain curve. The stress is related to the mean applied indenter pressure or Mean Hardness Pressure (MHP) and the strain is related to a ratio of the indenter contact diameter with the specimen to the

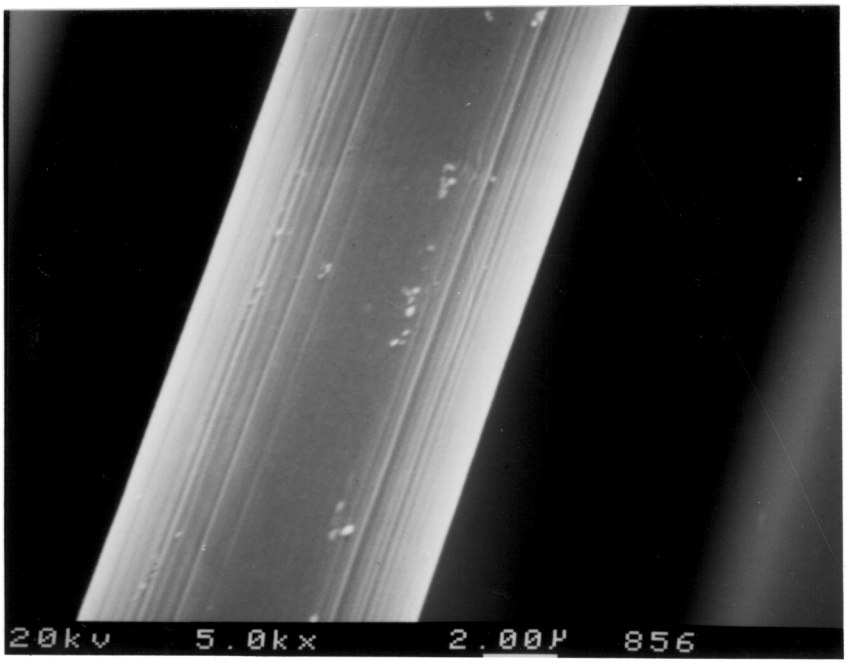

(a)

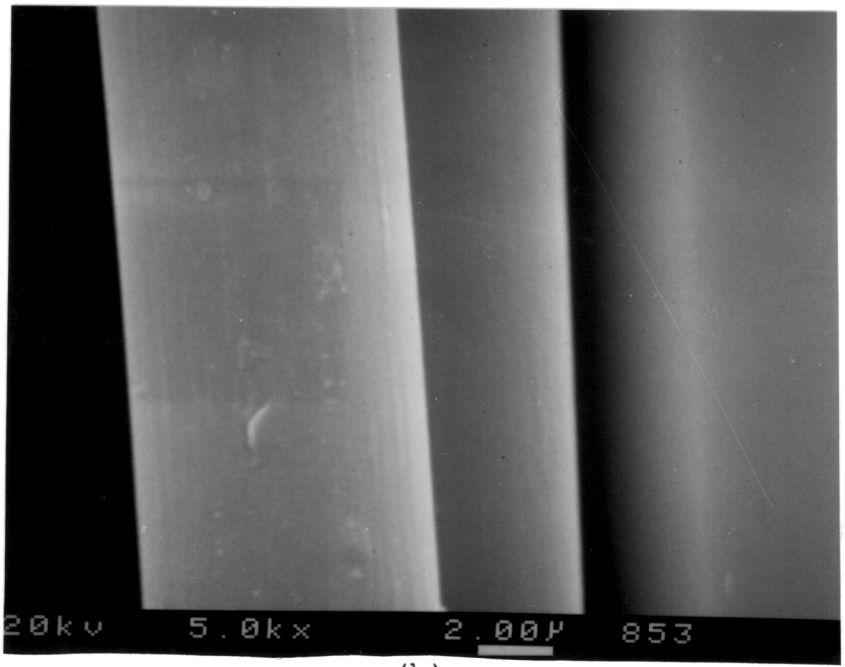

(b)

Figure 4-4: SEM photomicrographs for (a) AU4 fiber; (b) AS4(2) fiber; and (c) AS4CGP fiber.

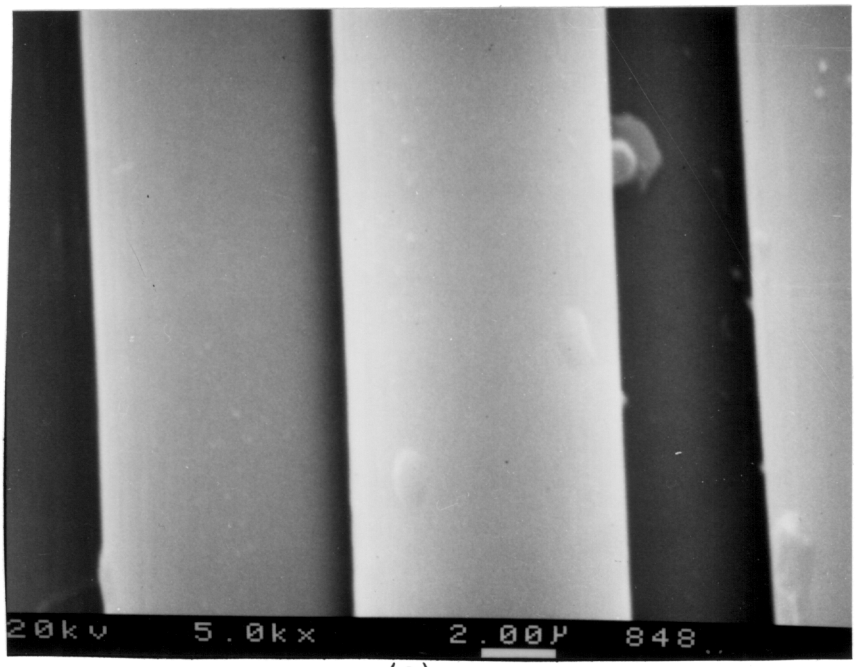

(c)

Figure 4-4: Continued

penetrator diameter. An elastic limit is observed in the indentation test which signifies the failure of the fiber/matrix interface corresponding to the Maximum Mean Hardness Pressure (MMHP). This value of applied indenter pressure is then input into a linear elastic micromechanics model [13] to yield a measure of the interfacial bond quality.

In Table 4-2 the meso-indentation results are presented for the AU4, AS4(2), and AS4CGP systems. When comparing the MMHP, the AU4 composite possesses the weakest interface by approximately 22% relative to the surface treated fibers. The AS4CGP and AS4(2) are essentially indistinguishable. Due to the limitations on the micromechanics model and what was observed in the tests, only approximate Interfacial Shear Strength (ISS) values were obtainable for three (highlighted by star) of the four systems. The ISS of ~77 MPa for the AU4 composite is typical for this non-surface treated fiber [14].

4.7 Summary

The surface treatment increases the polarity of the AS4(2) and AS4CGP fibers resulting in increasing the adhesion between the fibers and J2 polymer. The results obtained by the meso-indentation tests show the ISS of the

AS4(2)/J2 and AS4CGP/J2 composites was roughly 20% more than the AU4/J2 composites.

REFERENCES

[1] Bolvari, A. E. and Ward, T. C., "Determination of Fiber-Matrix Adhesion and Acid-Base Interactions," in Inverse Gas Chromatography: Characterization of Polymers and Other Materials, Ed. Lloyd, D. R., Ward, T. C., and Schreiber, H. P., ACS Symposium Series 391, 1989.

[2] Piggot, M. R., "Tailored Interphases in Fiber Reinforced Polymers," in Materials Research Society Symposium Proceedings, Vol. 170, Ed. by Pantano, C. G. and Chen, E. J. H., pp. 265-274.

[3] Bascom, W. D., Yon, K. J., Jensen, R. M., Cordner, L., "The Adhesion of Carbon Fibers to Thermoset and Thermoplastic Polymers," Journal of Adhesion, Vol. 34, 1991, pp. 79-98.

[4] Wilkinson, S. P., Ph.D. Dissertation, "Toughened Bismaleimides: Their Carbon Fiber Composites and Interphase Evaluation," Virginia Polytechnic Institute and State University, December, 1991.

[5] Fowkes, F. M., "Determination of Interfacial Tensions, Contact Angles, and Dispersion Forces in Surfaces by Assuming Additivity of Intermolecular Interactions in Surfaces," Journal of Physical Chemistry, Vol. 66, 1962, p. 382.

[6] Schultz, J., Cazeneuve, C., Shanahan, M. E. R., Donnet, J. B., "Fiber Surface Energy Characterization," Journal of Adhesion, Vol. 12, 1981, pp. 221-231.

[7] Gutmann, V., The Donor Acceptor Approach to Molecular Interactions, Plenum Press, 1978.

[8] Schultz, J., Lavielle, L., and Martin, C., "The Role of the Interface in Carbon Fiber-Epoxy Composites," Journal of Adhesion, Vol. 23, 1987, pp. 45-60.

[9] Ishida, H, private communication in his presentation at VPI&SU, on April 15, 1992.

[10] Plazek, D. J., and Frund, Z. N., "Epoxy Resins (DGEBA): The Curing and Physical Aging Process", Journal of Polymer Science: Part B, Vol. 28, pp. 431-448, 1990.

[11] Thomason, J. L. and Morsink, J. B. W., "Investigation of the Interphase in Glass-Fiber-Reinforced Epoxy Composites", in Interfaces in Polymer, Ceramic, and Metal Matrix Composites, Ed. by Ishida, H., Elsevier Science Publishing Co., 1988, pp. 503-512.

[12] Drzal, L. T., "Composite Interphase Characterization," SAMPE Journal, Vol. 5, 1983, pp. 7-13.

[13] Carman, G. P., Lesko, J. J., Reifsnider, K. L., and Dillard, D. A., "Micromechanical Model of Composite Materials Subjected to Ball Indentation," Submitted to Journal of Composite Materials, October, 1991.

[14] Lesko, J.J., Carman, G. P., Dillard, D. A., and Reifsnider, K. L., "Indentation Testing of Composite Materials as a Tool for Measuring Interfacial Quality," submitted for publication ASTM STP, March, 1991.

Chapter 5

MECHANICAL PROPERTIES OF J2 COMPOSITES

The properties of the interphase have been discussed in chapter 4. Both AS4(2)/J2 and AS4CGP/J2 composites have approximately the same ISS which are higher than that of the AU4/J2 composites. Thus, one would expect that the static mechanical properties of the AS4(2)/J2 and AS4CGP/J2 would be greater than those of the AU4/J2 composites. It is noticed that the AS4CGP fiber contains unreacted epoxy sizing which may result in a compliant interphase in the AS4CGP/J2 composites. This compliant interphase may yield a slightly different mechanical performance as compared to the AS4(2)/J2 composites.

5.1 Characteristic of the Composites

Figure 5-1 shows the appearance of the composite panels. The broken fibers can be seen in the AU4/J2 panel, as shown in Figure 5-1. The broken fibers are not only on the outside but also inside of the composite panels. These broken fibers are randomly distributed and tangle fiber tows to form a mat-like structure. Broken fibers are not observed on either the AS4/J2 or AS4CGP/J2 composites. Figure 5-2(a) shows resin rich layers in the AU4/J2

composites. The resin rich regions suggest little J2 resin contacts the AU4 fibers, which may be the effect of the broken fibers, i.e., the mat-like structure. Figure 5-2(b-c) show uniformly distributed fibers in both AS4/J2 and AS4CGP/J2 composites.

5.2 Mechanical Properties of J2 Composites

Mechanical properties of J2 composites are summarized in Table 5-1. Each entry in this table is an average of either four or five data points as indicated by round parentheses. The fiber volume fraction of each type of testing specimen is also listed in this table as shown by square parentheses. These experimental results will be discussed in detail in the following section.

5.2.1 $[0]_8$ Tensile Tests

Figure 5-3(a-c) shows the stress-strain curves of all the longitudinal tensile tests. The modulus of the specimen is determined over the strain range from 0.03% to 0.3%. The experimental results of the longitudinal tensile tests - tensile strength (σ^f_{11}), modulus (E_{11}), and Poisson's ratio (ν_{12}) - are given in Table 5-1. Except for the σ^f_{11} of the AS4/J2 composite, only a small variation (less than 5%) is observed among the composite systems for each kind of the mechanical property. The insensitivity of the fiber

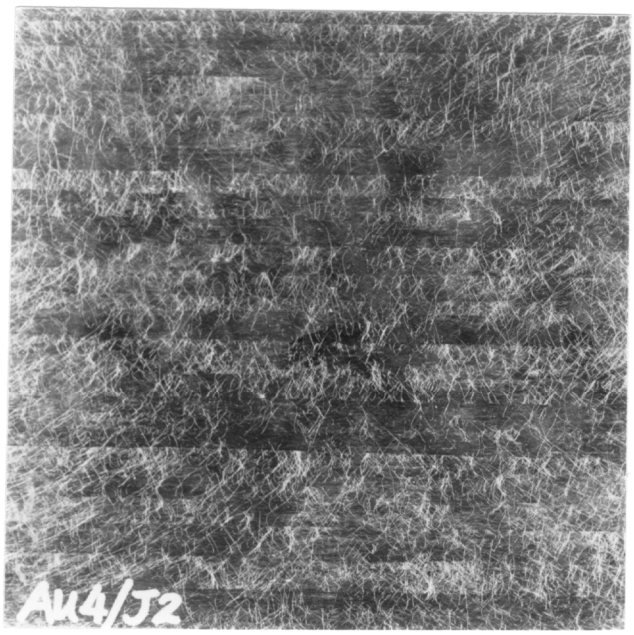

Figure 5-1: Broken fibers randomly distributed in the AU4/J2 composite panels. These broken fibers are not only on the outside but also inside of the composite panels.

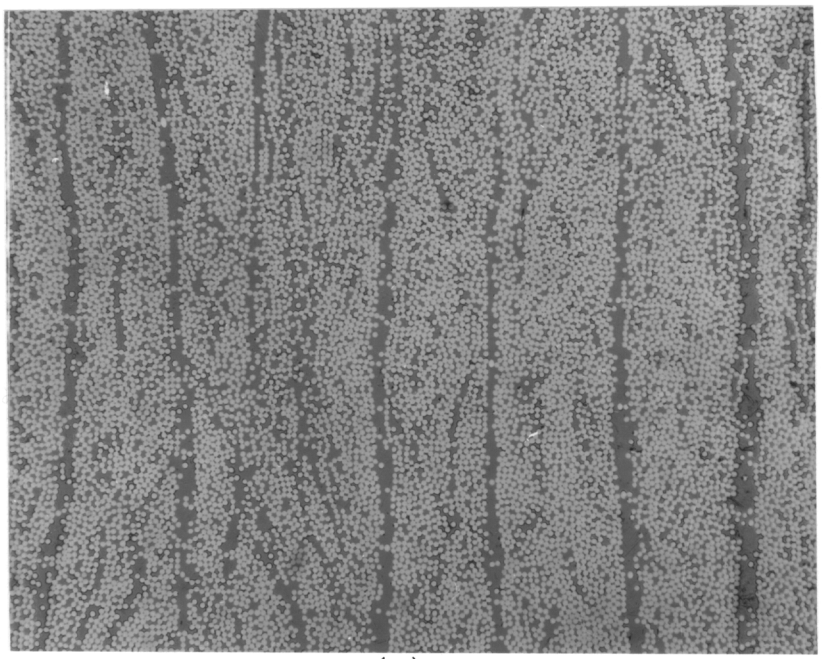

(a)

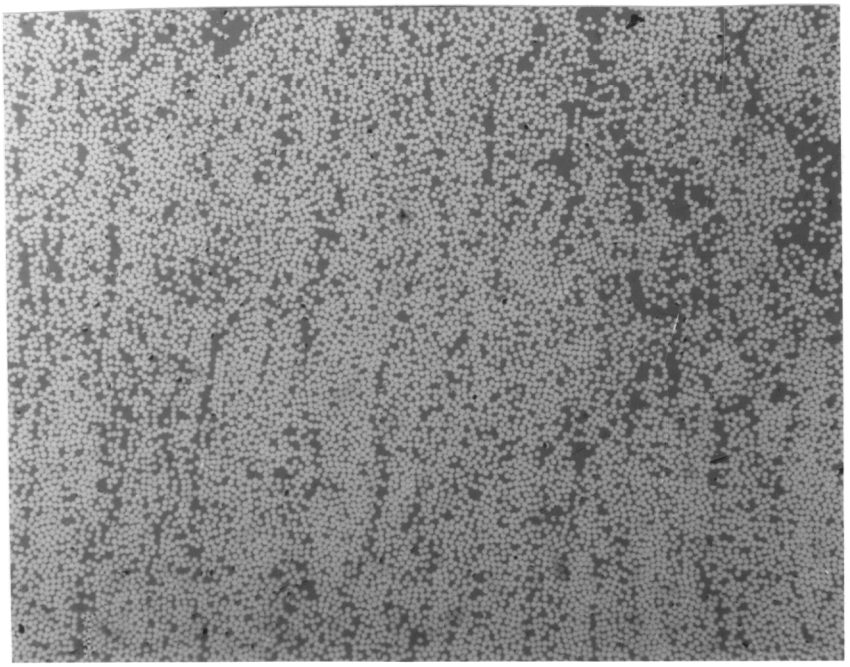

(b)

Figure 5-2: Fiber distribution on the cross section area of the (a) AU4/J2; (b) AS4(2)/J2; and (c) AS4CGP/J2 composite specimen.

(c)

Figure 5-2: Continued

Table 5-1 Mechanical properties of J2 composites

	AU4/J2	AS4/J2	AS4CGP/J2
Tensile $[0]_8$ Strength, GPa	1.61±0.08 *(5),[53.6%]	1.83±0.06 (5),[57.6%]	1.64±0.02 (5),[53.8%]
Tensile $[0]_8$ Modulus, GPa	122.94±3.85	124.42±2.77	126.02±7.42
Failure Strain	1.21%	1.31%	1.17%
Poisson's Ratio, ν_{12}	0.35±0.018	0.32±0.013	0.30±0.023
Tensile $[90]_{12}$ Strength, MPa	34.19±3.39 (5),[57.4%]	54.18±1.71 (4),[55.7%]	42.72±2.16 (5),[52.5%]
Tensile $[90]_{12}$ Modulus, GPa	8.95±0.22	8.47±0.35	8.34±0.26
Falure Strain	0.38%	0.62%	0.59%
Tensile $[\pm45]_{2s}$ Inplane Shear Strength, MPa	94.83±3.50 (5)	159.87±2.79 (4)	153.46±5.12 (4)
Tensile $[\pm45]_{2s}$ Inplane Shear Modulus, GPa	5.16±0.37	4.94±0.27	4.74±0.30
Iosipescu $[90]_{20}$ Shear Strength MPa	37.27±3.40 (5),[54.0%]	68.23±3.01 (4),[54.7%]	60.37±4.10 (5),[53.7%]
Iosipescu $[90]_{20}$ Shear Modulus GPa	5.22±0.11	5.10±0.12	4.97±0.10
$[\pm45/90_2]_s$ Strength, MPa	196/182	316/303	316/309
**Interfacial Shear Strength MPa	77.2 [54%]	~96.5 [54.7%]	~96.5 [53.7%]

* Numbers in the round and square parentheses denote the number of tested specimens and fiber volume fraction, respectively.

** Measured by meso-indentation tests.

direction properties to the ISS has also been reported in Refs. [1,2]. The failure strains are 1.21%, 1.31%, and 1.17%, for the AU4/J2, AS4/J2, and AS4CGP/J2 composites, respectively.

Since the fiber direction dominates the 0°-tension tests, it is expected that the highest fiber strength will yield the highest 0° tensile strength of composites provided the level of the fiber-matrix adhesion are very similar among the tested composites. Thus, according to Table 3-1, one would expect the σ^f_{11} of the AS4CGP/J2 composite to be the highest since the adhesion of the AS4CGP fiber to J2 is greater than those of the other composite systems. However, the tensile strength of AS4/J2 composites is greater than that of either the AU4/J2 or AS4CGP/J2 composite. Drzal [3] has suggested that a rigid interphase tends to transfer load more efficiently than a compliant interphase does. As a result, a rigid interphase yields a higher σ^f_{11} of composites than the compliant interphase does, which is the present case.

Figure 5-4 shows the photographs of failed $[0]_8$ specimens. It is seen that the AU4/J2 composites show extensive fiber-matrix splitting. Figure 5-4 also shows neat fracture surfaces for both AS4/J2 and AS4CGP/J2 specimens. It is also noticed that cracks propagate through the width of specimens and little fiber-matrix splitting

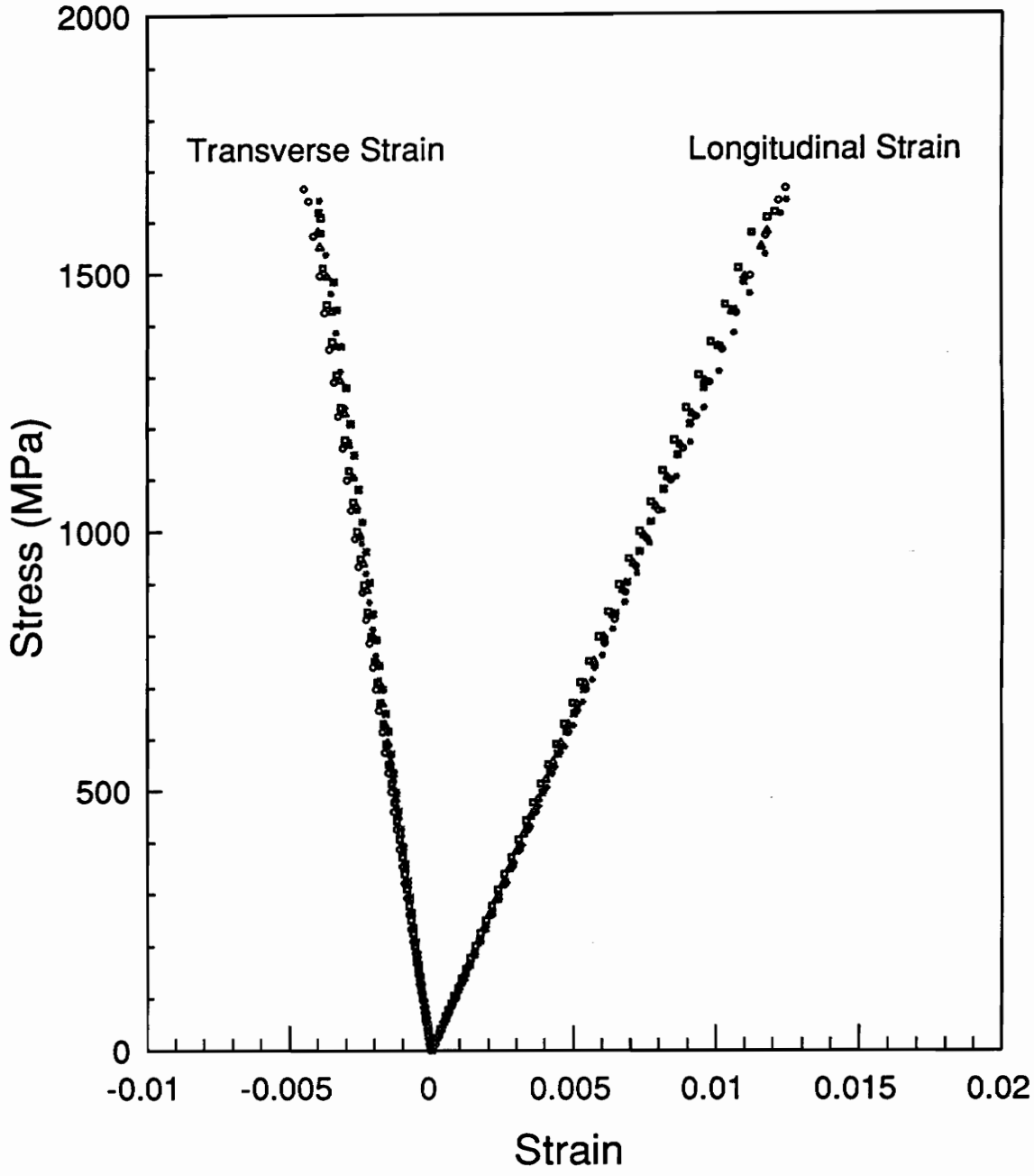

Figure 5-3(a): Stress-strain curves of [0] tension tests for AU4/J2 composites.

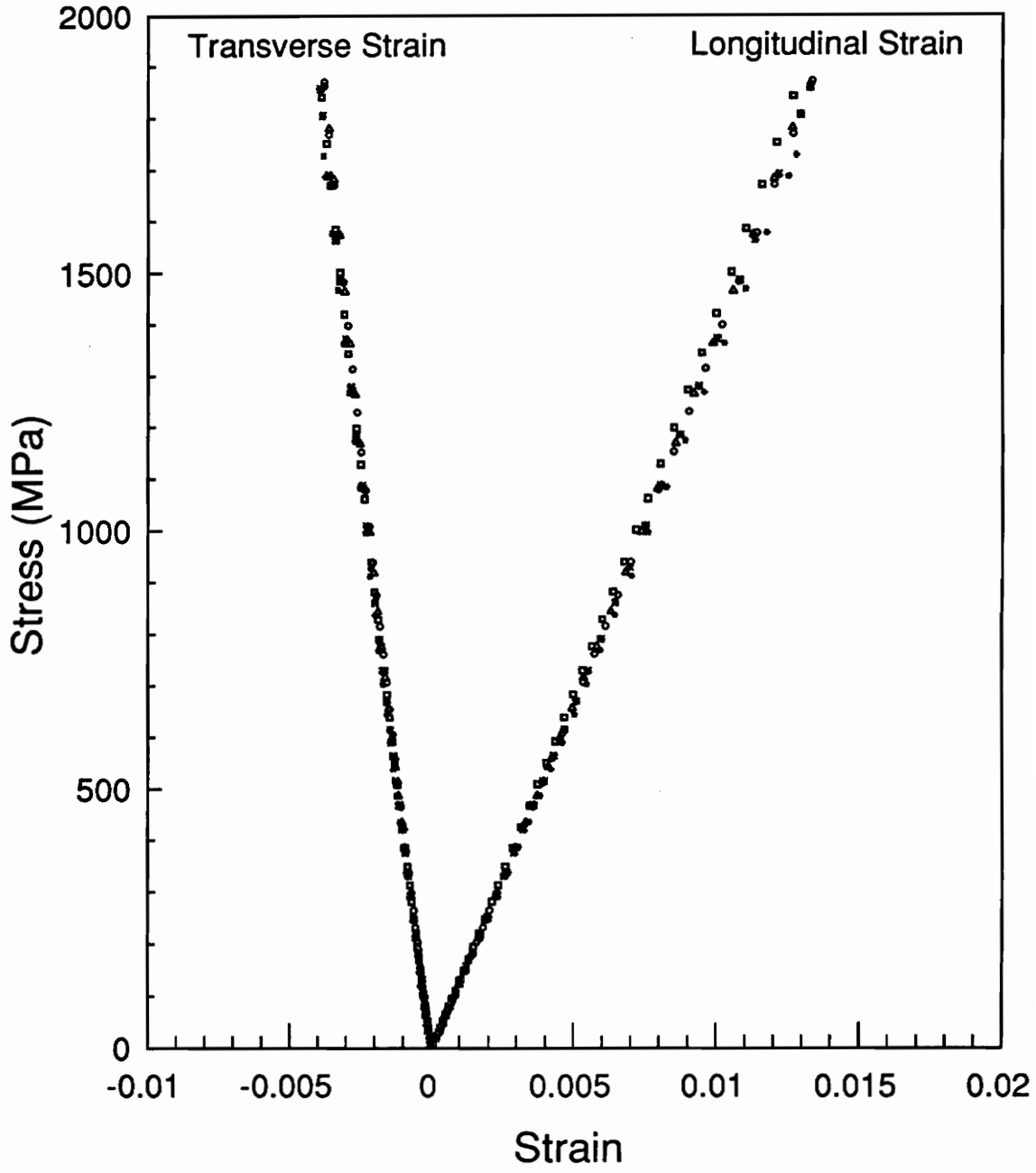

Figure 5-3(b): Stress-strain curves of [0] tension tests for AS4(2)/J2 composites.

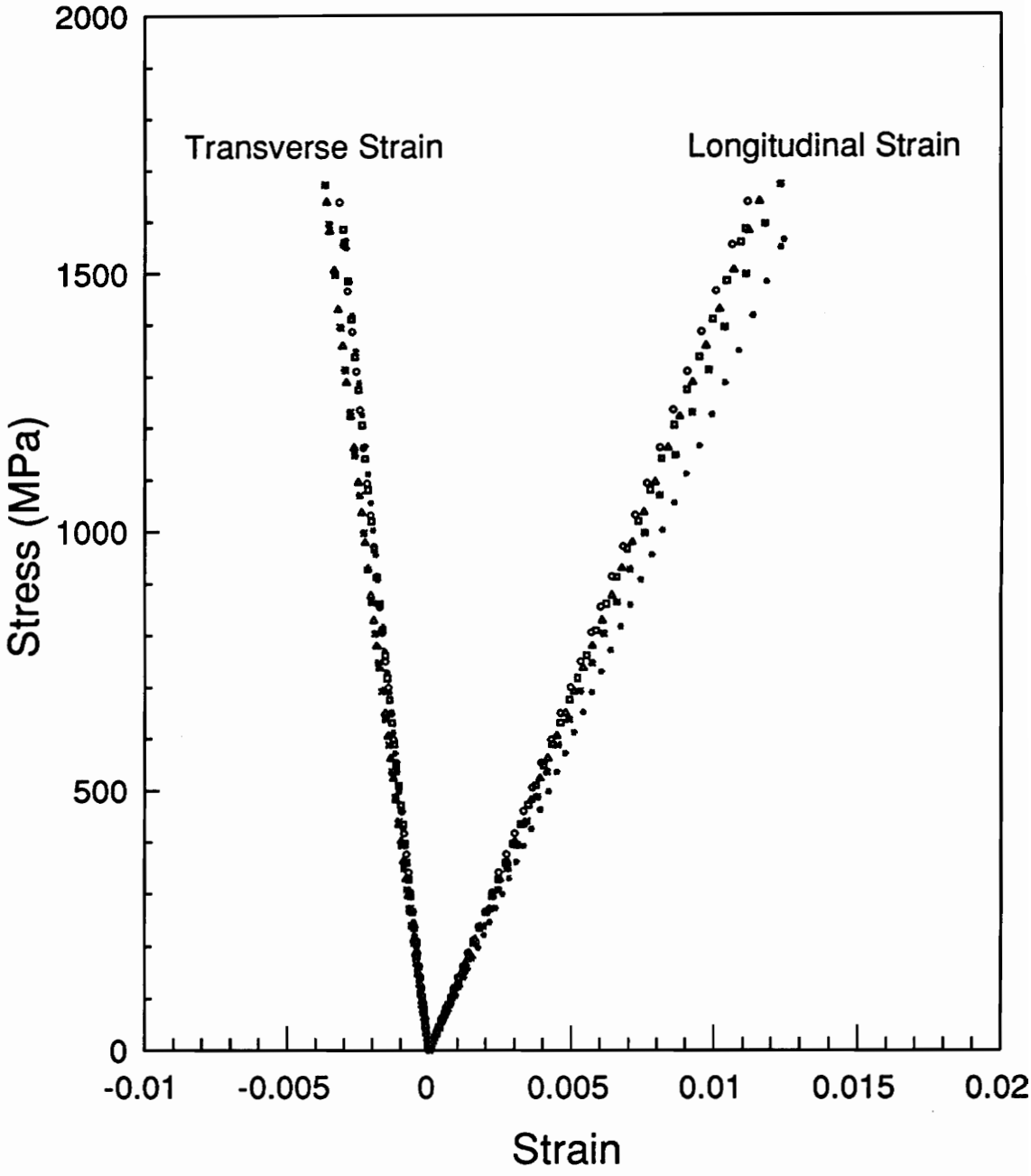

Figure 5-3(c): Stress-strain curves of [0] tension tests for AS4CGP/J2 composites.

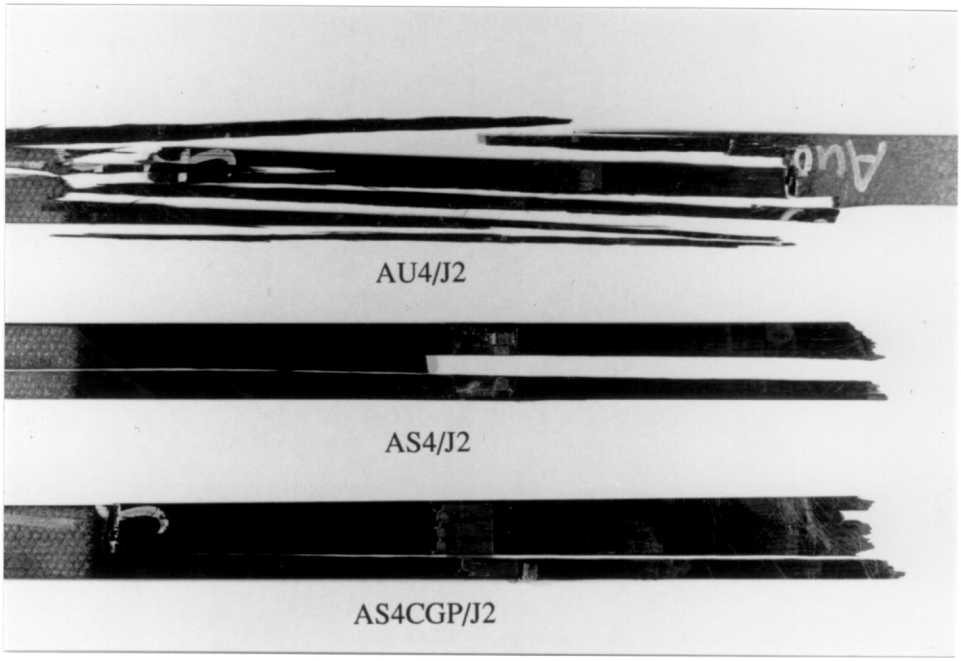

Figure 5-4: A photo for failed $[0]_8$ specimens. The AU4/J2 composite shows extensive fiber-matrix debonding. Both AS4(2)/J2 and AS4CGP/J2 composites show clean fracture surface.

exists. The responsible mechanisms for the above observations are suggested as follows.

Fibers are known to have a statistical distribution of flaws or imperfections such that fibers will fail at various stress levels [4]. Thus, for a composite at a certain stress level, a fiber breaks and causes a non-uinform stress state in the neighborhood of this broken fiber. It has been shown [4] that the maximum shear stress occurs near the end of the broken fiber. For weak interfacial adhesion between the fiber and matrix, this shear stress will exceed the interfacial shear strength. Therefore, an interfacial crack will propagate along the interface and result in fiber-matrix debonding. The role of the matrix is to transfer load from fibers to fibers. Thus, the breakdown of the matrix and/or interphase results in transferring the load to a distance. As the load increases, fiber breakage at different positions resulted from this load trsanfer process. Finally this will lead to the failure of the composite. This type of failure results from accumulation of random fiber breakage.

On the other hand, good interfacial adhesion between the fiber and matrix may yield an interfacial shear strength that is greater than the shear stress. Thus the load transfer from fibers to fibers is efficient and interfacial debonding will not be initiated. Thus, the fiber, next to

the single broken fiber, fails at the position close to the end of the single broken fiber. This process continues and results in a progressive fiber breakages from the adjacent fibers of the single broken fiber. Thus, the failed AU4/J2 composites, known to have poor interfacial adhesion, were brush-like; whereas the failed AS4/J2 and AS4CGP/J2 composites, both have good interfacial adhesion, show clean fracture surfaces (i.e., few fiber-matrix splitting.)

5.2.2 $[90]_{12}$ Tensile Tests

The results of the transverse tensile strengths (σ^f_{22}) and moduli (E_{22}) of the composites are given in Table 5-1. Figure 5-5(a-c) is the stress-strain curves for all the transverse tensile tests. The average failure strains are 0.38%, 0.62%, and 0.59% for AU4/J2, AS4/J2, and AS4CGP/J2 composites, respectively. The modulus of each specimen was determined over the strain range from 0.03% to 0.12%.

The order of the transverse tensile strength is the same as that of the longitudinal tensile strength for the tested composite systems. Presumably, the transverse tensile strength is the same for the tested composite systems because of the matrix dominating the transverse tensile properties. However, for the transverse tensile strength, the ratios of AS4/J2 to AU4/J2 and of AS4CGP/J2 to AU4/J2 are ~1.6 and ~1.4, respectively. Thus, it is clear

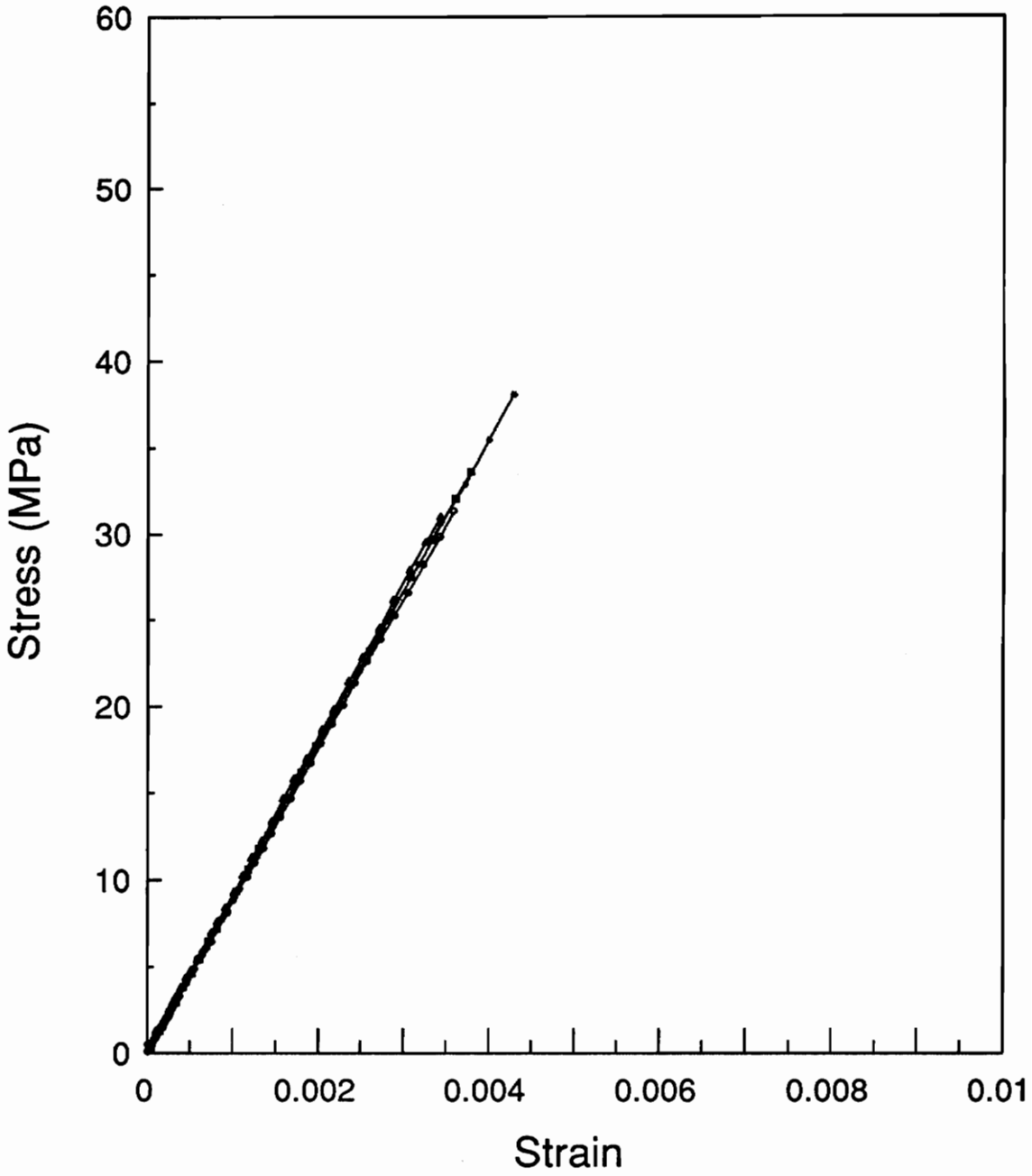

Figure 5-5(a): Stress-strain curves of [90] tension tests for AU4/J2 composites.

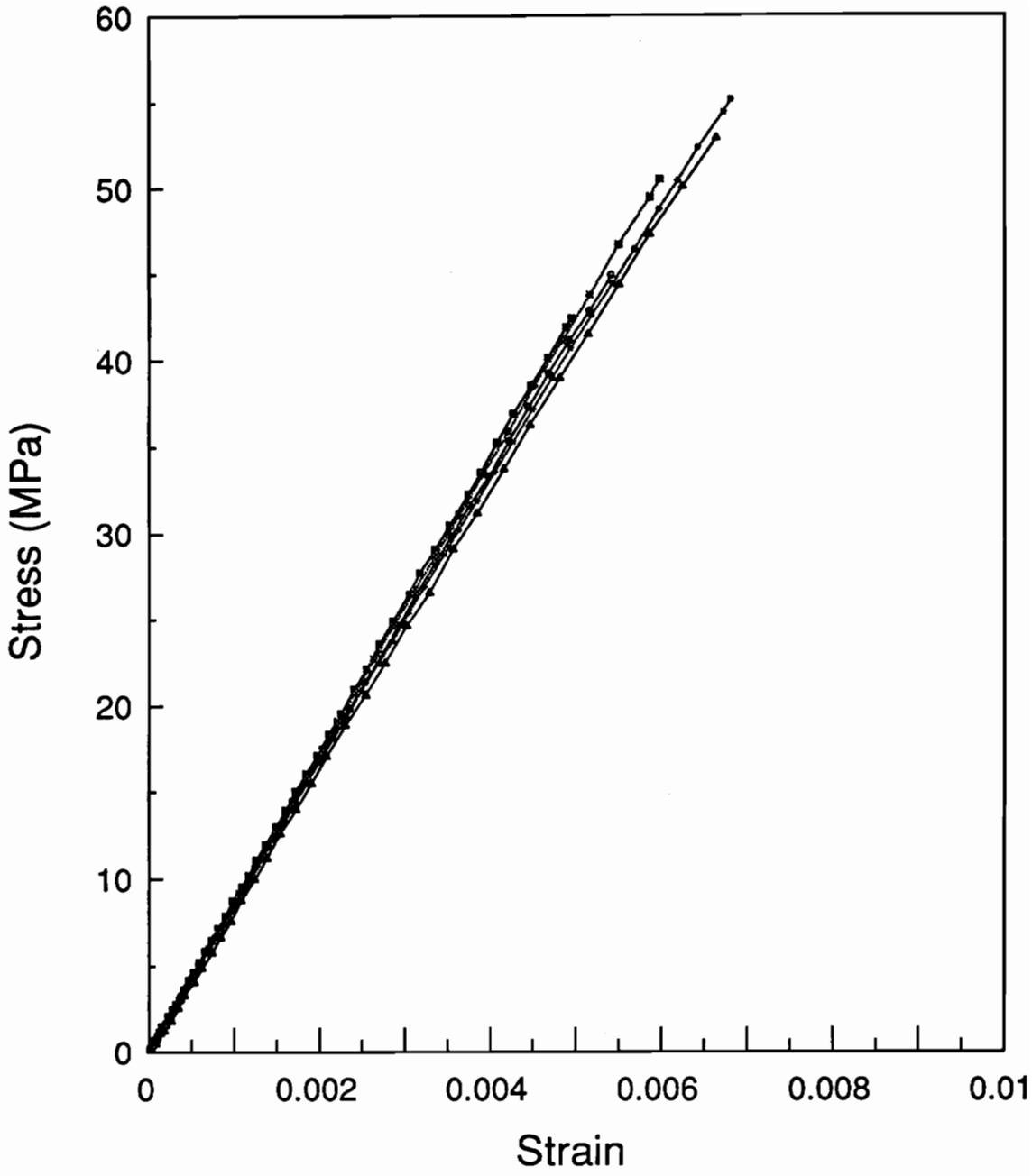

Figure 5-5(b): Stress-strain curves of [90] tension tests for AS4(2)/J2 composites.

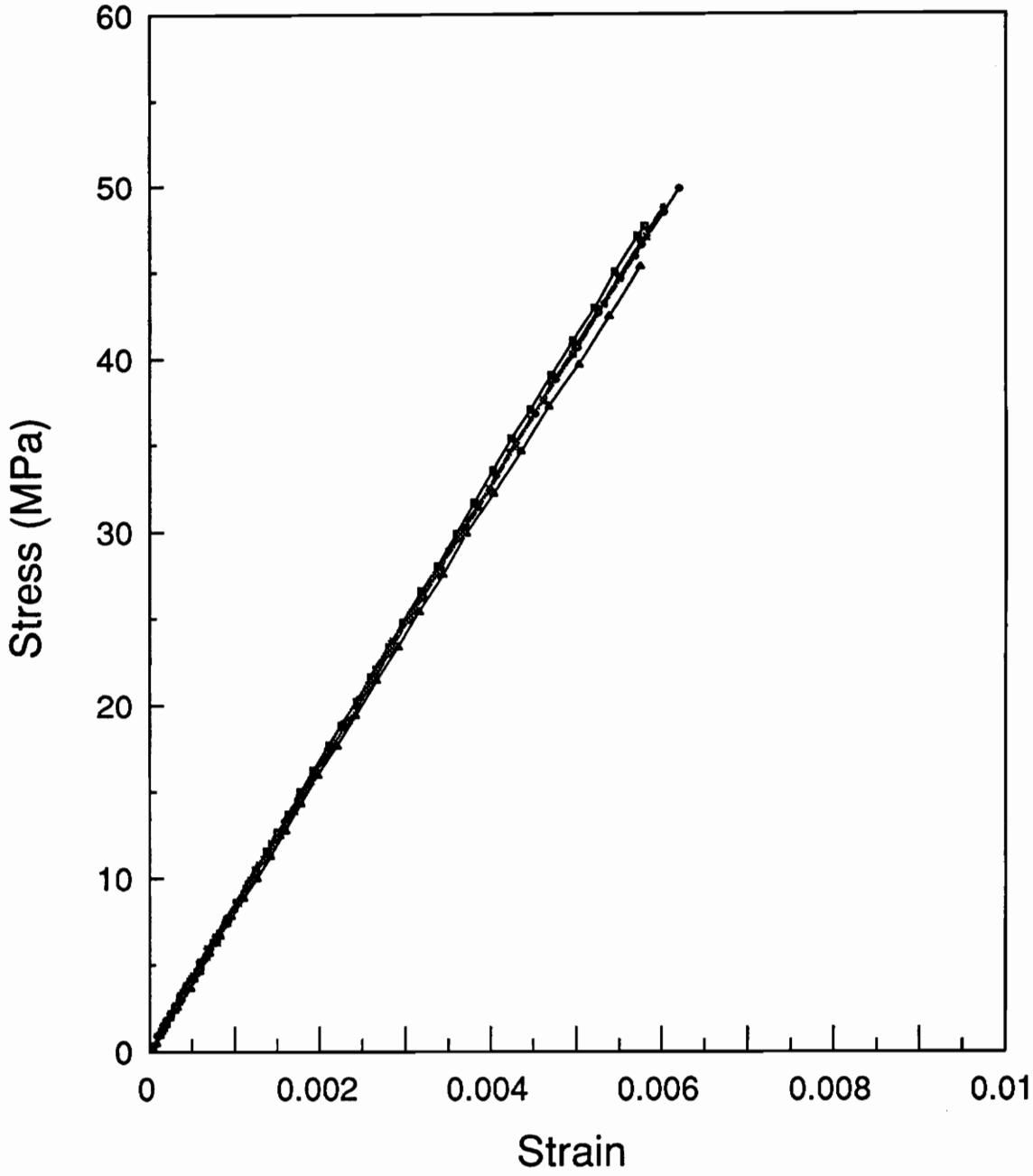

Figure 5-5(c): Stress-strain curves of [90] tension tests for AS4CGP/J2 composites.

that the interphase plays an important role in determining the transverse tensile strength. The highest σ^f_{22} value of the AS4/J2 composites is consistent with Drzal's results [3].

Carman et al. [5] have proposed that a compliant interphase in a composite tends to lower the stress concentration factor in the neighborhood of the fibers and results in increasing the transverse tensile strength of the composite. This result is based on a low fiber volume fraction and high ratio of the transverse modulus of the fiber to the matrix modulus. According to Carman et al. [5], however, the stress concentration factor is relatively small when a composite has the high fiber volume fraction and low ratio of the transverse modulus of the fiber to the matrix modulus, which applies for the present composite systems. In such a case, a compliant interphase does not make as large a contribution as the other case. In fact, a rigid interphase in a composite will increase the transverse tensile strength of the composite [3]. Our experimental results are in a good agreement with the trend suggested by Carman et al. [5].

SEM photomicrographs of the fracture surfaces for AU4/J2, AS4/J2, and AS4CGP/J2 specimens are shown in Figure 5-6(a-c). Figure 5-6(a) shows clean fibers in AU4/J2 composites, indicating weak interfacial adhesion for the AU4

fiber to J2 matrix. Figure 5-6(b-c) shows J2 polymer remaining on the AS4 and AS4CGP fibers, which suggests good adhesion for both composite systems. A distinguishing feature is observed when comparing Figure 5-6(b) and (c). It is seen that the AS4CGP/J2 specimen has more hackles than the AS4/J2 specimen does; and the matrix has been torn apart in the AS4/J2 composites, i.e., a cohesive failure of the matrix. These two photos have suggested that a ductile failure mode is exhibited in the AS4CGP/J2 composites; whereas a brittle failure mode occurs in the AS4/J2 composites.

The variation of the transverse tensile modulus (E_{22}) between composite systems is small. However, the order of the transverse tensile moduli (E_{22}) is reversed from that of the longitudinal tensile moduli (E_{11}). In addition, as will be demonstrated in next few sections, the shear moduli (G_{12}) show a similar trend to the order of E_{22} although the variation between the G_{12}'s is also very small. Thus, it leads us to investigate possible responsible mechanisms.

As for the AU4/J2 composites, the broken fibers are randomly distributed in the specimens. Referring to Figure 5-1, these broken fibers are randomly oriented in a two-dimensional fashion. These broken fibers will form a planar layer between each ply, which is similar to a short fiber reinforced composite. For transverse tensile tests, the

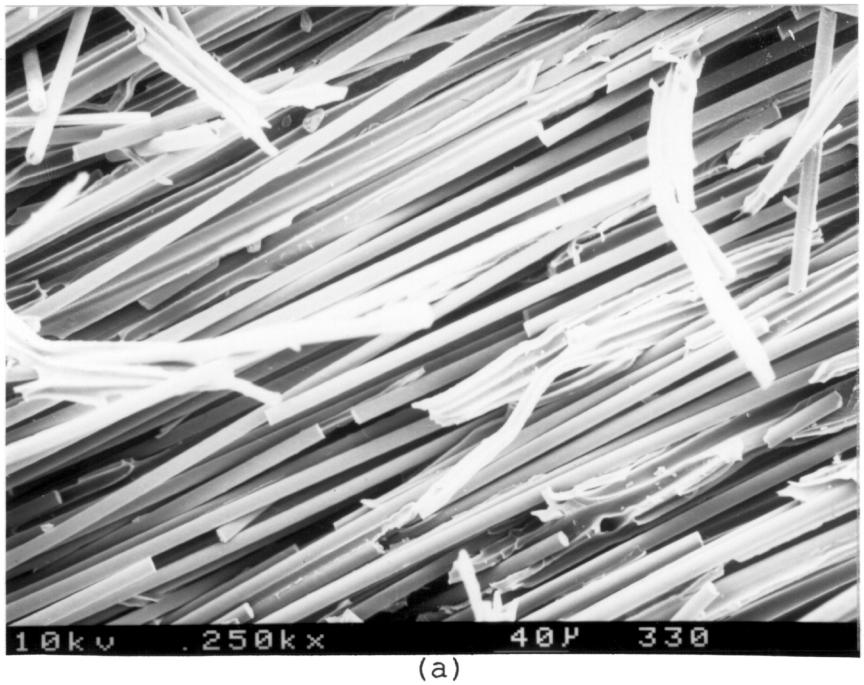

(a)

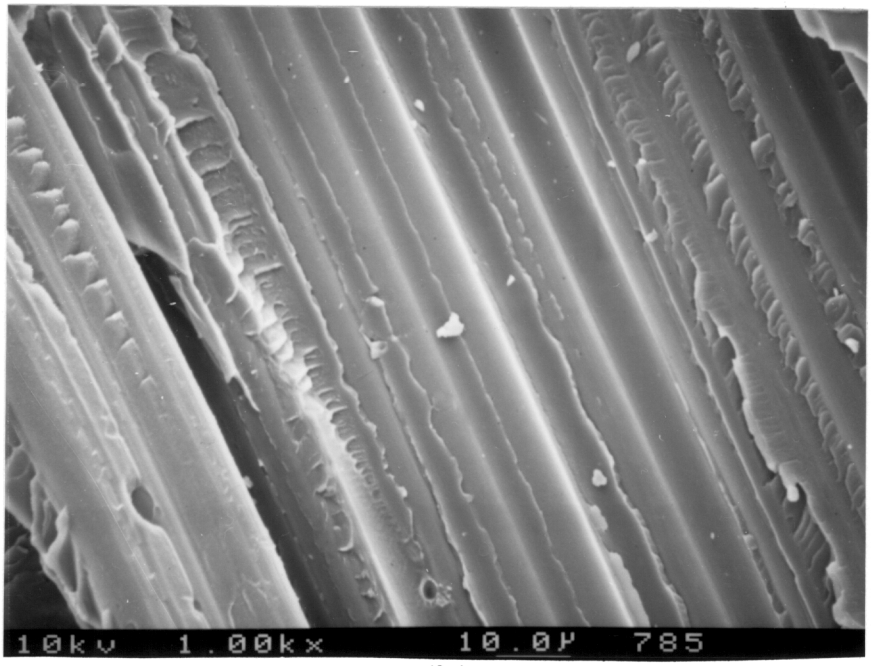

(b)

Figure 5-6: SEM photomicrographs of failed $[90]_{12}$ specimens for (a) AU4/J2; (b) AS4(2)/J2; and (c) AS4CGP/J2 composites.

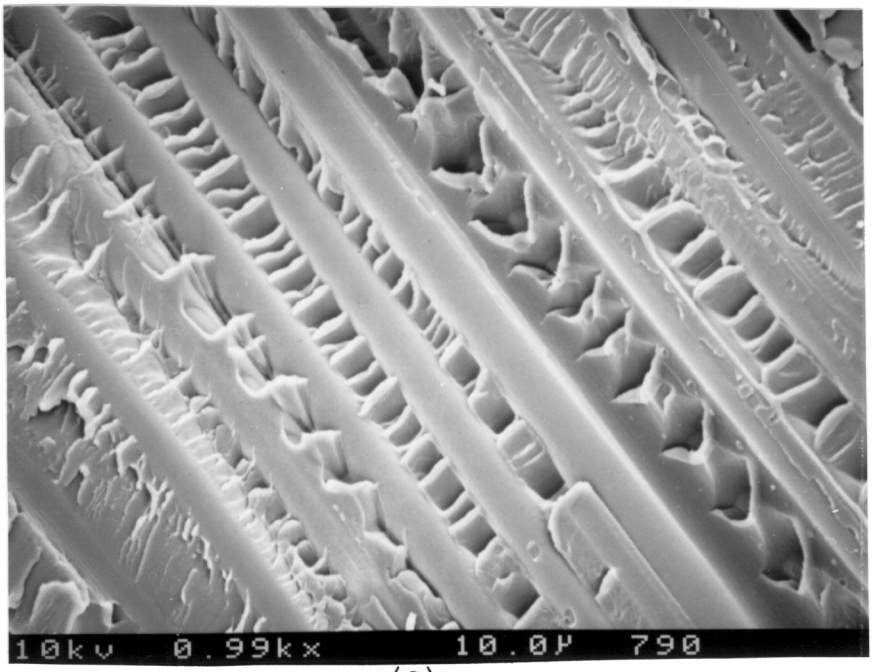

(c)

Figure 5-6: Continued

broken fiber layers are along the loading direction. It is obvious that the layers reinforce the AU4/J2 composites. Thus, it is clear that the AU4/J2 composites have the highest E_{22} value among the tested $[90]_{12}$ specimens. On the other hand, the interphase, known to be compliant, in the AS4CGP/J2 composite is loaded perpendicular to the loading direction. Therefore, the modulus of the AS4CGP/J2 composites is expected to be the lowest.

5.2.3 $[\pm 45]_{2s}$ Tensile Tests

The summary of the $[\pm 45]_{2s}$ tensile test results including shear moduli and shear strengths is listed in Table 5-1. Shear stress-shear strain curves for all $[\pm 45]_{2s}$ specimens are nonlinear, as shown in Figure 5-7(a-c). The shear modulus is caculated within the shear strain range from 0.01% to 0.4%. The shear strengths of the AS4/J2 and AS4CGP/J2 composites are ~65% greater than that of the AU4/J2 composites.

Figure 5-8 show photographs of failed $[\pm 45]_{2s}$ specimens. Figure 5-8 shows fibers pulling out and no significant fiber breakage in the fracture surfaces. This type of failure mode is the result of poor interfacial adhesion. Carefully comparing Figure 5-8, it is noticed that the AU4/J2 specimens do not exhibit much necking phenomenon. This premature failure suggests that the low

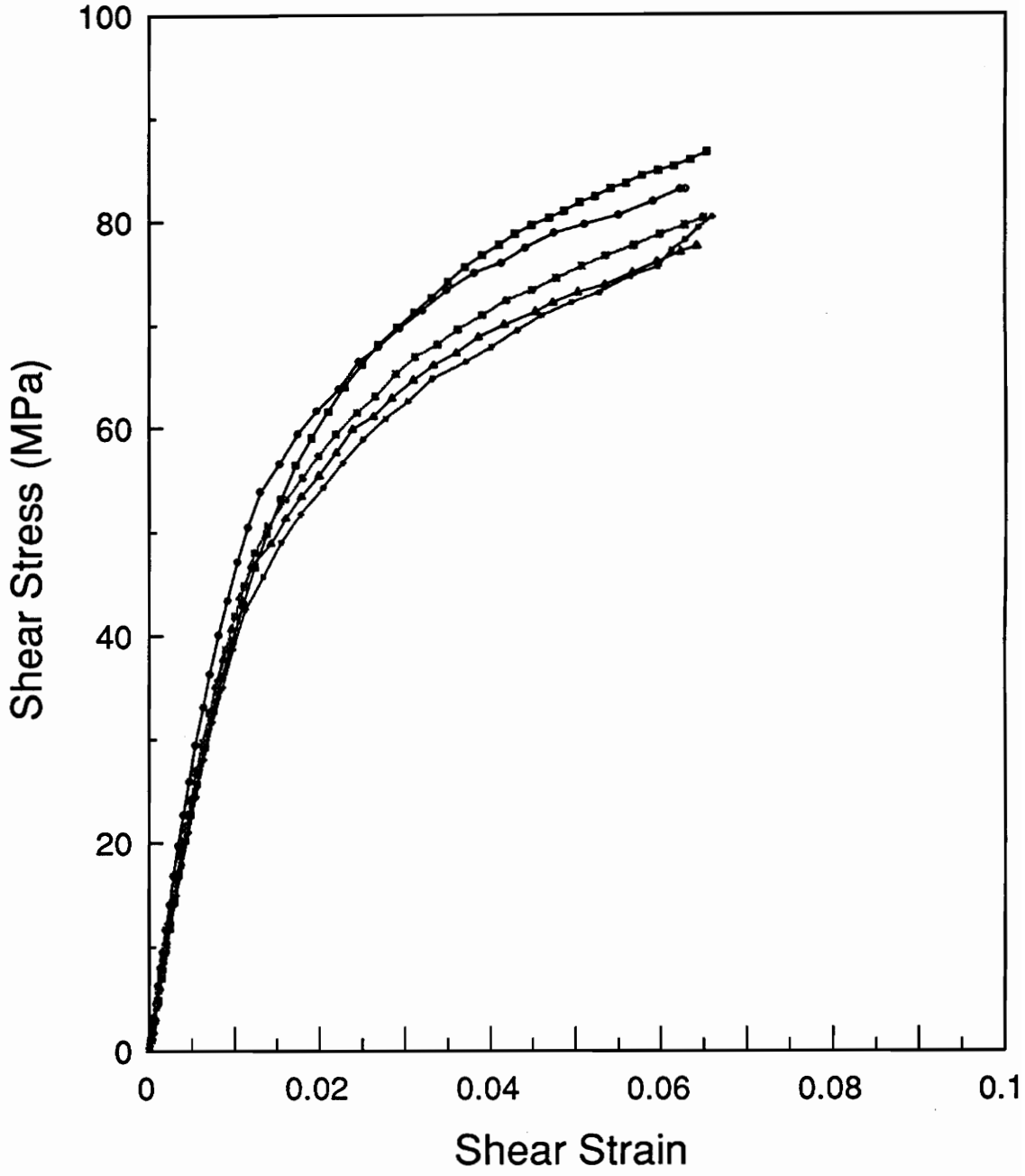

Figure 5-7(a): Shear stress - shear strain curves of in-plane tension tests for AU4/J2 composites.

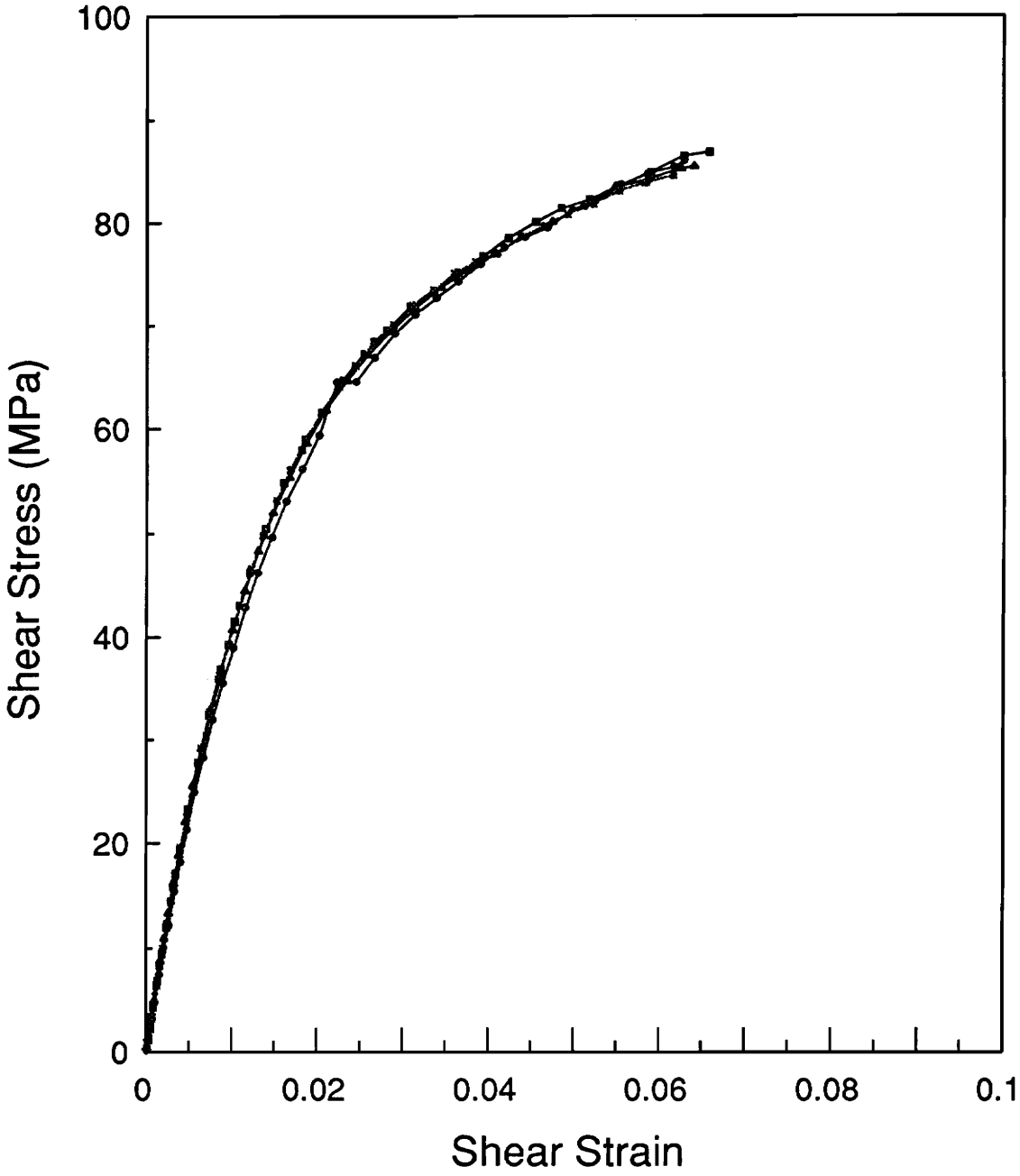

Figure 5-7(b): Shear stress - shear strain curves of in-plane tension tests for AS4(2)/J2 composites.

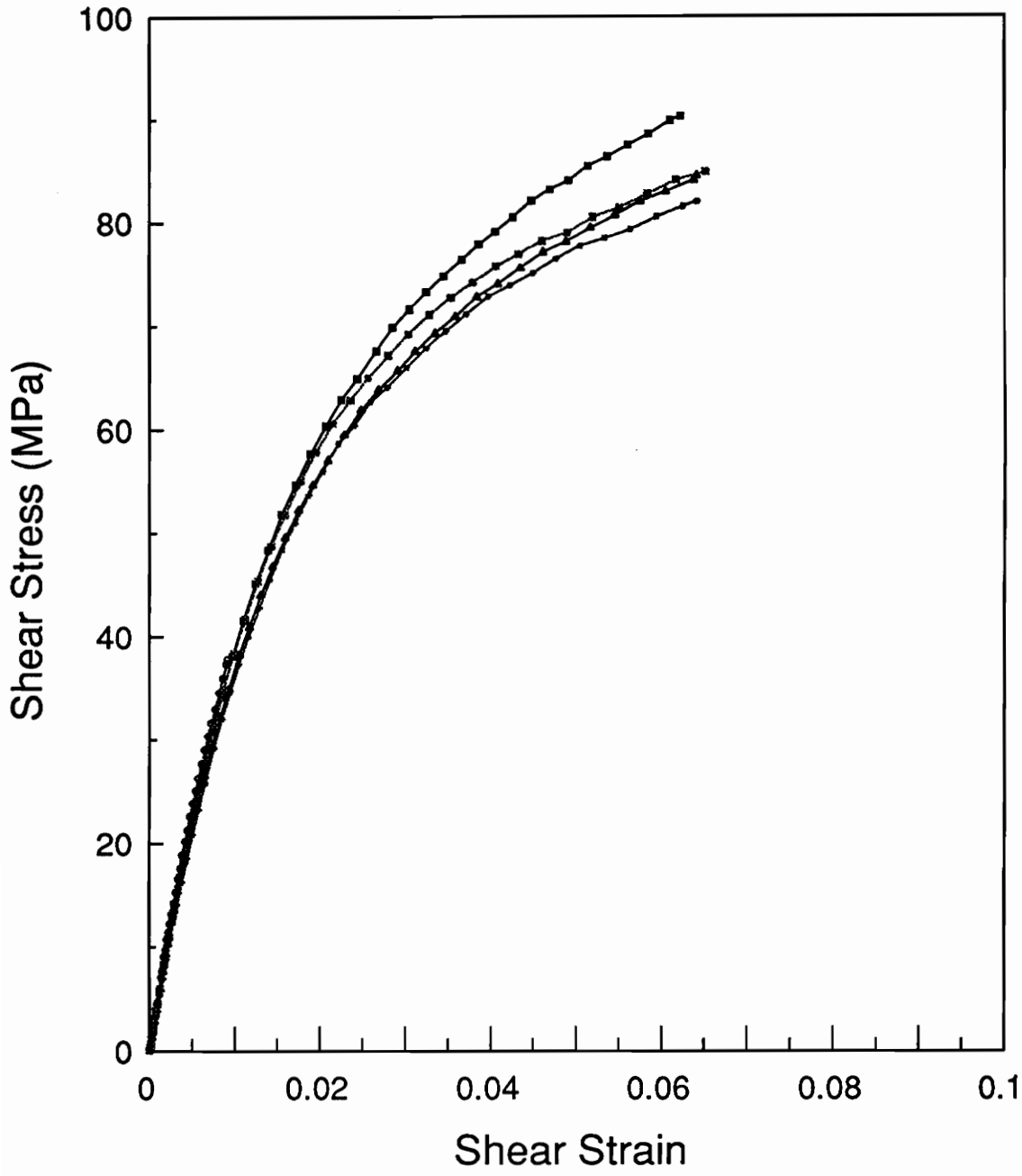

Figure 5-7(c): Shear stress - shear strain curves of in-plane tension tests for AS4CGP/J2 composites.

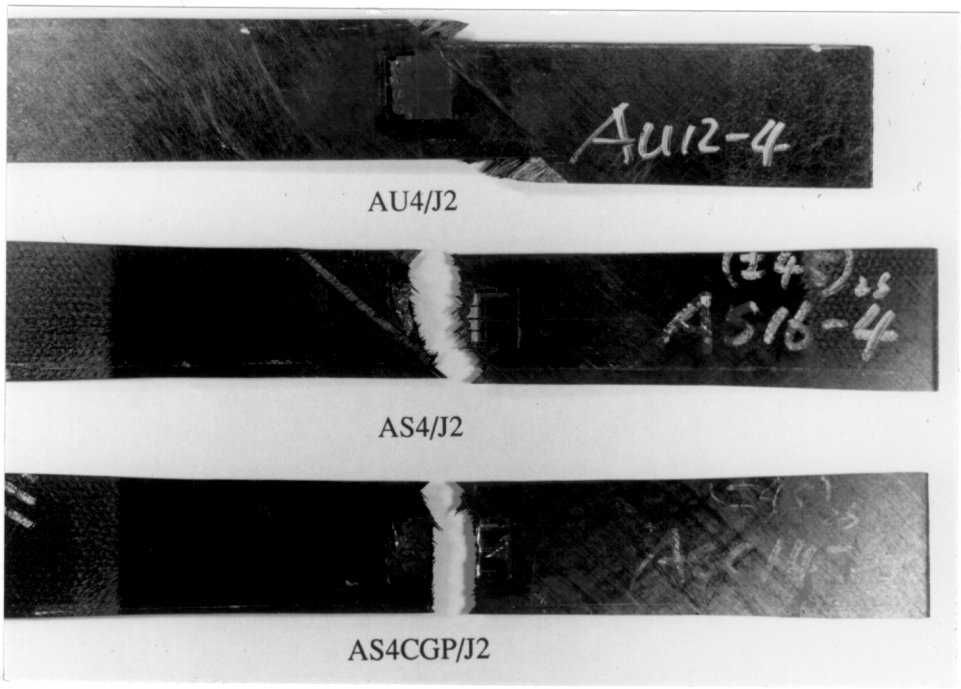

Figure 5-8: A photograph for failed $[\pm 45]_{2s}$ specimens. Fiber slippage is a predominant failure mode in the AU4/J2 composites. Fiber breakage is a predominant failure mode in both AS4(2)/J2 and AS4CGP/J2 composites.

ISS of the AU4/J2 specimens is unable to resist the applied shear stress.

Figure 5-8 shows that both the AS4/J2 and AS4CGP/J2 specimens have experienced severe necking before the failure of the composites occurs. In general, thermoset composites do not exhibit necking phenomenon, as shown in Ref. [8]. The necking behavior in the AS4/J2 and AS4CGP/J2 composites is due to (1) the more ductile nature of thermoplastic polymers without a crosslink structure and (2) good interfacial adhesion in the composites. Also, Figure 5-8 reveals that fiber breakage is a dominant failure mode for both AS4/J2 and AS4CGP/J2 composites. In addition, SEM photomicrographs for the fracture surfaces of the $[\pm 45]_{2s}$ specimens (Figure 5-9(a-c)) show the same fracture features as those of the Figure 5-6(a-c). These observations strongly suggest good adhesion in both AS4/J2 and AS4CGP/J2 composite systems.

5.2.4 Iosipescu Tests

Figure 5-10(a-c) shows shear stress-shear strain curves for all Iosipescu specimens, which are all nonlinear and similar to Figure 5-7(a-c). The shear modulus is calculated in the linear range of the shear strain from 0.05% to 0.4%. The shear moduli of the composites obtained by the Iosipescu tests differ from those obtained by the in-plane shear tests

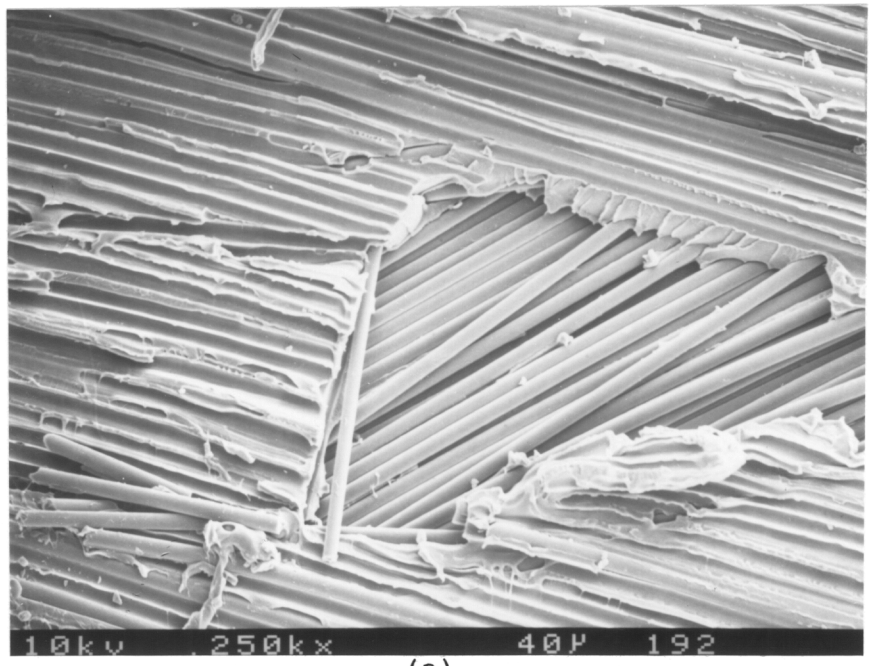

(a)

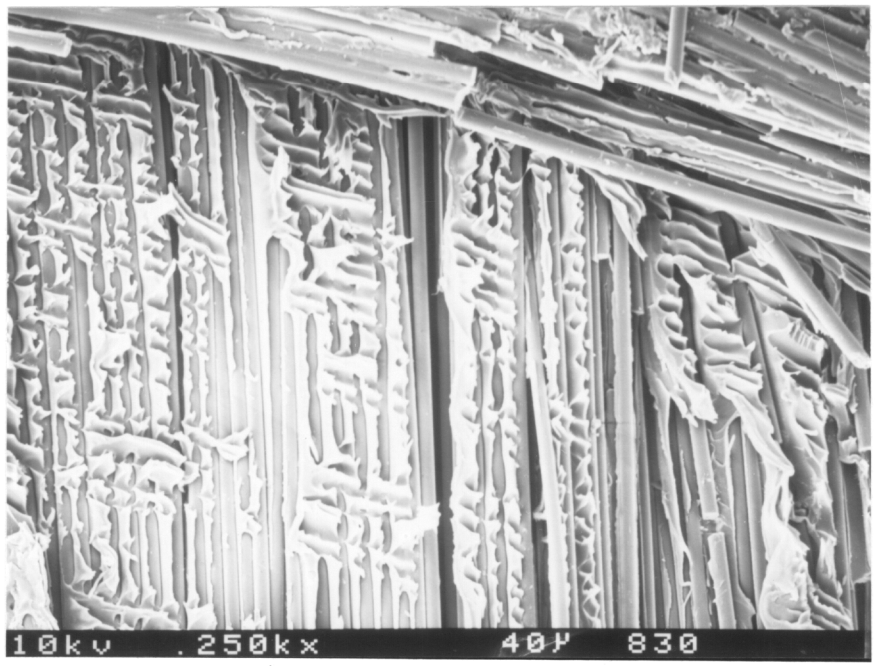

(b)

Figure 5-9: SEM photomicrographs of failed $[\pm 45]_{2s}$ specimens for (a) AU4/J2; (b) AS4(2)/J2; and (c) AS4CGP/J2 composites.

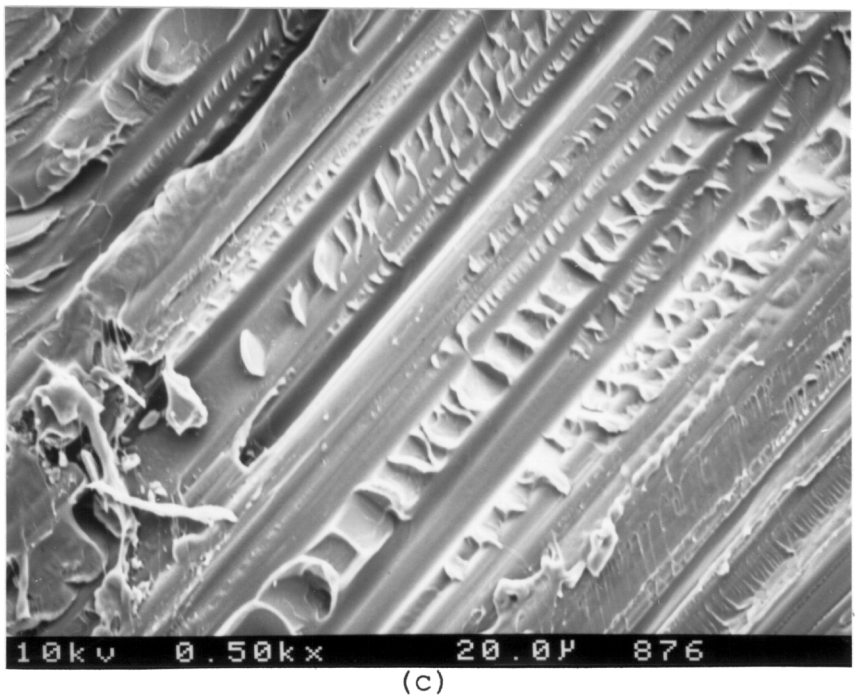

(c)

Figure 5-9: Continued

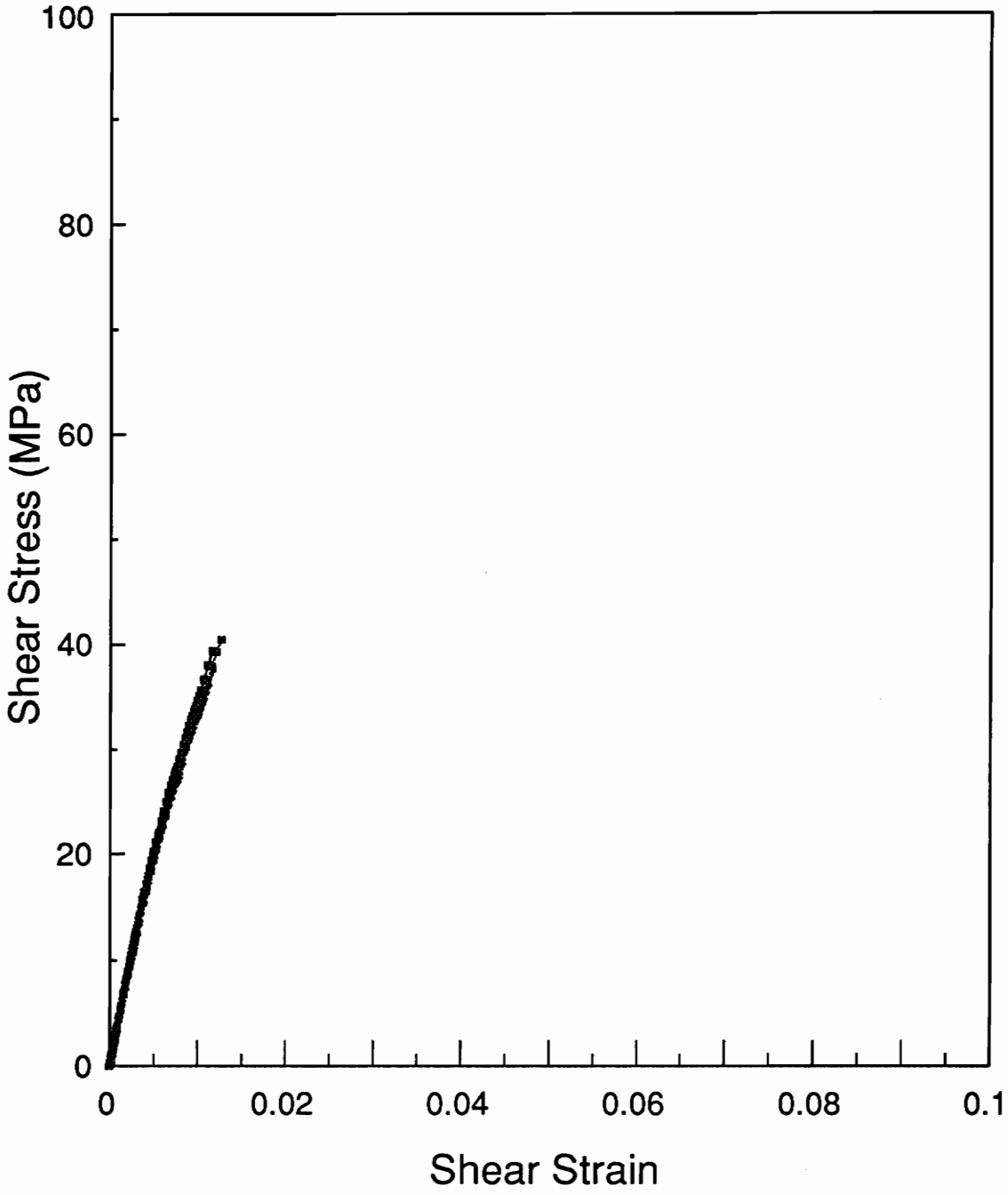

Figure 5-10(a): Shear stress - shear strain curves of Iosipescu tests for the AU4/J2 composites.

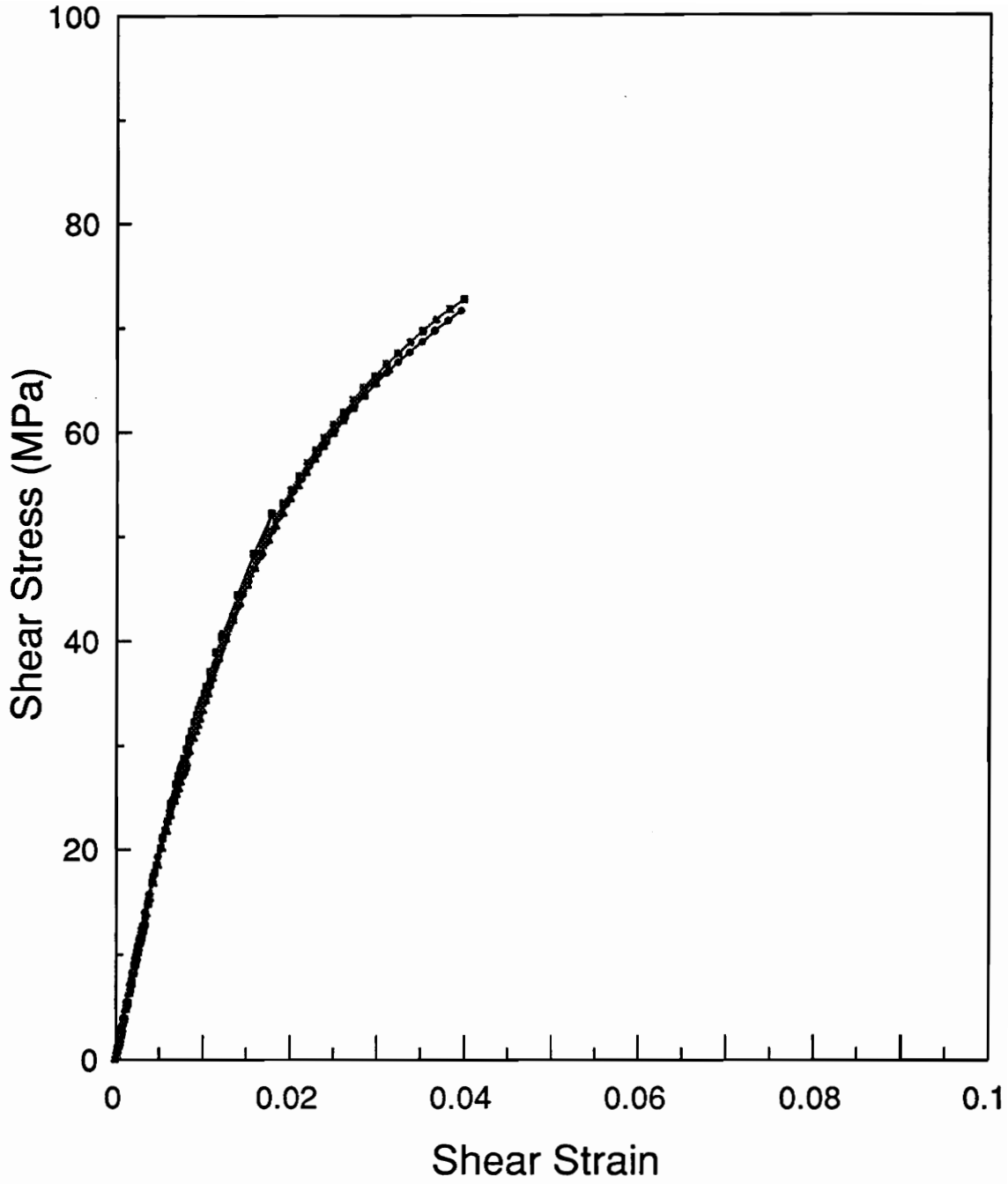

Figure 5-10(b): Shear stress - shear strain curves of Iosipescu tests for the AS4(2)/J2 composites.

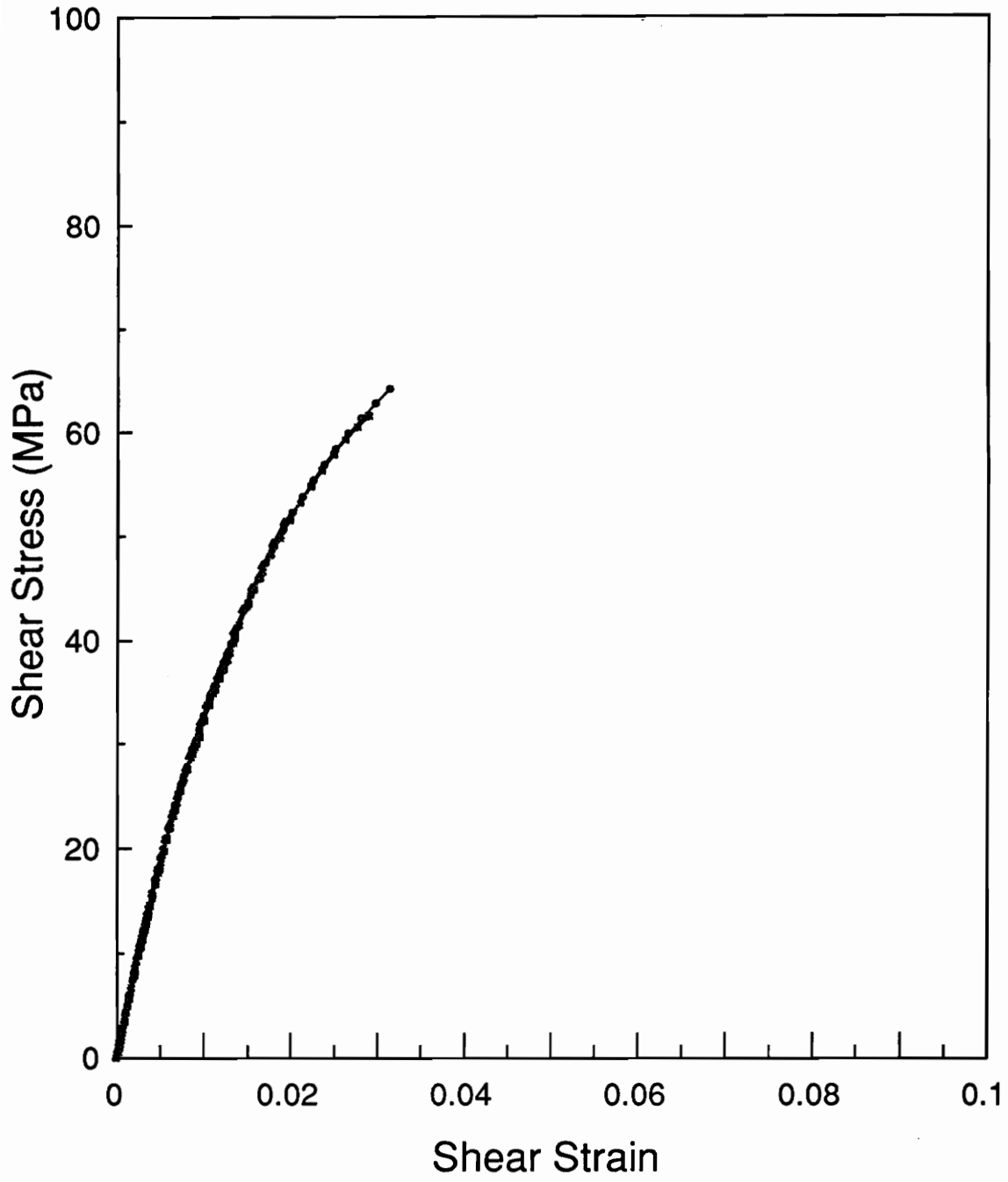

Figure 5-10(c): Shear stress - shear strain curves of Iosipescu tests for AS4CGP/J2 composites.

insignificantly; the difference is less than 5%. This kind of good agreement has been observed for several thermoset composites [9].

SEM photomicrographs of the fracture surfaces for the Iosipescu specimens are shown in Figure 5-11(a-c). Again, clean fiber surfaces are seen in the AU4/J2 specimen and there is little matrix material held in the fibers, as shown in Figure 5-11(a). Figure 5-11(b) shows a large bundle of fiber breakages in the fracture surface. The authors have observed several occurences of this type of fiber breakage in the AS4/J2 specimens. However, many single fiber breakages can be seen in the AS4CGP/J2 specimens. Furthermore, one can see that the direction of hackles in the AS4/J2 specimen is from upper-right to lower-left, which suggests a dominant shear mode failure. (Note that the applied load is along the fiber direction.) On the other hand, Figure 5-11(c) shows that the direction of hackles is upward and the broken fibers are all popped up and toward readers. This phenomenon suggests that a mixed mode failure, the tensile and shear failure, results in the AS4CGP/J2 specimen. Since to break a large bundle of fibers and develop pure shear mode failure requires more energy than to break many single fibers and develop mixed mode failure, it is not surprising that the shear strength of the

AS4/J2 composites is greater than that of the AS4CGP/J2 composites.

5.2.5 $[\pm 45/90_2]_s$ Laminates

We have reported that the transverse tensile and shear strengths of the AS4/J2 composites are greater than those of the AS4CGP/J2 composites. However, the failure strength of the AS4/J2 and AS4CGP/J2 laminates ($[\pm 45/90_2]_s$) are approximately the same. These results show a different order between the laminate failure strength and transverse tensile and shear strength. Noita et al. [2] have also observed a similar phenomena. This inconsistency may be due to the minor effect of the interfacial adhesion in determining the failure strength of composite laminates. Figure 5-12 (a) and (b) are the photos of the failed J2 composite laminates ($[\pm 45/90_2]_s$). Figure 5-12(a) shows a predominant fiber slippage failure in the AU4/J2 composites and fiber breakage failure in the AS4(2)/J2 and AS4CGP/J2 composites. These type of failure modes are similar to those observed for $[\pm 45]_{2s}$, as shown in Figure 5-8. Figure 5-12(b) also shows intraply (90° layers) delaminations in the AU4/J2 laminates. However, the delaminations are not developed in both AS4(2)/J2 and AS4CGP/J2 composite laminates.

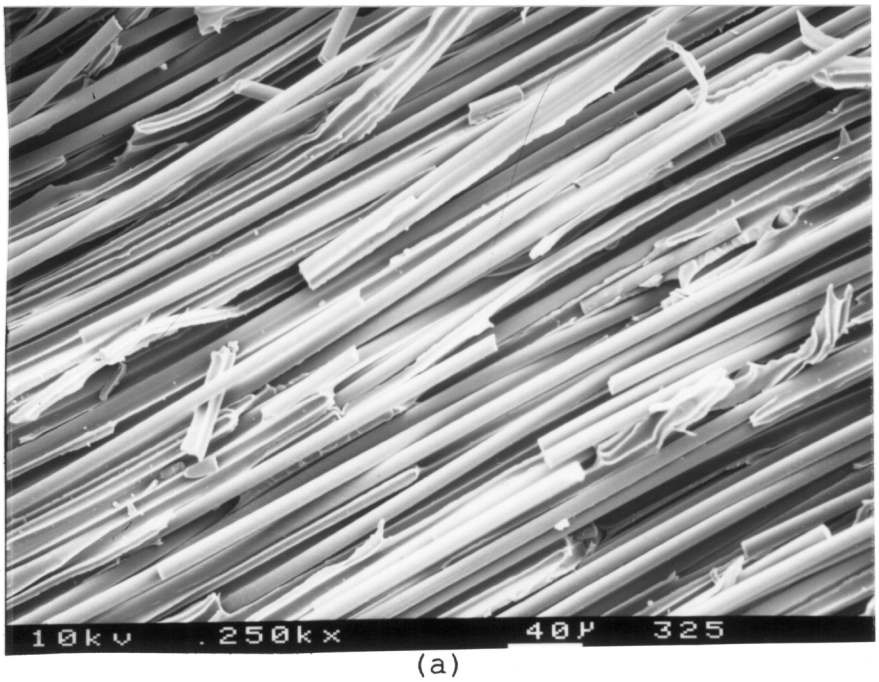

(a)

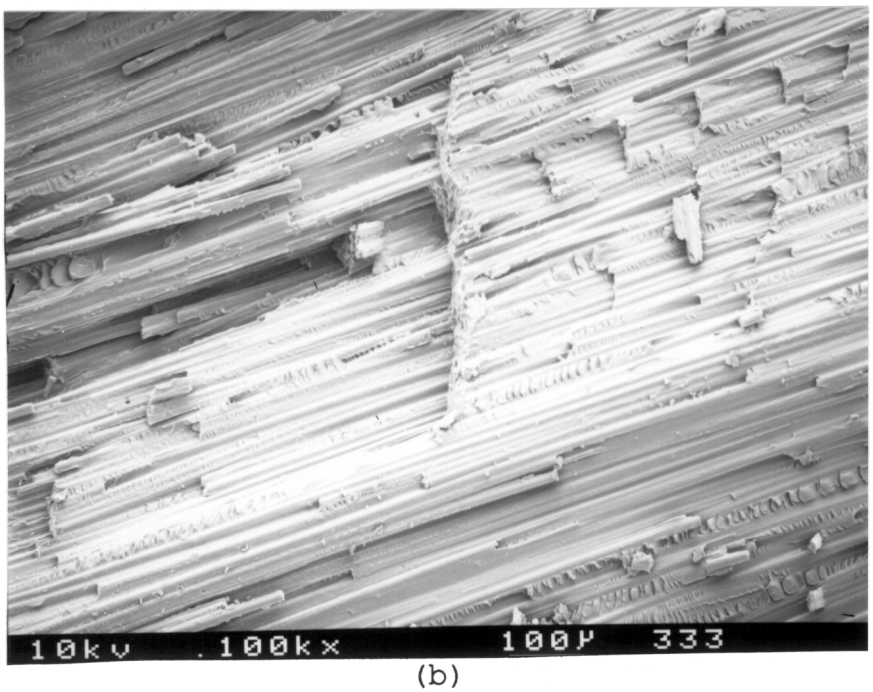

(b)

Figure 5-11: SEM photomicrographs of failed Iosipescu specimens for (a) AU4/J2; (b) AS4(2)/J2; and (c) AS4CGP/J2 composites.

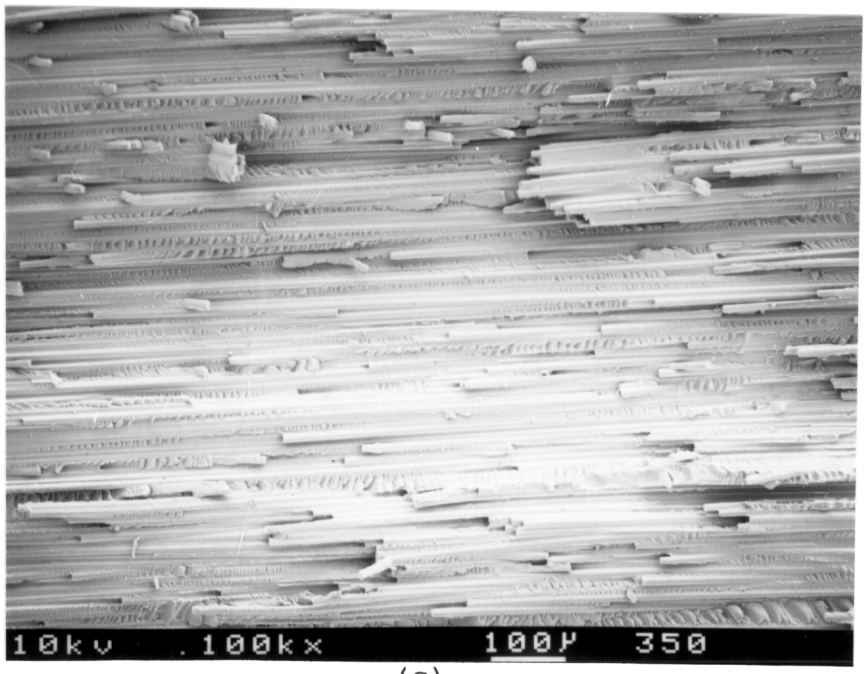

(c)

Figure 5-11: Continued

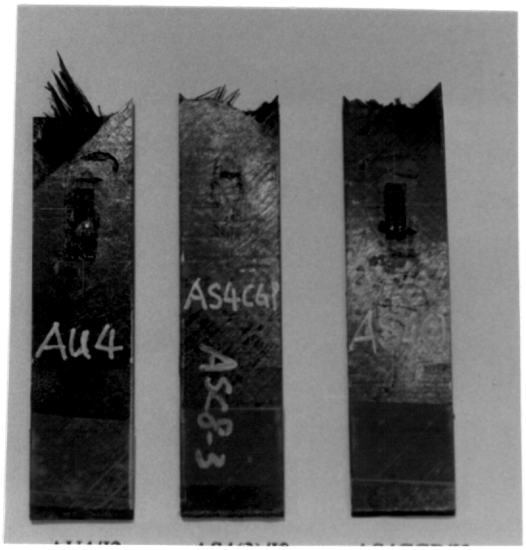

(a)

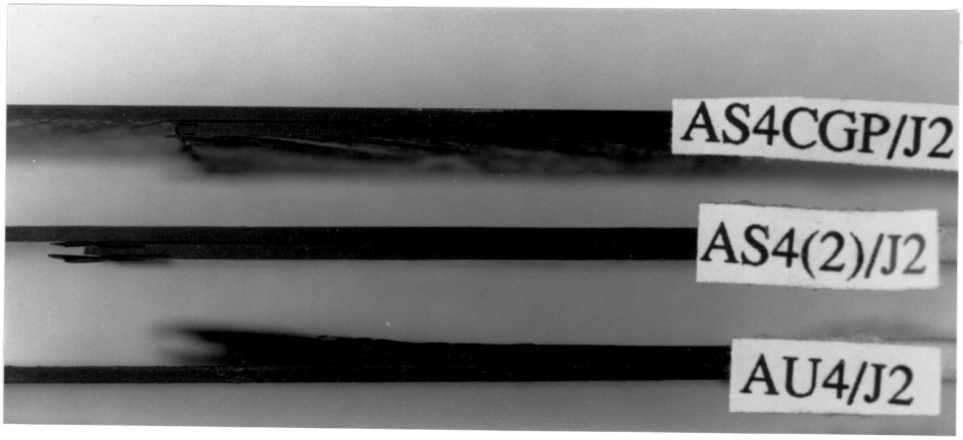

(b)

Figure 5-12: Photos of failed $[\pm 45/90_2]_s$ specimens for J2 composites. (a) top view: fiber slippage in the AU4/J2 composites and (b) side view: delamination in the AU4/J2 composites.

5.3 Summary

With an increase of ~22% of the ISS in the AS4(2)/J2 and AS4CGP/J2 composites, both the transverse tensile and shear strengths increase roughly 60% over that of the AU4/J2 composites. The static moduli of the AU4/J2, AS4(2), and AS4CGP/J2 composites are insensitive to the ISS. The lamina strengths of the AS4(2)/J2 composites are greater than those of the AS4CGP/J2 composites. However, the laminate strengths for both AS4(2)/J2 and AS4CGP/J2 composites are approximately the same.

REFERENCES

[1] Madhukar, M. S. and Drzal, L. T., "Fiber-Matrix Adhesion and Its Effect on Composite Mechanical Properties: II. Longitudinal (0°) and Transverse (90°) tensile and Flexure Behavior of Graphite/Epoxy Composites", Journal of Composite Materials, Vol. 25, 1991, pp. 958-991.

[2] Norita, T., Matsui, J., and Matsuda, H. S., "Effect of Surface Treatment of Carbon Fiber on Mechanical Properties of CFRP", in Composite Interfaces, Ed. by, Ishida, H. and Koenig, J. L., Elsevier Science Publishing Co., 1986, pp. 123-132.

[3] Drzal, L. T., "Composite Interphase Characterization," SAMPE Journal, Vol. 5, 1983, pp. 7-13.

[4] Rosen, B. W., "Tensile Failure of Fibrous Composites," American Institute for Aerospace and Aerodynamic Journal, Vol. 2, No. 11, 1964, pp. 1985-1991.

[5] Carman, G. P., Averill, R., Reifsnider, K. L., and Reddy, J. N., "Optimization of Fiber Coating to Minimize the Stress State in Composite Materials," Submitted to Journal of Composite Materials, April, 1992.

[6] Christensen, R. M., and Waals, F. M., "Effective Stiffness of Randomly Oriented Fiber Composites", Journal of Composite Materials, Vol. 6, pp. 518-532, 1972.

[7] Williams, J. G., Donnellan, M. E., James, M. R., and Morris, W. L., "Elastic Modulus of the Interphase in Organic Matrix Composites", in Interfaces in Composites, Ed. by Pantano, C. G. and Chen, E. J. H., Materials Research Society Symposium Proceedings Vol. 170, pp.285-290, 1989.

[8] Madhukar, M. S. and Drzal, L. T., "Fiber-Matrix Adhesion and Its Effect on Composite Mechanical Properties: I. Inplane and Interlaminar Shear Behavior of Graphite/Epoxy Composites", Journal of Composite Materials, Vol. 25, 1991, pp. 932-958.

[9] Lee, S., Munro, M., and Scott, R. F., "Evaluation of Three In-Plane Shear Test Methods for Advanced Composite Materials", Composites, Vol. 21, no. 6, pp. 495-502, 1990

Chapter 6

CREEP AND CREEP RUPTURE OF J2 COMPOSITES

Static mechanical properties of the AU4/J2, AS4(2)/J2, and AS4CGP/J2 composites have been characterized and discussed in chapter 5. It has been shown that the lamina strengths of the AS4(2)/J2 composites are greater than those of the AS4CGP/J2 composites. However, the laminate strengths are approximately the same for the AS4(2)/J2 and AS4CGP/J2 composites. This chapter will then focus on the effect of the interphase properties on the creep rupture life of the three composite systems.

6.1 Dynamic Mechanical Properties of Composites

The T_g's of the composites are shown in Table 6-1. It should be noted that the T_g's (shown in Table 6-1) were an average of three samples; the T_g's of each composite systems had ~0.5°C deviation, according to the DMA results. The T_g's of the composites are ~20°C higher than that of the J2 polymer [1]. The increase of the T_g has been attributed to the interaction between the fiber and matrix. The interaction restricts the mobility of polymer molecules and results in raising the T_g [2,3]. The T_g's for each type of composite laminates do not differ significantly, as shown in

Table 6-1. Ko et al. [4] have also shown that there is little difference in the T_g of the AU4 and AS4 fiber in EPON-828/mPDA. The present results are in good agreement with Ko's results. Thus, the surface treatment on the AS4(2) and AS4CGP fibers does not have a significant effect on the T_g's of the J2 composites.

Table 6-1 T_g and Height of the tan(δ) Peak

	AU4/J2 T_g/Height	AS4(2)/J2 T_g/Height	AS4CGP/J2 T_g/Height
$[0°]_8$*	179/0.572	180/0.541	179/0.479
$[\pm 45°]_{2s}$*	181/0.549	181/0.600	179/0.711
$[90°]_{12}$**	181/0.709	178/0.954	178/1.06

* : measurement at 1 Hz; **: measurement at 3.2 Hz.

Figure 6-1(a-c) shows the traces of the log(E') and tan(δ) vs. temperature for $[0]_8$, $[\pm 45]_{2s}$, and $[90]_{12}$ specimens. It should be noted that the results in Figure 6-1(b) were obtained at 3.2 Hz because the tan(δ) (at 1 Hz) does not form a peak at the T_g's. The authors have observed a "bump" (not a sharp peak) at about 275°C for both $[0]_8$ and $[\pm 45]_{2s}$ specimens. Thomason [5] has concluded that the bump was an artefact and was formed due to a complex combination of the instrument parameters and sample properties. Thus, the authors do not show the data for temperatures that are beyond 200°C in Figure 6-1(a-b). Figure 6-1(a-c) shows only a small difference for the E' of the composites in the

glassy state, suggesting a minor influence of the interphase. This also confirms a small difference in the E_{11}, E_{22} and G_{12} of the $[0]_8$, $[\pm45]_{2s}$ and $[90]_{12}$ specimens. However, the difference of the E′ becomes distinguishable in the glass transition and rubbery regions. For the matrix dominated composite laminates, the E′ of the AS4CGP/J2 composites is the lowest perhaps because of the existence of the compliant interphase. In addition, the highest value for the E′ in the AU4/J2 composites may be due to the broken fiber effect, as mentioned in the previous section.

The heights of the tan(δ) vs. temperature at T_g for $[\pm45]_{2s}$ and $[90]_{12}$ specimens are also listed in Table 6-1. Since loss factor (tan(δ)) is the ratio of loss modulus (E") to storage modulus (E′), a smaller E′ results in a higher tan(δ) value. For most advanced polymeric composites at a temperature below T_g, a storage modulus (E′) was approximately equal to the corresponding Young's modulus, e.g., E_{22} of $[90]_{12}$ specimens. Figure 6-1 has shown that the trends of the E′ for the $[0]_8$, $[90]_{12}$ and $[\pm45]_{2s}$ specimens are consistent with the trends of the E_{11}, E_{22} and G_{12}. Thus the trends for the height of the tan(δ) peaks for the $[0]_8$, $[\pm45]_{2s}$, and $[90]_{12}$ specimens are in a reversed order to those of the E_{11}, E_{22} and G_{12} of the composites. The present observations are consistent with the published results [4].

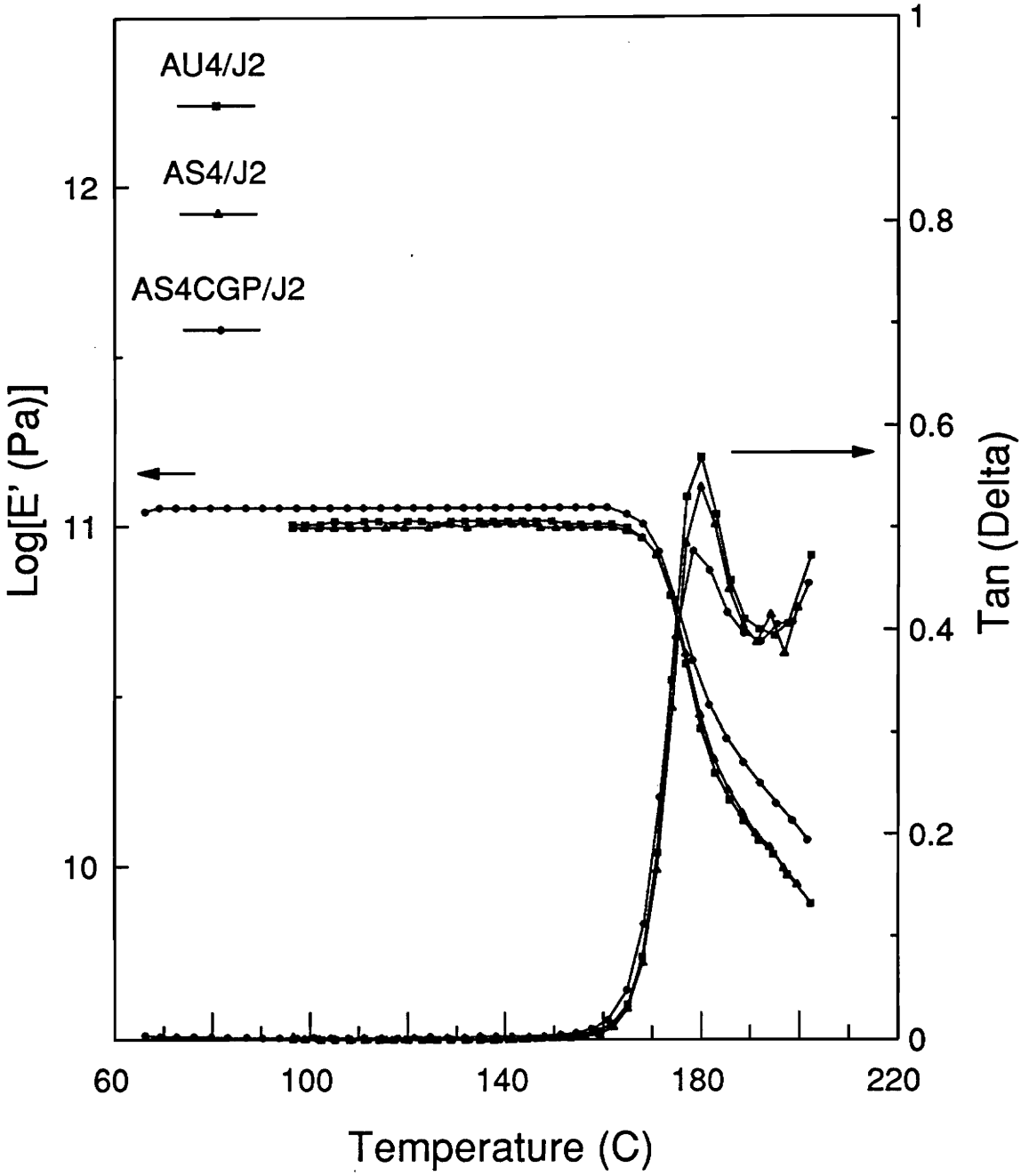

Figure 6-1(a): DMA results of Log(E') and Tan(Delta) vs. Temperature plot for [0] specimens at 1 Hz.

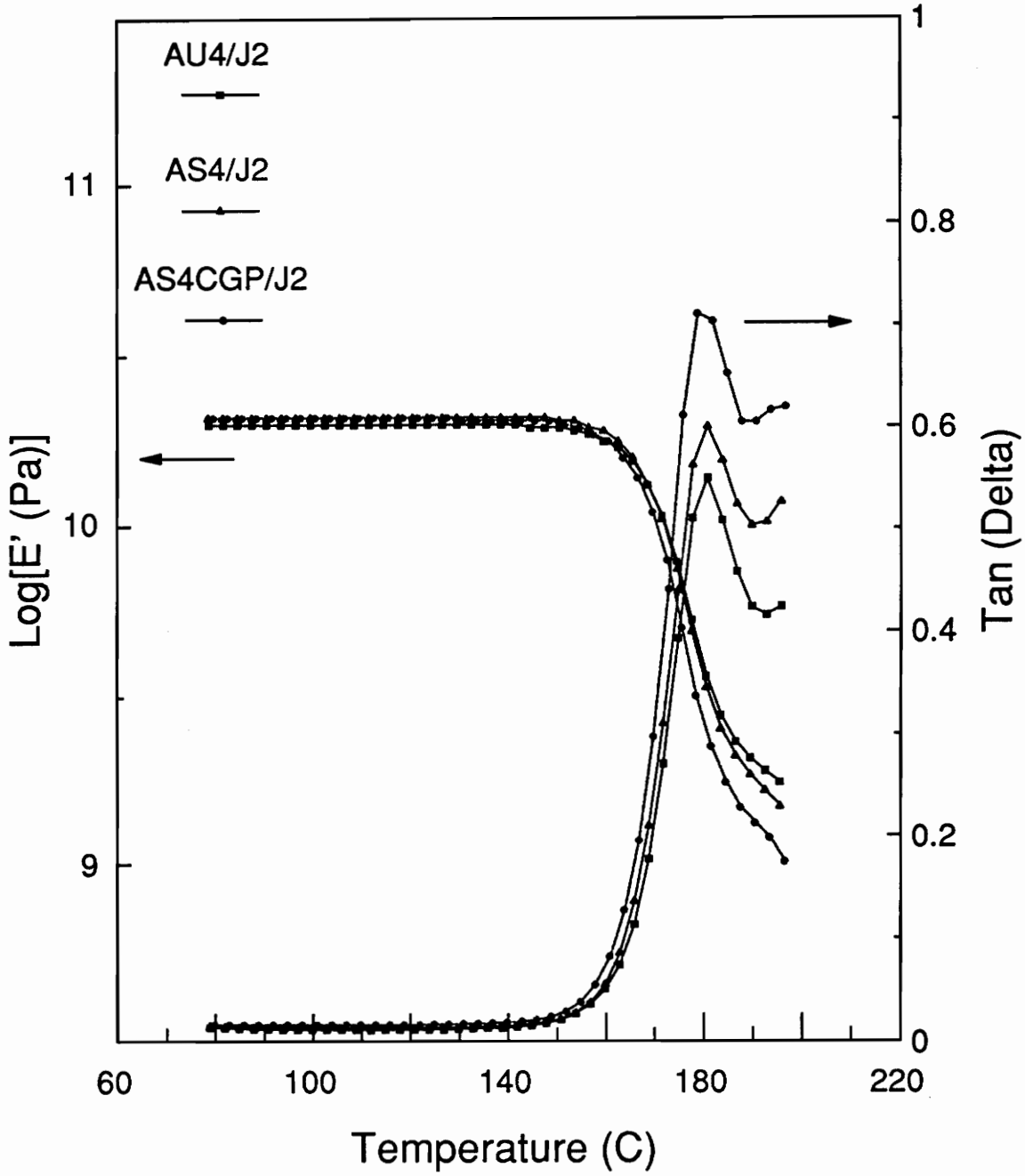

Figure 6-1(b): DMA results of Log(E') and Tan(Delta) vs. Temperature plot for [45/-45](2s) specimens at 1 Hz.

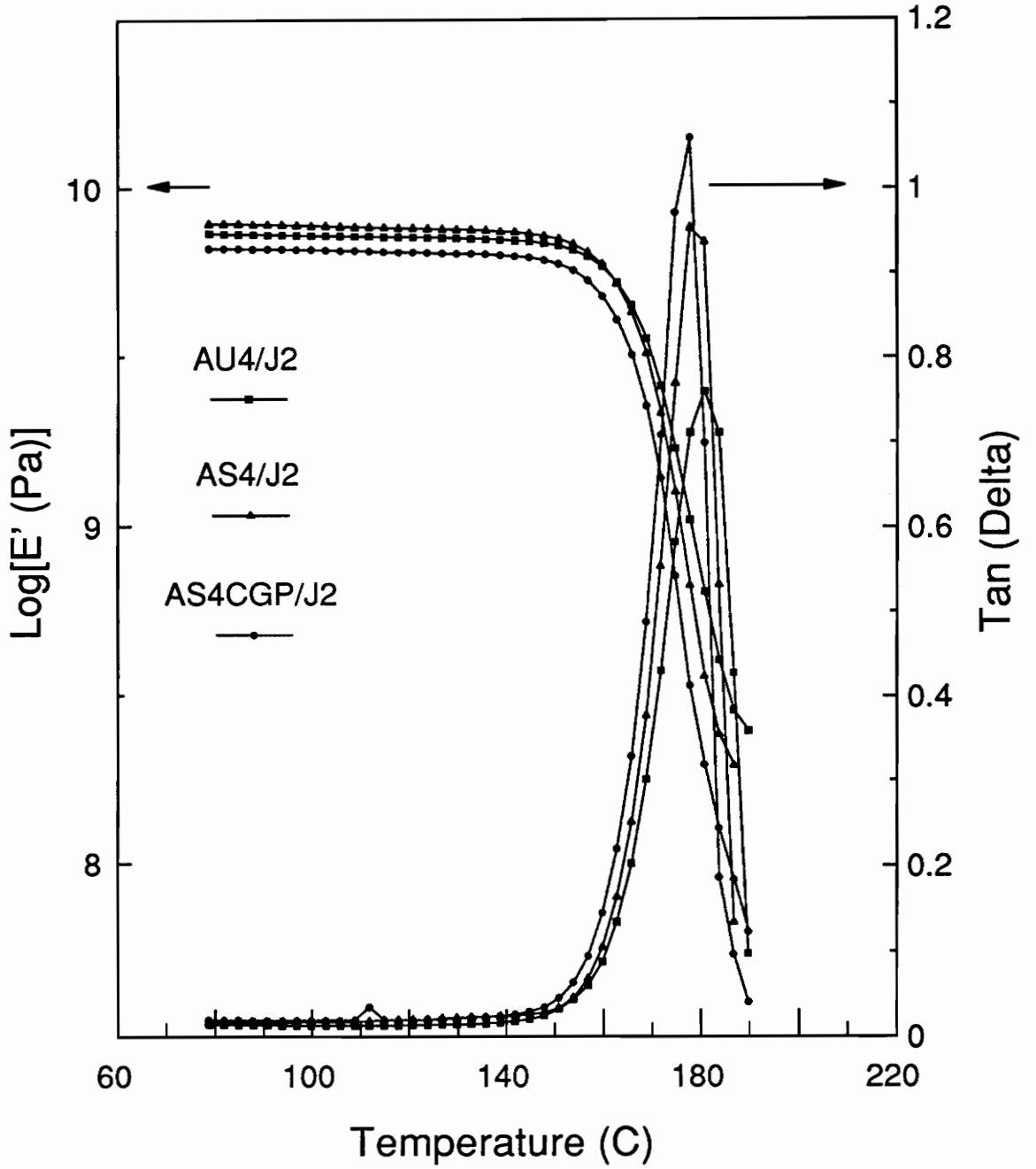

Figure 6-1(c): DMA results of Log(E') and Tan(Delta) vs. Temperature plot for [90](12) specimens at 3.2 Hz.

6.2 Creep and Creep Rupture of J2 Composites

Short term creep and recovery tests have been conducted at low stress levels. According to the user's manual [6], the maximum strain of the outer surface is ~0.1% for the tested J2 composite laminates with known dimensions. Thus, it is believed that the creep and recovery tests were performed in the linear viscoelastic range.

A typical plot for creep compliance curves at elevated temperatures of AS4CGP/J2 $[90]_{12}$ specimen is shown in Figure 6-2. Based on the time-temperature superposition principle (TTSP) [7], a master curve can be formed by shifting creep compliance curves horizontally with respect to a reference curve. The scheme to shift the creep compliance curve has been described in detail in Ref. [7]. Shift factors ($\log(a_T)$) are obtained by shifting each curve along the log(time) axis with respect to the reference curve. The reference temperature for all master curves is 109°C. The master curves of the annealed and unannealed composite $[90]_{12}$ specimens are shown in Figure 6-3. It is known that the annealing process densifies polymers and results in increasing the modulus of the polymers [8]. Thus, as expected, the annealed specimens become stiffer and thus the corresponding master curves shift to the right, when compared to the unannealed specimens. Figure 6-3 also shows that the AU4/J2 composites are stiffer than the AS4(2)/J2

and AS4CGP/J2 composites, which is in good agreement with the corresponding E_{22}. To reach the same compliance level at elevated temperatures, the annealed specimens require more time, ~1.2 decades, than the unannealed specimens do for AU4/J2, AS4(2)/J2, and AS4CGP/J2 composites. The same amount of time difference is within our expectation because the composites used for the DMA creep tests are $[90]_{12}$ laminates which are matrix dominated. Figure 6-4 shows the master curves of the annealed $[\pm 45]_{2s}$ specimens, which show a similar trend to that of Figure 6-3.

The Arrhenius type equation is commonly used to describe the relationship between the $\log(a_T)$ and 1/T below the T_g. The Arrhenius equation is

$$\log(a_T) = \frac{-H_a}{2.303R}\left(\frac{1}{T} - \frac{1}{T_0}\right) \qquad (6.1)$$

where H_a is the activation energy, T_0 is the reference temperature. An Arrhenius type equation is generally applicable below the T_g. The activation energy can be obtained from the slope of the $\log(a_T)$ vs. 1/T plot. Typical Arrhenius plots for the tested composites are shown in Figure 6-5. It is apparent that the data falls onto two straight lines which intersect at approximately 145°C. The

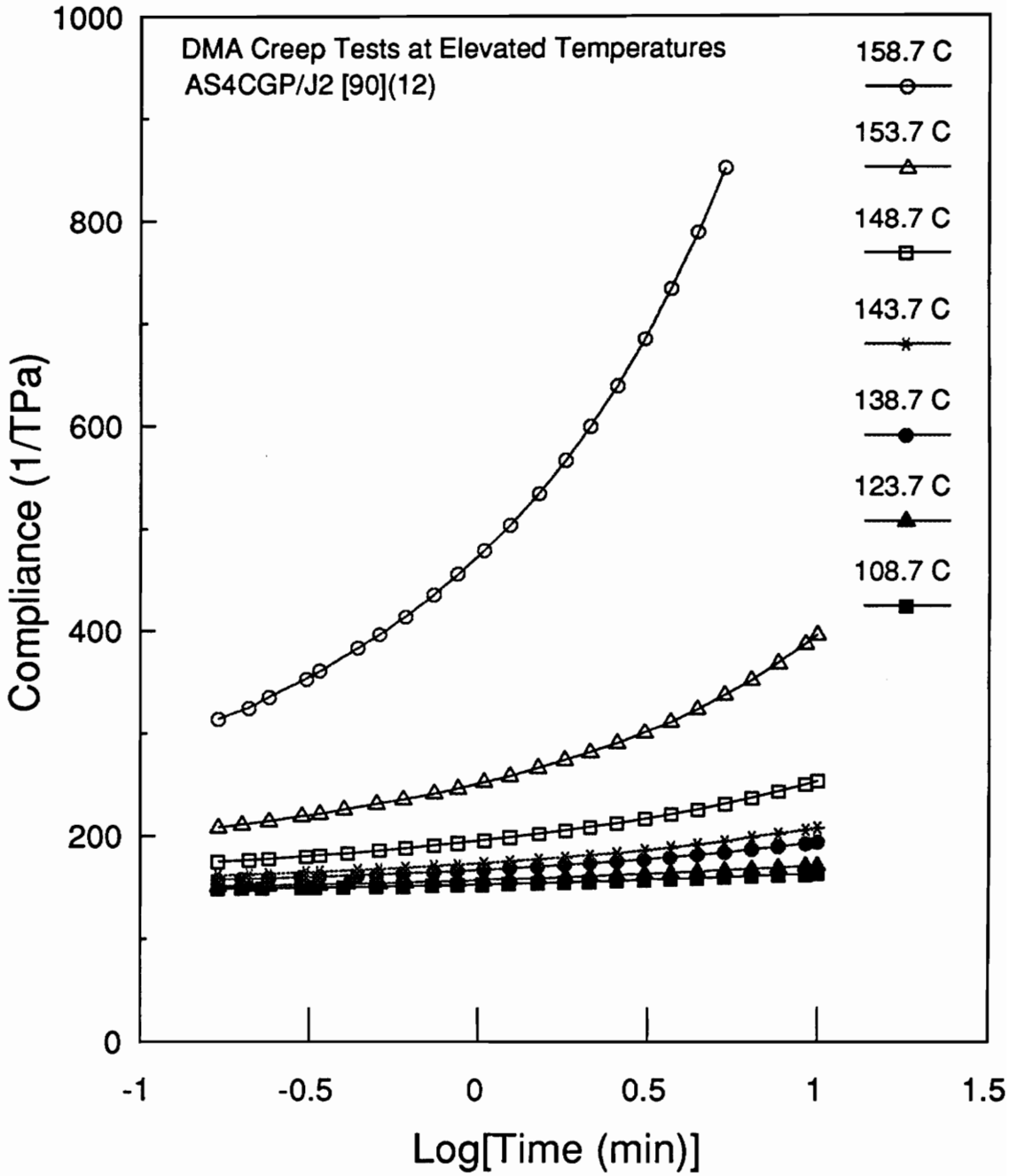

Figure 6-2: Typical creep compliance curves at elevated temperatures for the AS4CGP/J2 [90](12) specimen.

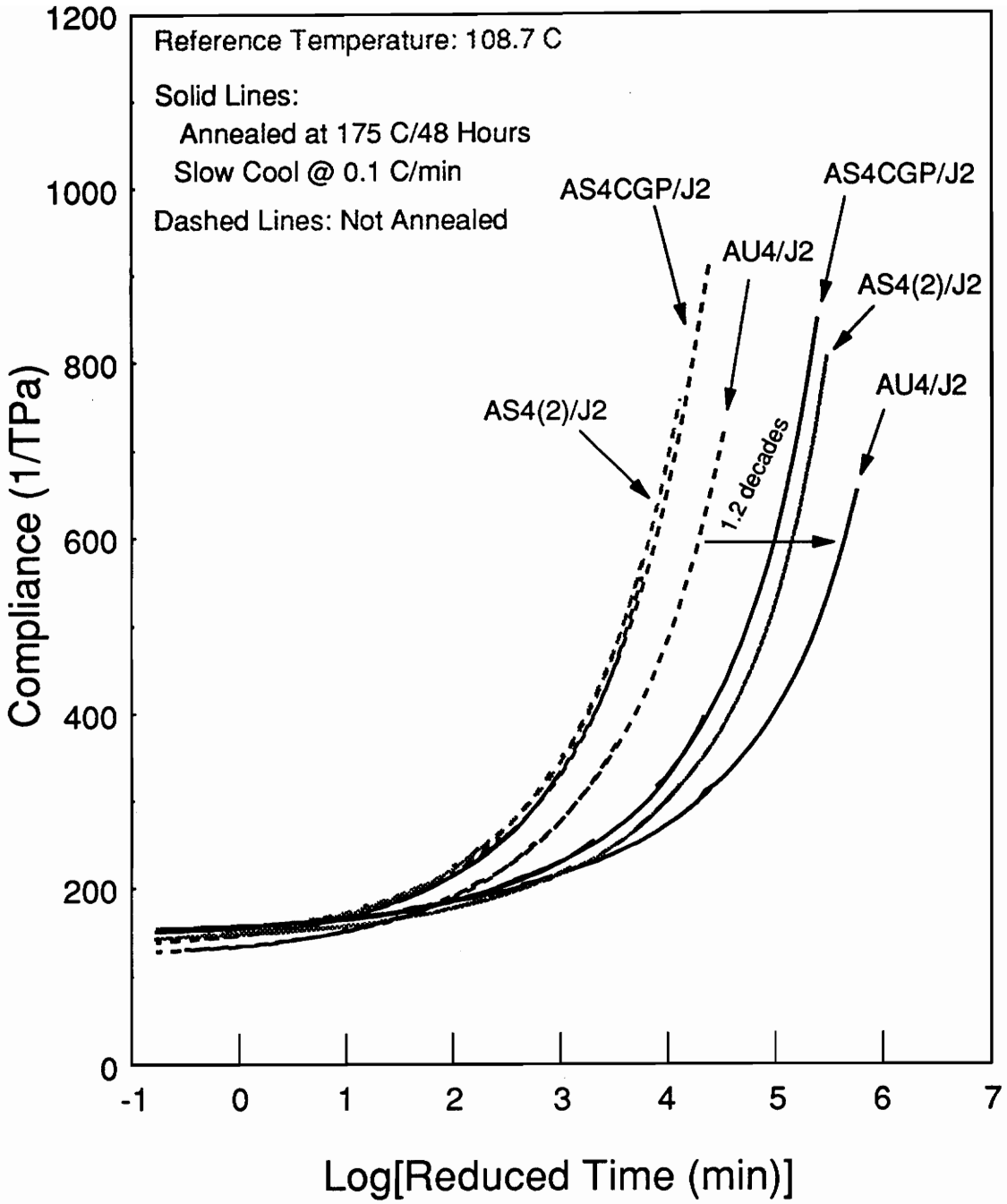

Figure 6-3: Master curves of J2 composite [90] specimens.

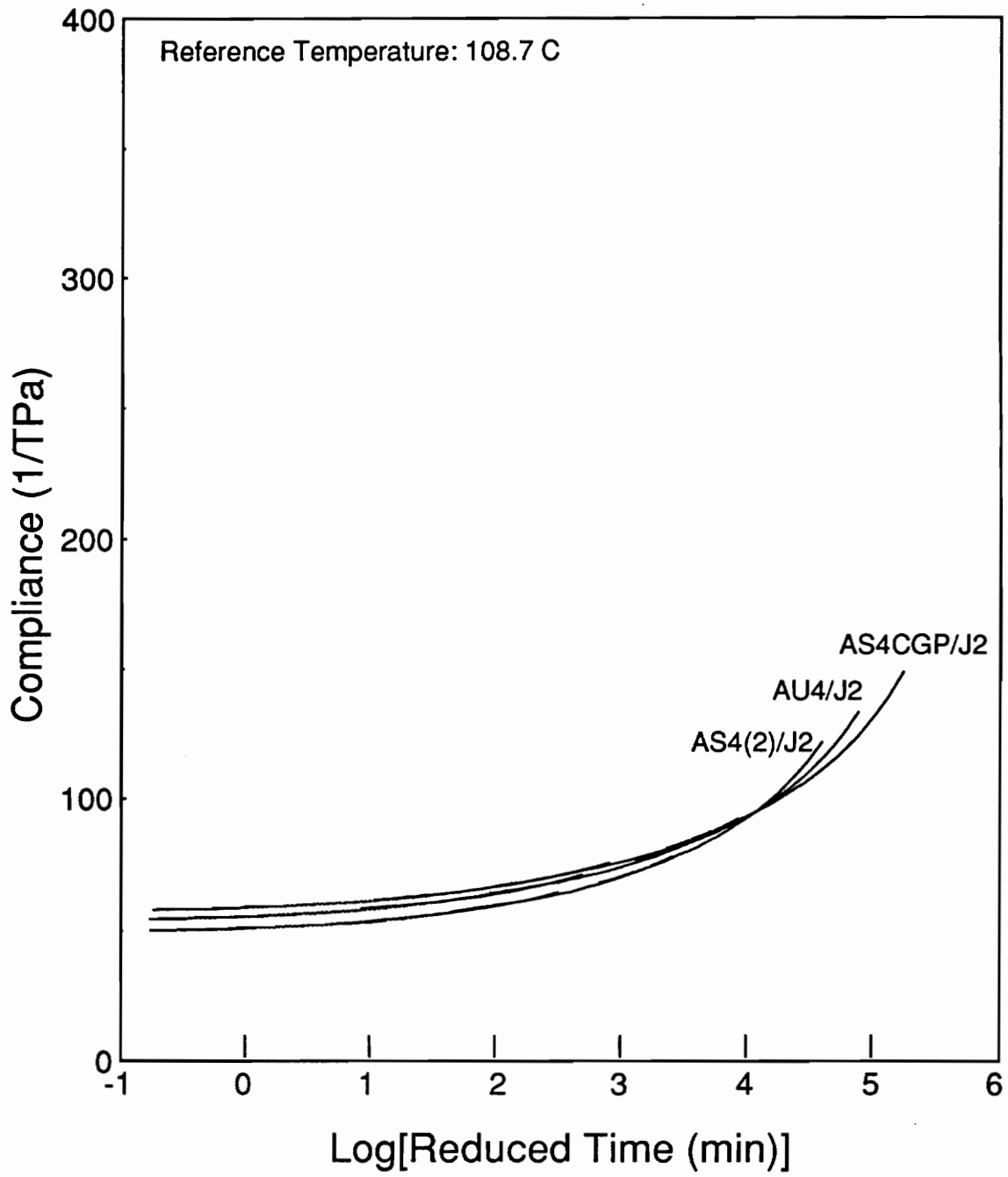

Figure 6-4: Master curves of J2 composite [45/-45](2s) specimens.

change of the slope can be confirmed by referring to Figure 6-1. Figure 6-1 shows that tan(δ) starts to increase and log(E') starts to drop at approximately 145°C, which is the onset temperature of the glass transition region. Thus the change of the slope suggests a change of relaxation mechanism of molecular motion; i.e., from the glassy state to the glass transition region. In the glassy state, the relaxation is due to the motion of side-groups. However, within the glass transition region, the relaxation depends on main-chain motion. The main-chain motion requires more energy than the side-group motion does. As a result, the activation energy of the glass transition region is higher than that of the glassy state, as indicated in Figure 6-5. It is noticed that the difference in the activation energy of the $[90]_{12}$ and $[\pm 45]_{2s}$ is minor. Figure 6-5 shows that the slopes of the three sets of data for the $[90]_{12}$ specimens are very close to each other. This suggests the interphase has little influence on the activation energy. Similarly, one can see that the slopes of the three sets of data for the $[\pm 45]_{2s}$ specimens are also nearly equal. This insensitivity of the ISS to activation energy has been also reported by Kimoto [9].

Figure 6-6 shows the creep rupture results for the AU4/J2, AS4(2)/J2, and AS4CGP/J2 laminates ($[\pm 45/90_2]_s$). The data are within the experimental scatter and show a

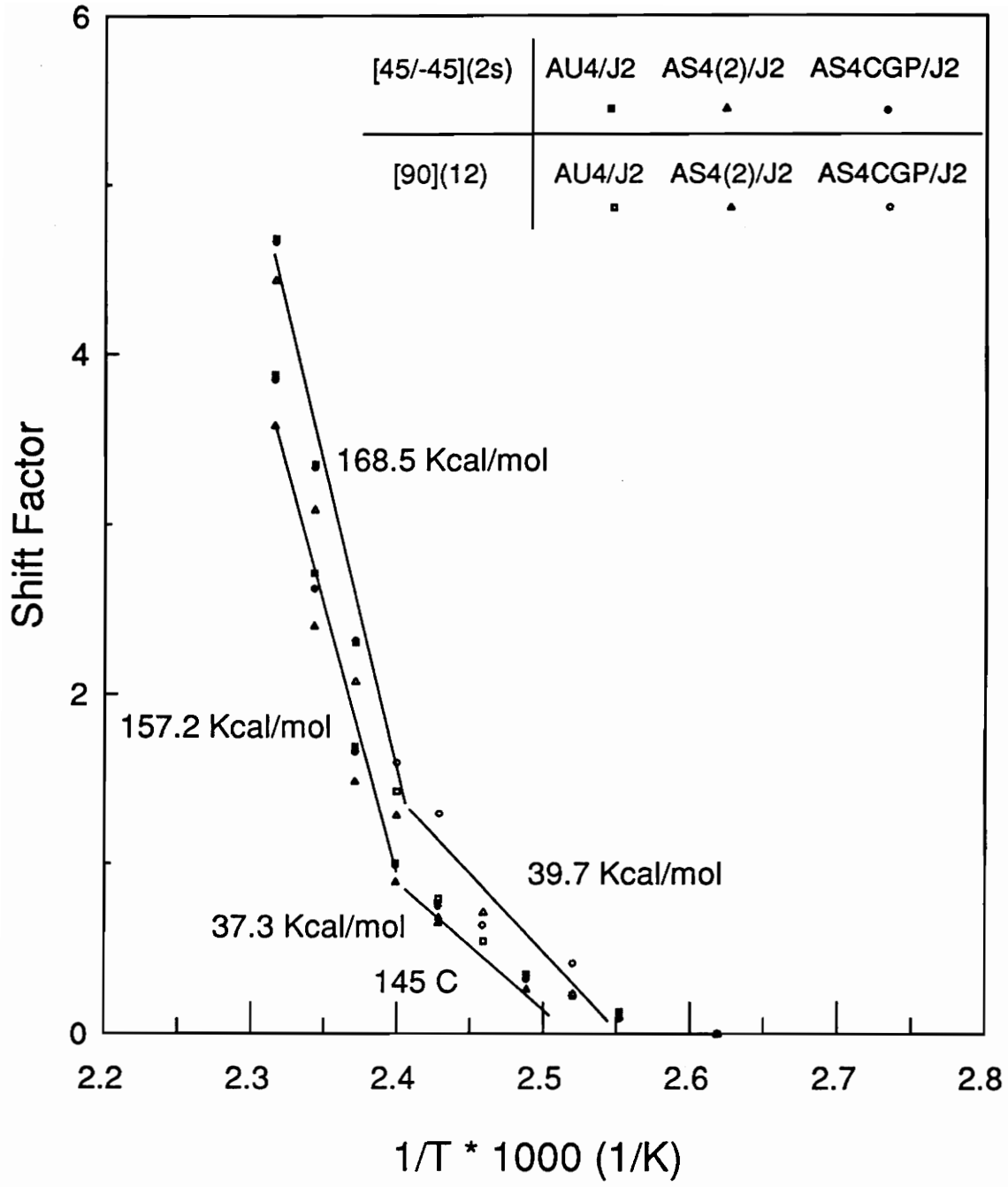

Figure 6-5: Arrhenius plots for J2 composites.

distinguishable trend for each composite system. As shown in Figure 6-6, these lines are fairly parallel to each other. This suggests that the degradation rate of the creep rupture strength for these three laminates is approximately the same. It is noticed that the creep rupture strengths of the composite laminates degrade approximately 9% within five decades.

The degradation rate of the creep rupture strength of the AU4/J2, AS4(2)/J2, and AS4CGP/J2 laminates is insensitive to the fiber surface properties, although interfacial quality does change the static mechanical properties. On the other hand, the fiber-matrix bond characteristics do affect the long term mechanical performance. One may recall that the quasi-static tensile strengths of the ($[\pm 45/90_2]_s$) laminates are approximately the same for both AS4(2)/J2 and AS4CGP/J2 composites. However, the creep rupture strength of the AS4CGP/J2 composites is greater than that of AS4(2)/J2 composites. It is believed that fiber fracture played an important in the creep performance of these laminates. Except for the AU4/J2 laminate, fiber breakage is a dominant failure mode, as illustrated in Figure 5-12. This type of failure mode is also observed on laminates under the creep rupture tests. According to Batdrof [10], the strength of the composites can be improved by reducing the stress concentration in the

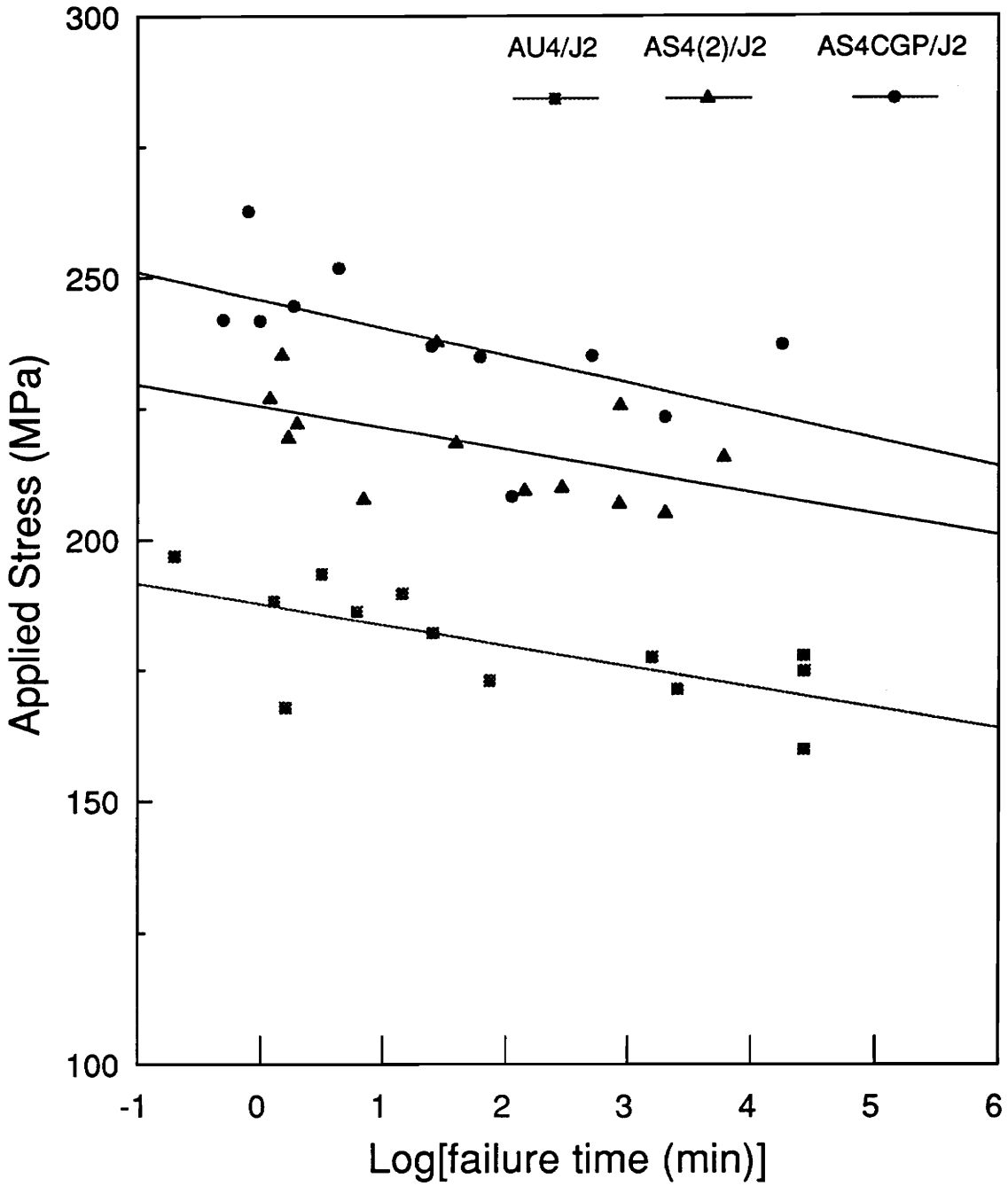

Figure 6-6: Creep rupture tests at 120 C for the AU4, AS4(2)/J2, and AS4CGP/J2 laminates ([45/-45/90(2)](s)).

neighborhood of broken fibers. Thus, the presence of a deliberately applied interphase, e.g., the epoxy sizing of the AS4CGP/J2 composites, could tend to blunt and/or arrest the cracks and result in lowering the stress concentration. Consequently, for a fixed life-time, the creep rupture strength of the AS4CGP/J2 laminates is greater than that of the AS4(2)/J2 laminates.

Figures 6-7 and 6-8 show the fracture surfaces of the specimens failed at an intermediate and long creep rupture life for AU4/J2, AS4(2)/J2, and AS4CGP/J2 laminates. Figure 6-7(a) shows clean fiber surfaces (at 45/-45 plies) in AU4/J2 laminates. Figure 6-7(b) shows that matrix was pulled up toward the readers at the 45/-45 interface in the AS4(2)/J2 laminates. River patterns were observed in Figure 6-7(c) for the AS4CGP/J2 laminates at the 45/-45 interface.

For long creep rupture life, severe plastic deformation was observed in the other three composite systems, see Figure 6-8(b) and 8(c). Nonetheless, clean fiber surfaces were still observed in AU4/J2 composites.

6.3 Summary

The T_g's of the J2 composites are insensitive to the interfacial adhesion between fibers and J2 matrix. In addition, the creep response of the tested J2 composites is not affected by the fiber-matrix adhesion. Despite the

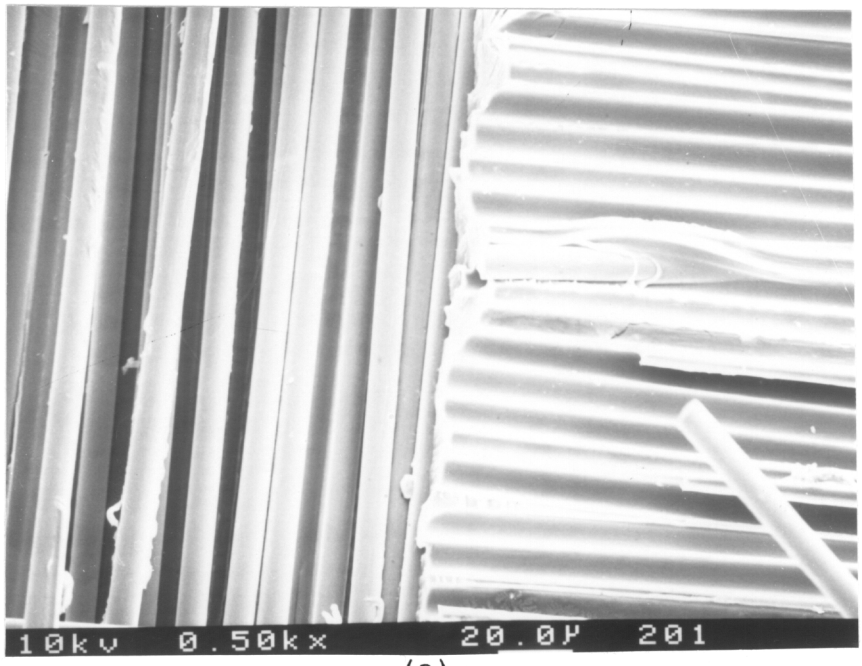

(a)

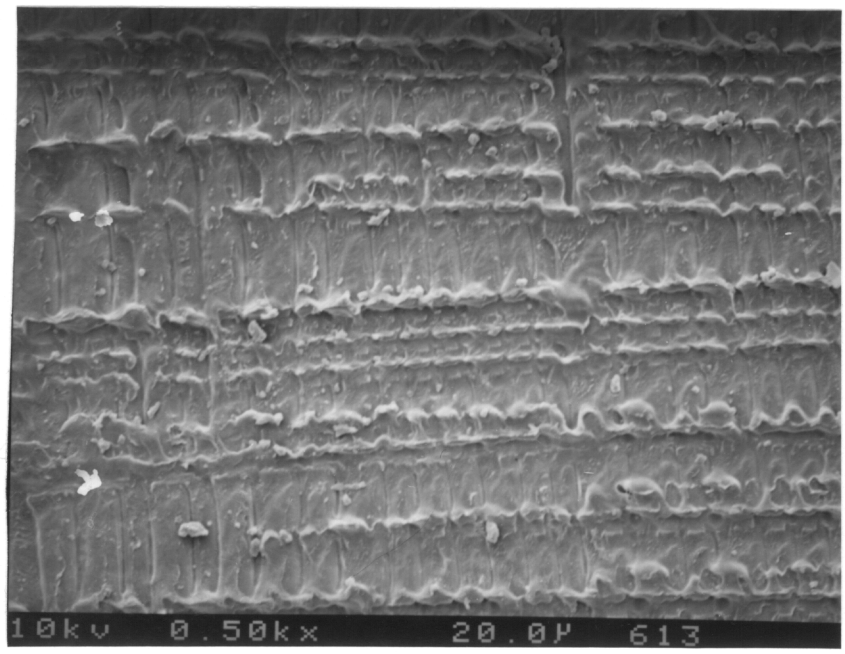

(b)

Figure 6-7: SEM photomicrographs of failed specimens ($[\pm 45/90_2]_s$) with intermediate creep rupture life for (a) AU4/J2; (b) AS4(2)/J2; and (c) AS4CGP/J2 composites.

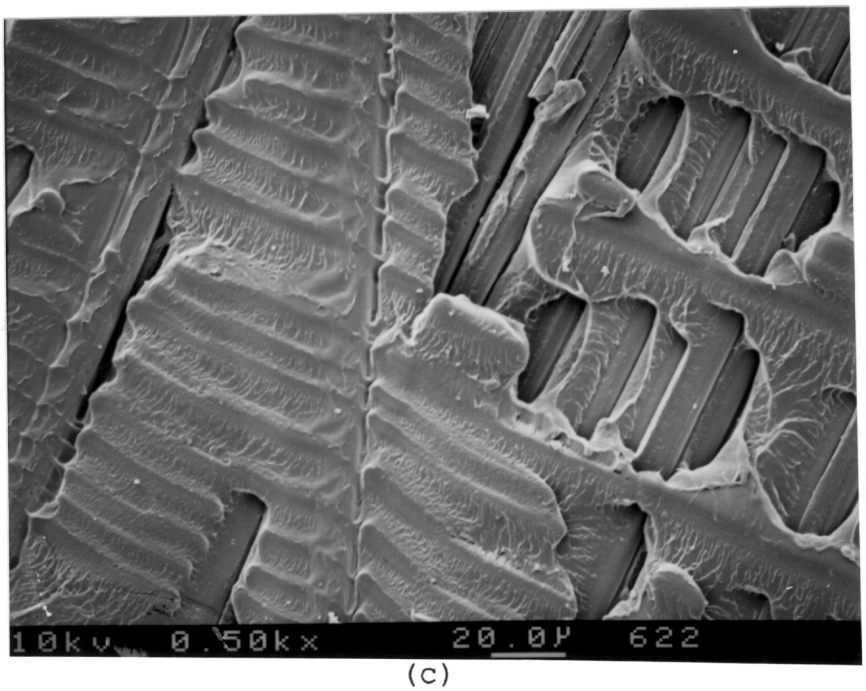

(c)

Figure 6-7: Continued

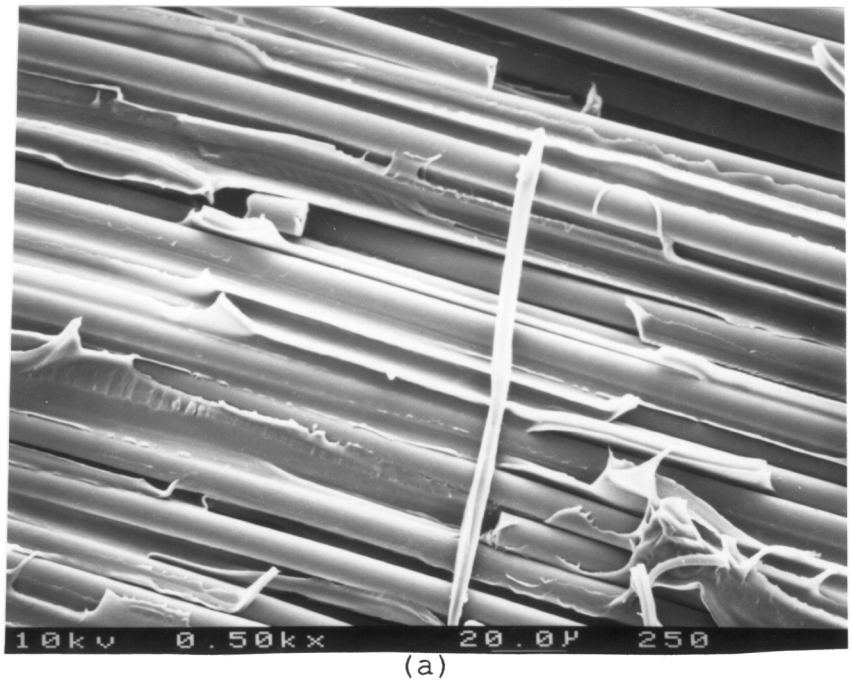

(a)

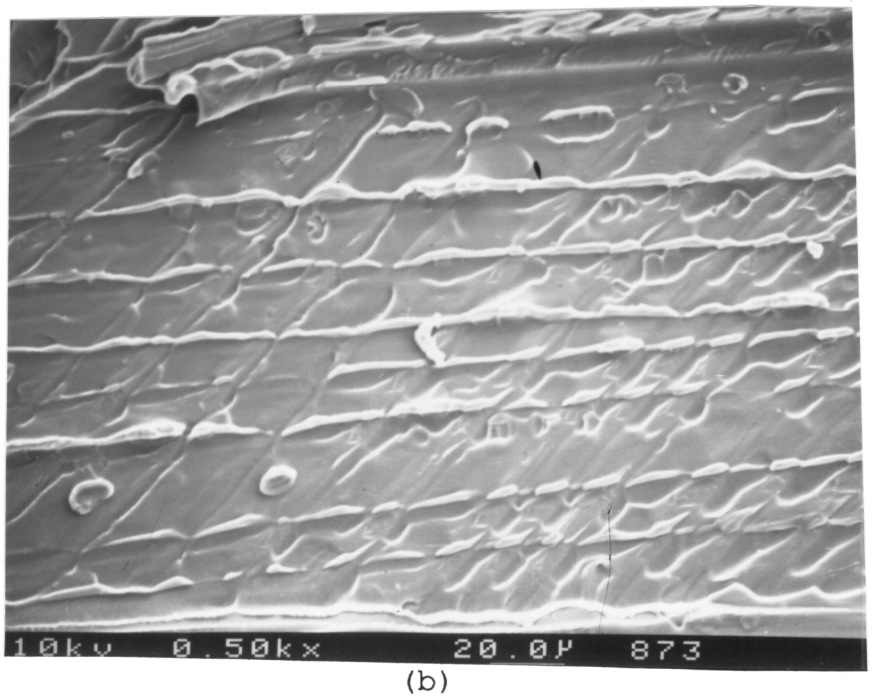

(b)

Figure 6-8: SEM photomicrographs of failed specimens ($[\pm 45/90_2]_s$) with long creep rupture life for (a) AU4/J2; (b) AS4(2)/J2; and (c) AS4CGP/J2 composites.

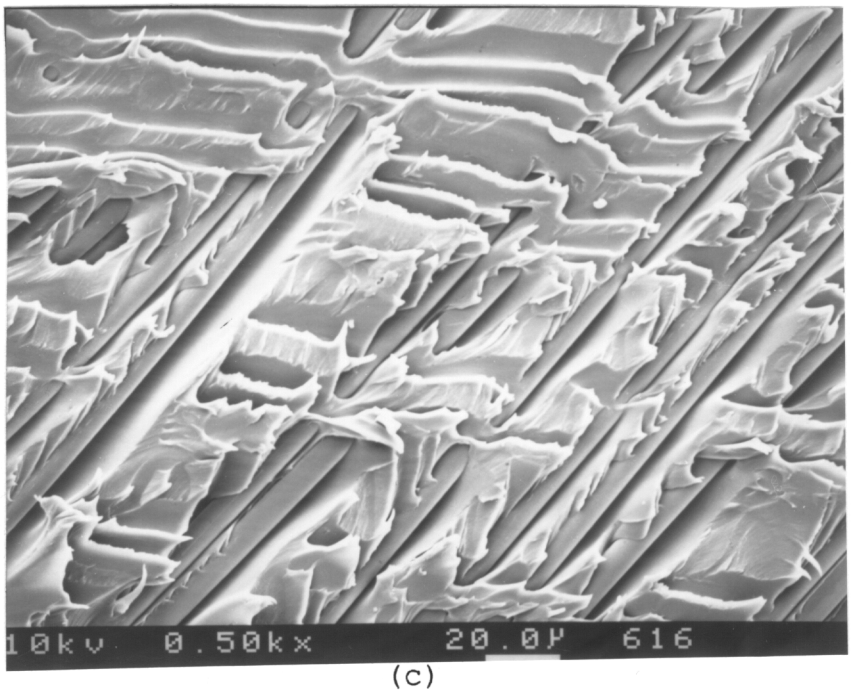

(c)

Figure 6-8: Continued

AS4(2)/J2 composites have higher static strengths, creep rupture strength of the AS4CGP/J2 laminates is greater than that of the AS4(2)/J2 laminates.

REFERENCES

[1] Krueger, W. H., Khan, S., Croman, R. B., and Chang, I. K., "High Performance J-2 Thermoplastic Matrix Composite Reinforced with Kevlar Aramid Fiber," in Proceedings of 33rd SAMPE symposium, Anaheim, March 7-10, 1988, pp. 181-193.

[2] Shalaby, S. W., "Thermoplastic Polymers", in Thermal Characterization of Polymeric Materials, Ed. by Turi, E. A., Academic Press, London, 1981.

[3] Kodama, M., Karino, I., and Kuramoto, K., "Polar-Polar Interaction and Boundary Phase Structure Between Reinforcement and Matrix in a Polymer Composite", Polymer-Plastics Technology and Engineering, Vol.27, no. 1, pp. 127-153, 1988.

[4] Ko, Y. S., Forsman, W. C., and Dziemianowicz, T. S., "Carbon Fiber-Reinforced Composites:Effect of Fiber Surface on Polymer Properties", Polymer Engineering Science, V. 22(13), 1982, pp. 805-814.

[5] Thomason, J. L., "Investigation of Composite Interphase Using Dynamic Mechanical Analysis: Artifacts and Reality", Polymer Composites, Vol. 11, no. 2, pp. 105-113, 1990

[6] In DuPont DMA-983 user's manual: DMA Standard Data Analysis Program.

[7] Aklonis, John J. and MacKnight, William J., Chapter 3, in Introduction to Polymer Viscoelasticity, Second Edition, John Wiley, New York, 1983.

[8] LeGrand, D. G., "Annealing," in Encyclopedia of Polymer Science and Engineering, Vol. 2, 1984, pp. 43-55.

[9] Kimoto, M., "Flexural Properties and Dynamic Mechanical Properties of Glass Fiber-Epoxy Composites", Journal of Materials Science, Vol. 25, pp.3327-3332, 1990.

[10] Batdrof, S. B., "Tensile Strength of Unidirectionally Reinforced Composites - I," Journal of Reinforced Plastics and Composites, Vol. 1, 1981, pp. 153-177.

Chapter 7

COMPARISON BETWEEN AS4(1)/J2 AND AS4(2)/J2 COMPOSITES

Higher degradation rate in the creep rupture strength of the AS4(1)/J2 composite laminates motivated the present research. At that time, the cause was thought to be the interphase (interface) region effect. However, as discussed in the last chapter, the interphase region did not affect the degradation rate of the creep rupture strength for the second batch of J2 composite laminates. Therefore, the author was led to investigate possible factors that might cause these inconsistent observations.

7.1 Surface Properties of AS4(1) and AS4(2) fiber

The surface chemistry of both AS4(1) and AS4(2) fiber was characterized by using the XPS technique. Due to the lack of the AS4(1) fiber in a tow form, the fiber samples used for XPS were taken from their corresponding prepregs. For comparison purposes, the AS4(2) fiber, taken from spools, was also examined due to its availability.

The XPS results are summarized in Table 7-1. It was found that the compositions of carbon/oxygen/nitrogen are very close for the AS4(2) fiber taken from the spool and prepreg. This indicates that the fibers taken from the

prepregs were not influenced by either the low molecular weight (M.W.) polymer (J2) or other contaminants. Thus, the XPS results of AS4(1) fibers should be reliable and show the compositions of oxygen and nitrogen are different from those of the AS4(2) fibers. It is observed that AS4(1) fiber has a higher nitrogen composition than AS4(2) fiber does. In addition, the oxygen composition of the AS4(1) fiber is smaller than that of the AS4(2) fiber. It should be noted that the first batch of the AS4(1)/J2 prepreg was received on September, 1989; whereas the AS4(2) fiber was purchased on December, 1990. Thus, according to the XPS results, the supplier might have used a different process parameters to produce the AS4(1) and AS4(2) fiber.

Table 7-1 XPS Results of AS4(1) and AS4(2) fibers

	AS4(1)*	AS4(2)*	AS4(2)**
Carbon	89.2%	87.5%	85.9%
Oxygen	5.6%	9.9%	11.6%
Nitrogen	4.2%	2.6%	2.5%

* : Fibers were taken from prepregs.
**: Fibers were taken from the spool.

7.2 DMA Results

Figure 7-1 shows the dynamic modulus components as a function of temperature, for the J2 composites including

unannealed AS4(1)/J2, as well as annealed AS4(1)/J2 and AS4(2)/J2 specimens. The specimens used for the DMA tests were $[90]_{12}$ laminates, i.e., the testing direction is matrix dominated. The transition temperatures of unannealed AS4(1)/J2 and annealed AS4(1)/J2 and AS4(2)/J2 specimens are 168°C, 172.3°C, and 168.8°C, respectively. Although the T_g values of the tested composite systems do not deviate significantly, the high and low values encountered on the annealed AS4(1)/J2 and AS4(2)/J2 systems become important. The high T_g value observed for the annealed AS4(1)/J2 specimens may be due to good adhesion between fiber and matrix [19] and/or different J2 matrix (with higher molecular weight) being used.

7.3 Mechanical Properties of AS4(1)/J2 and AS4(2)/J2 Composites

The mechanical properties of both AS4(1)/J2 and AS4(2)/J2 composites are listed in Table 7-2. The ISS of the AS4(1) appears to have the greatest bond strength by roughly 31% over the AS4(2) composites. This may be explained, in part, by the differences in fiber lot and/or processing conditions for the AS4(1) and AS4(2). It should be noted that the AS4(1)/J2 system has the highest transverse tensile strength. Again, this may be due to good adhesion and/or the different batch of J2 resin used.

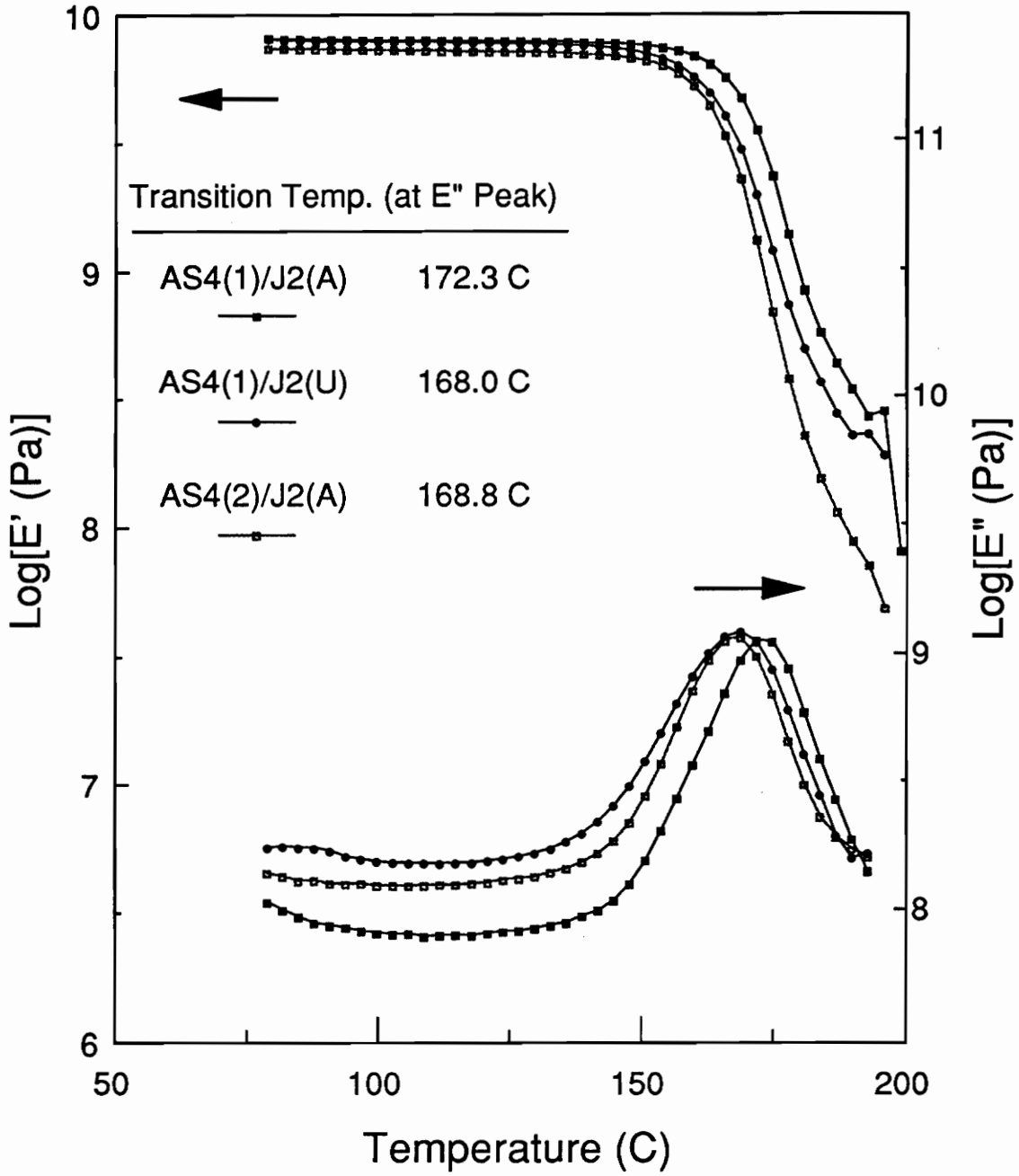

Figure 7-1: DMA results of Log(E') and Log(E") vs. Temperature plot for [90](12) specimens at 3.2 Hz. "A" represents annealed; "U" stands for unannealed.

However, the ultimate $[\pm 45/90_2]_s$ tensile strength of the AS4(1)/J2 is lower than that of the AS4(2)/J2. Several possible explanations are given.

Table 7-2 Mechanical Properties of AS4(1)/J2 and AS4(2)/J2

	AS4(1)/J2	AS4(2)/J2
ISS, [MPa]	~124.1	~96.5
Transverse Tensile Strength [MPa]	70.0±3.3 (4)*, [54.4%]**	54.2±1.7 (4)*, [55.7%]**
Transverse Tensile Modulus [GPa]	8.8±0.6	8.5±0.4
Failure Strength $[\pm 45/90_2]_s$ [MPa]	280±20 (4)	316/303

* : Number denotes the number of tested specimens.
**: Number represents fiber volume fraction.

Figure 7-2(a) shows a fiber breakage failure in the AS4(1)/J2 laminates. Figure 7-2(b) illustrate severe intraply (90° layers) delaminations on both edges of the AS4(1)/J2 laminates. However, the AS4(2)/J2 composites do not delaminate. This suggests that AS4(1)/J2 composites may possess either poor interfacial adhesion between fibers and J2 polymer or defects in the composites. The first possible factor is ruled out since good adhesion is observed from the meso-indentation results. Also, as will be confirmed later in the SEM photomicrographs, matrix remains on the fibers of the failed specimens suggesting a "good" adhesion in the

AS4(1)/J2 composites. As mentioned in the Chapter 3, the author has observed resin starved regions spreading out in the AS4(1)/J2 prepreg. However, the author is not certain if the resin starved regions create microvoids in the AS4(1)/J2 laminates. Thus the potential presence of resin starved regions is believed to cause the severe delaminations observed in the AS4(1)/J2 composite laminates. Therefore, the development of the delamination of the AS4(1)/J2 composite laminates alters the failure mode resulting in a lower failure strength.

7.4 Creep and Creep Rupture of AS4(1)/J2 and AS4(2)/J2 Composites

For the purpose of comparison, the master curves of AS4(1)/J2 and AS4(2)/J2 specimens ($[90]_{12}$), including annealed and unannealed conditions, are shown in Figure 7-3. The annealed specimens become stiffer and result in shifting the master curves to the right when compared to the unannealed specimens. As discussed in the last chapter, it requires ~1.2 dcades to shift the master curve of the unannealed AS4(2)/J2 specimen to match the master curve of the annealed AS4(2)/J2 specimen.

On the other hand, for the AS4(1)/J2 composites, there is roughly a 2.5 decades difference in time between the annealed and unannealed specimens at the same level of

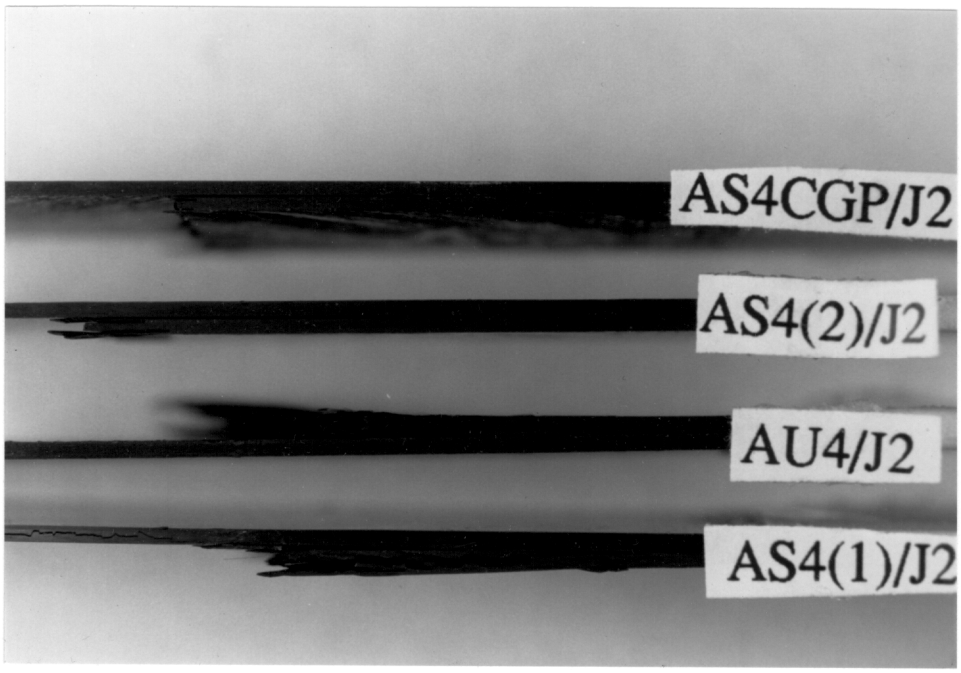

Figure 7-2: A photograph for failed J2 composite specimens ($[\pm 45/90_2]_s$). Severe intraply delamination occurs in the AS4(1)/J2 composites.

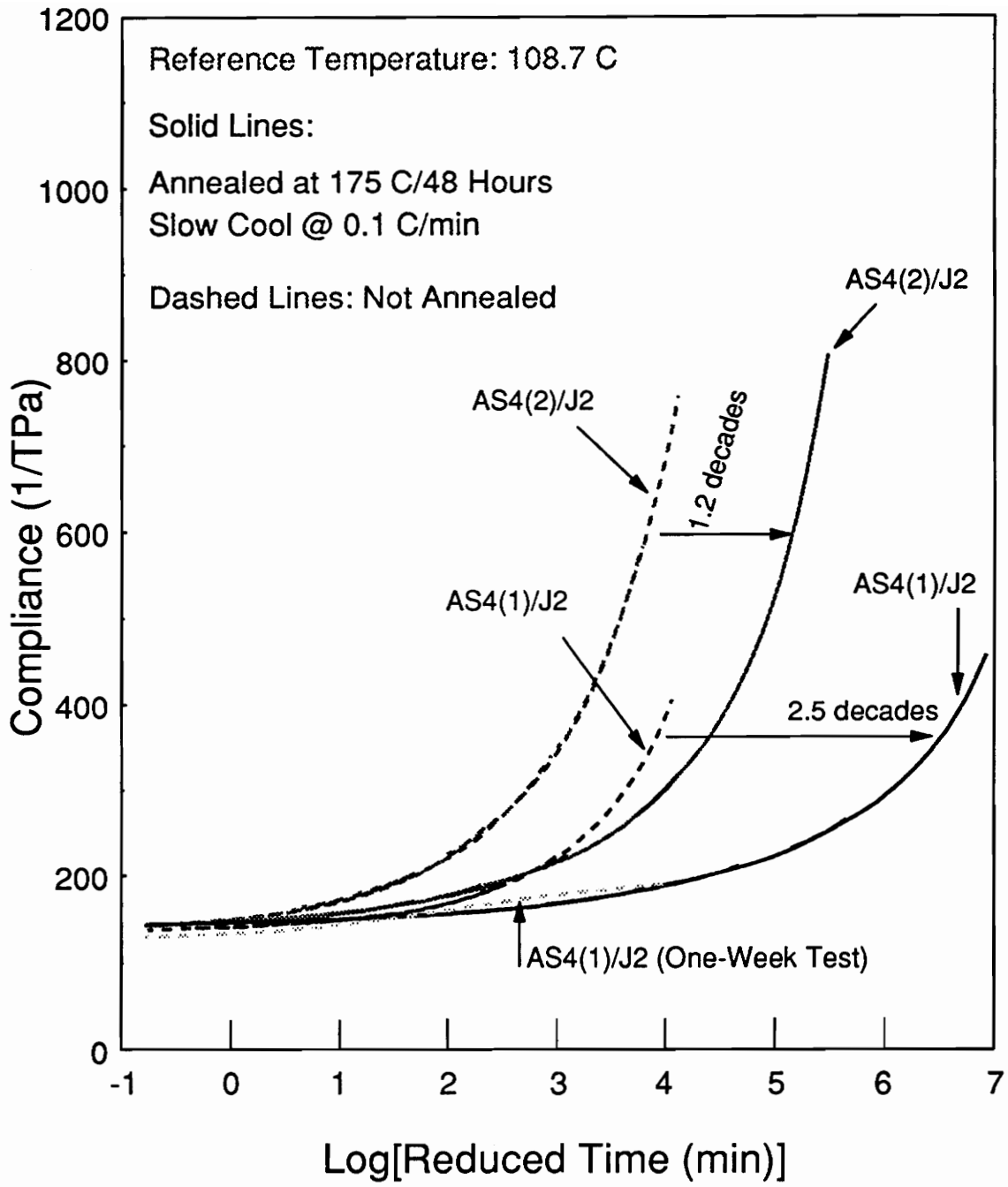

Figure 7-3: Master curves of AS4(1)/J2 and AS4(2)/J2 [90](12) specimens. A one-week creep test is also shown in the figure.

compliance, which is greater than the AS4(2)/J2 composite. This indirect measurement further implies that the matrix used in the AS4(1)/J2 and AS4(2)/J2 is dissimilar. In addition, the transverse tensile strength of the AS4(1)/J2 composite is ~30% higher than that of the AS4(2)/J2 composite. This suggests the matrix used for the AS4(1)/J2 composite may be quite stiff. If this is true, then the matrix is expected to become even stiffer with annealing.

As mentioned before, the authors did not consider that different thermal history of the AS4(1)/J2 composites would be a siginificant factor. Thus, a one-week DMA creep test was also conducted at 109°C for an unannealed AS4(1)/J2 $[90]_{12}$ laminate. This one-week creep test was to simulate the unannealed AS4(1)/J2 specimens under creep rupture tests and to investigate the long-term creep response.

The creep curve for the one-week creep test is also shown in Figure 7-3. This curve almost overlaps with the master curve of the annealed AS4(1)/J2 composites. The correspondence indicates that the unannealed specimen was aged and embrittled during the creep test, an observation discussed in detail by Struik [1].

For the convenience of comparison, the creep rupture results of all J2 composites are redrawn in Figure 7-4 and restated as follows. The creep rupture strength of the AS4(1)/J2 laminates degrades approximately 19% within four

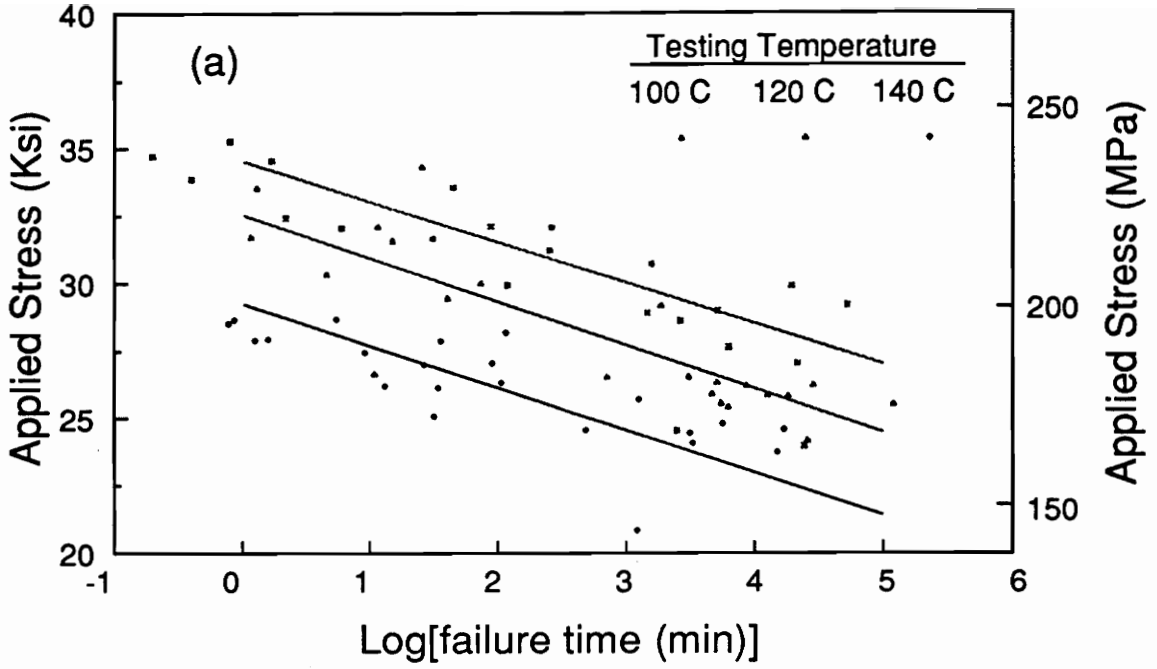

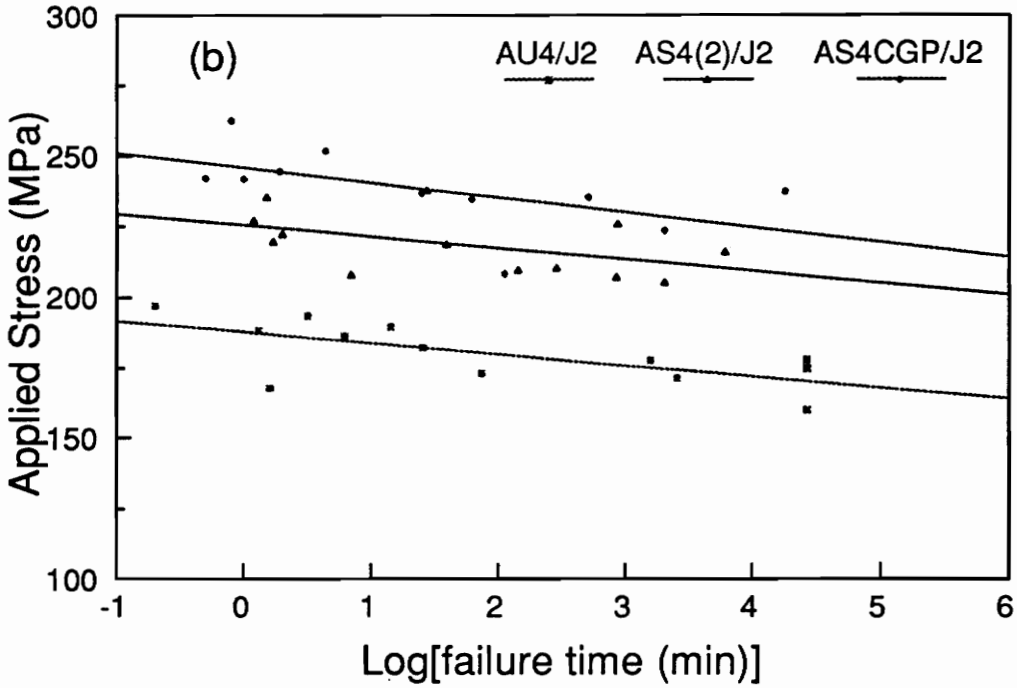

Figure 7-4: A redrawn figure for the creep rupture results of (a) Figure 1-1 and (b) Figure 6-6.

decades of time period at all testing temperatures, including 100°C, 120°C, and 140°C. The creep rupture strength of the other three composite systems degrades approximately 9% within five decades of time period, which is less than half of the values for the AS4(1)/J2 laminates. This substantial difference is illustrated in Figure 7-5 which shows normalized creep rupture strengths for J2 composites tested at 120°C. Figure 7-5 is obtained using the following scheme. Based on Figures 1-1 and 6-6, the best curve fitting method is employed to find the creep rupture strength at 1 min. For each composite system, creep rupture strengths are then normalized to the calculated creep rupture strength. Figure 7-5 shows that the best fit curves of the second batch of J2 composites do not deviate very much from each other. This suggests that the creep rupture strengths of J2 composites are not dependent upon the interphase/interface characteristics, as discussed in Chapter 6. Figure 7-5 clearly shows the creep rupture strengths of the AS4(1)/J2 composite degrade much faster than the other three composite systems. Possible explanations are stated in the following discussion.

Recall that Figure 7-2 shows severe delaminations in the AS4(1)/J2 composites, which are also observed in creep rupture tests. The embrittlement of the J2 could lead to the delamination observed. Since creep rupture tests are

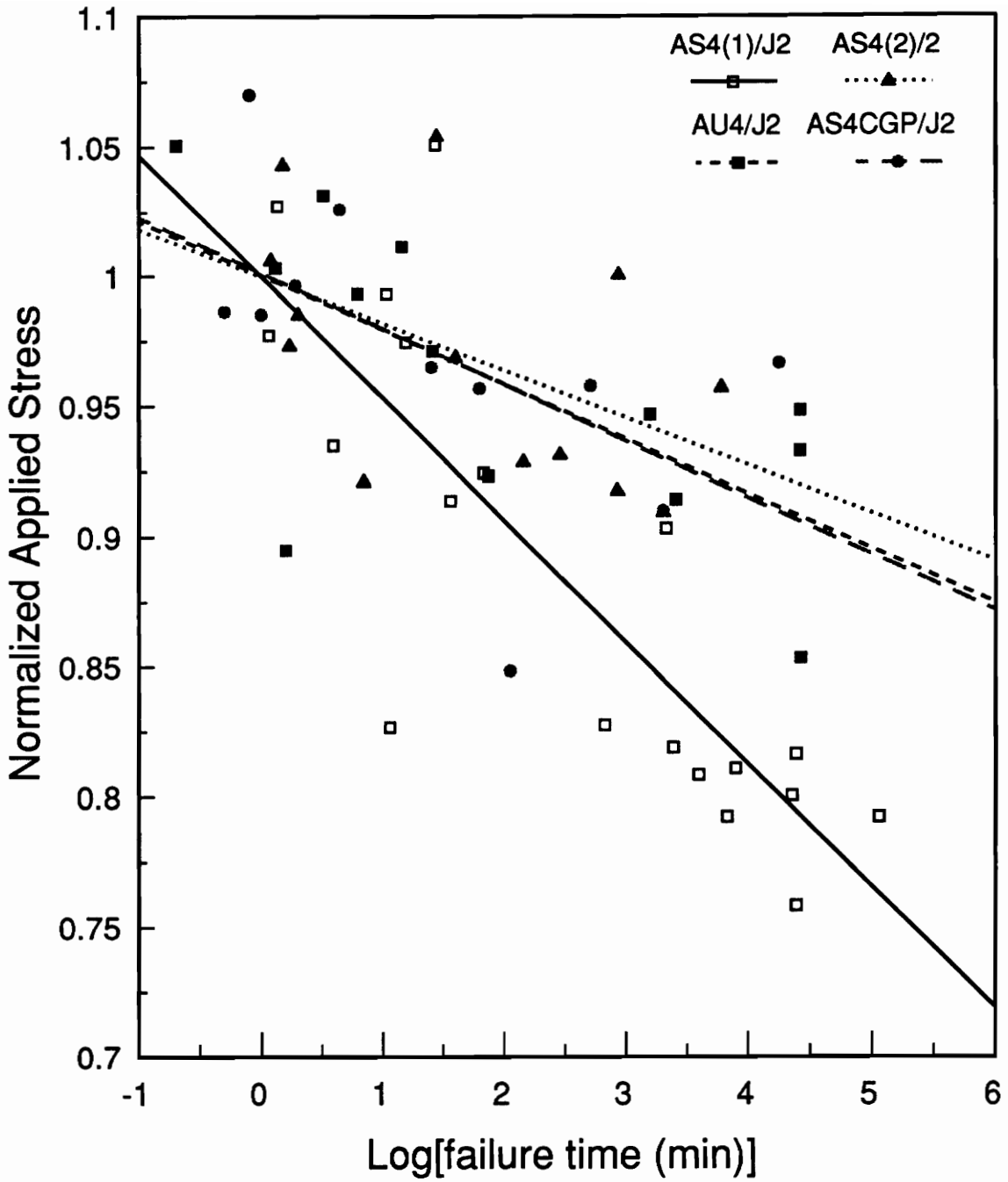

Figure 7-5: Normalized creep rupture strengths for J2 composites at 120 C.

long term mechanical tests, the aging process proceeds during the course of the experiment. This increases the brittleness of the testing specimens, particularly for the unannealed specimens. The viability of this scenario is experimentally verified for a one-week creep test of an unannealed AS4(1)/J2 composite and shown in Figure 7-3. These circumstances may explain why the AS4(1)/J2 laminates degrade faster than the other composite laminates.

Figures 7-6 and 7-7 show the fracture surfaces of the specimens failed at an intermediate and long creep rupture life for AS4(1)/J2 and AS4(2)/J2 laminates. Figure 7-5(a) shows that matrix was smeared at the -45/90 interface. It also shows good adhesion is obtained in AS4(1)/J2 system, which confirms the previous argument. Figure 7-6(a) shows flake-shape hackles in AS4(1)/J2 composites, suggesting a brittle failure mode. Both Figures 7-5(b) and 6(b) show a relatively ductile failure mode for the AS4(2)/J2 laminates when compared to the AS4(1)/J2 laminates.

7.5 Summary

Both XPS and DMA results suggest the fiber and J2 polymer may be different from one batch to the other. The AS4(1)/J2 composites have the highest ISS among the tested J2 composites. However, the transverse tensile strength of the AS4(1)/J2 composites is smaller than that of the

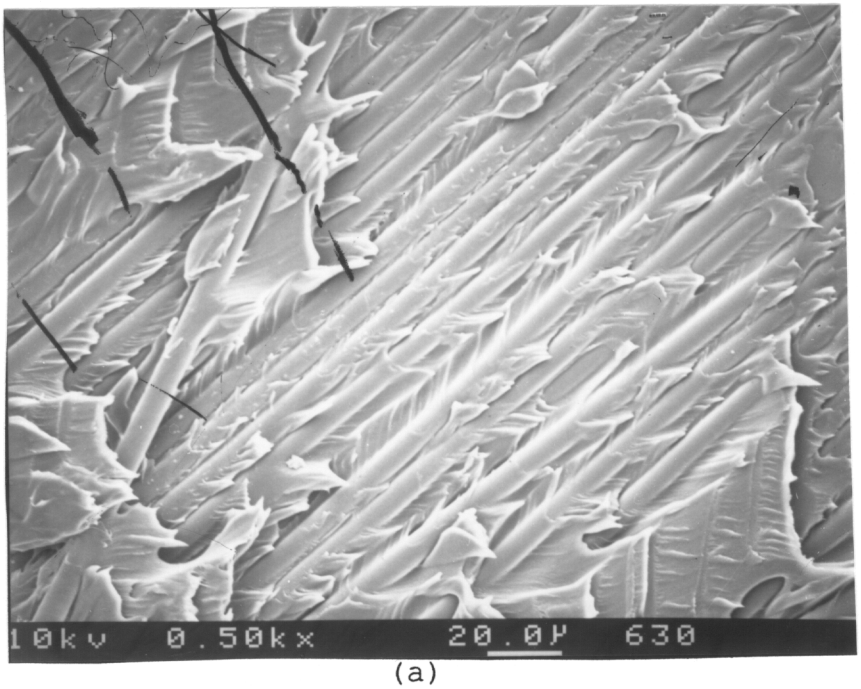

(a)

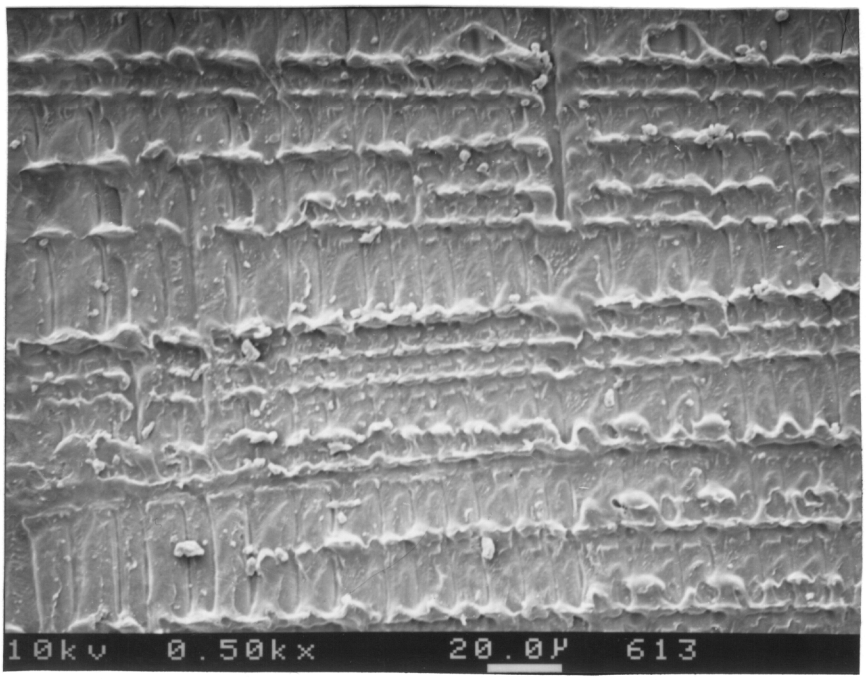

(b)

Figure 7-6: SEM photomicrographs of failed specimens ($[\pm 45/90_2]_s$) with intermediate creep rupture life for the (a) AS4(1)/J2 and (b) AS4(2)/J2 composite.

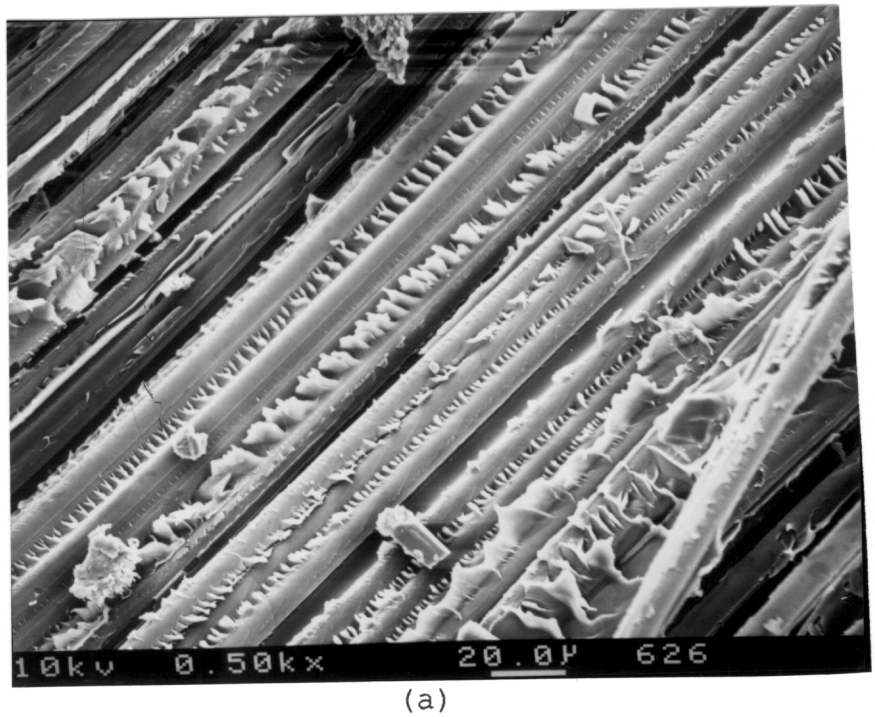

(a)

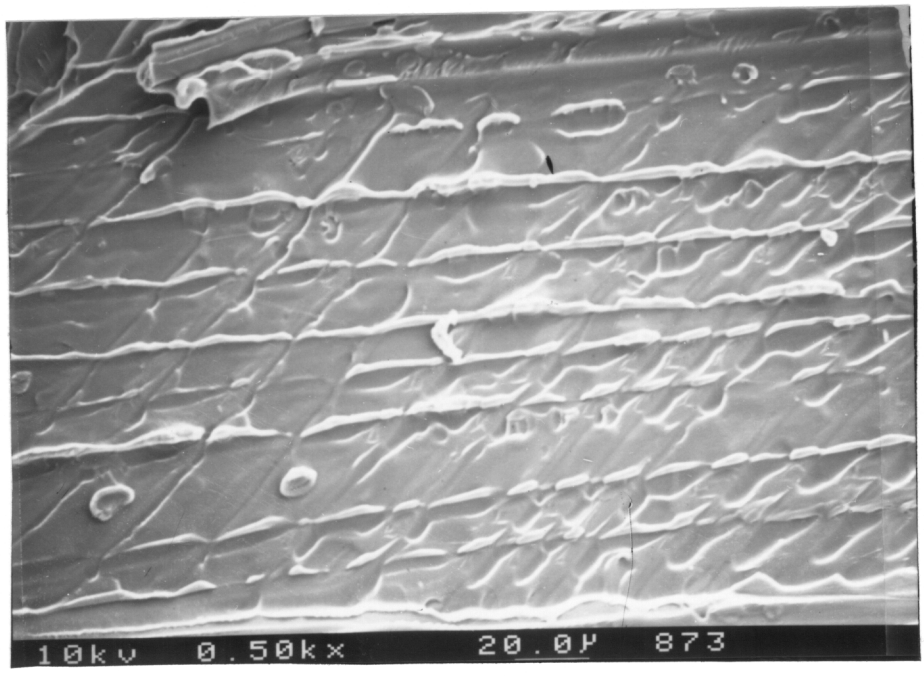

(b)

Figure 7-7: SEM photomicrographs of failed specimens ($[\pm 45/90_2]_s$) with long creep rupture life for the (a) AS4(1)/J2 and (b) AS4(2)/J2 composite.

AS4(2)/J2 composites. Severe delamination develops in the AS4(1)/J2 composite laminates.

REFERENCES

[1] Struik, L. C. E., Physical Aging of Polymers and Other Materials, 1978, Elsevier Publishing, NY.

Chapter 8

CONCLUSIONS and RECOMMENDATIONS

8.1 Conclusions

The objective of this research was to investigate the effect of the interphase and/or interface region on the creep and creep rupture behavior of J2 composites. The following conclusions were made:

- The surface analysis results suggest: (a) the surface treatment increases the polarity of the AS4(2) and AS4CGP fibers; (b) good adhesion is expected for the AS4(2) and AS4CGP fiber to J2 polymer.
- Due to the absence of the curing agent in the epoxy sizing, AS4CGP/J2 composites have a compliant interphase.
- The additional sizing, e.g., epoxy sizing for the present research, does not improve the ISS further, which is consistent with the surface analysis results.
- The strengths of the J2 composites are improved as ISS increases; whereas the effect of interphase/interface characteristics on the moduli of the J2 composites, e.g., E_{11}, E_{22}, and G_{12}, is minor.
- Both AS4(2)/J2 and AS4CGP/J2 composites have the same ISS. The static strengths ($[0]_8$, $[90]_{12}$, and $[\pm 45]_{2s}$) of

the AS4(2)/J2 composites are higher than those of the AS4CGP/J2 composites. However, the quasi-static tensile strengths of laminates ($[\pm 45/90_2]_s$) are about the same for both AS4(2)/J2 and AS4CGP/J2 composites. The creep rupture strength of the AS4CGP/J2 composites is greater than that of the AS4(2)/J2 composites.

- Creep response of J2 composites is not dependent upon the interphase/interface characteristics.
- The degradation rate of the creep rupture strength for the tested J2 composites is not affected by the interphase/interface properties.
- For J2 composites, "*high*" short-term static strength may not result in "*high*" creep rupture strength.

The conclusions of the comparison between the AS4(1)/J2 and AS4(2)/J2 composites are given as follows:

- Surface analysis results suggest the AS4(1) and AS4(2) fibers are different in chemical compositions.
- Thermal analysis results suggests J2 polymers that used in both batches are slightly different.
- The AS4(1)/J2 composites have the highest ISS and transverse tensile strength among the tested J2 composites.
- Severe delamination of the AS4(1)/J2 laminates changes the failure mode and possibly results in a higher degradation rate of the creep rupture strength.

- The aging process is also a possible factor that causes the unannealed AS4(1)/J2 laminates to fail faster than the other composite systems.
- For the present research, the use of different batches of J2 prepregs and different thermal history of J2 composites cuases difficulty in comparing the results.

8.2 Recommendations

As mentioned in the Chapter 7, the author did not consider different thermal histories of the AS4(1)/J2 would be a significant factor when the preliminary investigation was initiated. Thus, it becomes difficult to compare the results obtained from two batches of composites with different thermal histories. This will be especially true for composites under the creep rupture tests which involve the aging process imposing on the composites. Therefore, based on the present observation, it is necessary to further understand the effect of aging on the creep rupture life of the composites.

A possible approach is proposed here: Expose composites to a series of aging times. Conduct creep and creep rupture tests for the various aged composites. Incorporate the effective time theory [1] with VISCAP procedures [2] to model the creep response of the composites. Use this creep response model in MRLIFE7

procedures [3], based on critical element model, to predict creep rupture life of the aged composites.

It is noticed that the composite laminates ($[\pm 45/90_2]_s$) used for the creep rupture tests were not a structural lay-up. For practical applications, composite laminates are designed to allow fibers to bear most of the imposed load. However, some considerations limited the present research when the initial investigation began. These are (a) fibers do not creep and (b) the capacity of the existing equipment is small for testing fiber direction composites. Therefore, to overcome these problems and to simulate the real applications, the composite laminates can be designed with lower fiber angle orientation, e.g., 10°.

Present research suggests the creep rupture strength is affected by the epoxy sizing which is believed to cause a compliant interphase. Thus, to further investigate the role of the interphase in determining the long-term behavior, a systematic study is required. The study should at least involve interphases that are extremely rigid and compliant and intermediate. The interphases can be created by either different surface treatments or different sizings.

REFERENCES

[1] Struik, L. C. E., Physical Aging in Amorphous Polymers and Other Materials, Elsevier Science Publishing, NY, 1978.

[2] Gramoll, K. C., Ph.D. Dissertation, "Thermo-viscoelastic Characterization of Viscoelastic Composite Materials," Virginia Polytechnic Institute and State University, March, 1988.

[3] Reifsnider, K. L., "The Critical Element Model: A Modeling Philosophy," Mechanics of Damage and Fatigue, Pergamon Press, 1986, pp. 739-750.

VITA

Mr. Yeou Shin Chang was born 12 February, 1957 in Lo-Tung, Taiwan. He graduated from Chemical Engineering Department of National Chen-Kung University in 1980. After completing military service, he worked at a chemical plant for one year. He then attended Material Engineering Department of Auburn University, Alabama and received Master of Science degree in 1986. He enrolled in the Materials Engineering Science Program of Virginia Tech in August, 1986. Upon completion of his degree, he will return to his country. He is married to Ms. Chun-Yuan Cheng and has a son Eric, age 4.